„Untersuchung der Endothelfunktion von retinaler Arteriolen in drei Krankheitsmodellen”

Dissertation
zur Erlangung des Grades
„Doktor der Naturwissenschaften“
im Promotionsfach Pharmazie

am Fachbereich Chemie, Pharmazie,
Geographie und Geowissenschaften
der Johannes Gutenberg-Universität in Mainz

Jenia Kouchek Zadeh

geb. in Kirn, Deutschland

Mainz, 2020

Meiner Familie gewidmet

Tag der mündlichen Prüfung: 02. November 2020

Die vorliegende Dissertation wird am Fachbereich Chemie, Pharmazie und Geowissenschaften der Johannes Gutenberg-Universität in Mainz (D77) eingereicht und setzt sich kumulativ aus folgenden Publikationen zusammen:

I. **Zadeh JK**, Ruemmler R, Hartmann EK, Ziebart A, Ludwig M, Patzak A, Xia N, Li H, Pfeiffer N, Gericke A. *Responses of Retinal Arterioles and Ciliary Arteries in Pigs with Acute Respiratory Distress Syndrome (ARDS).* Exp. Eye Res. 2019 Jul; 184:152-161. PMID: 31022399.

II. **Zadeh JK**, Garcia-Bardon A, Hartmann EK, Patzak A, Ludwig M, Xia N, Li H, Pfeiffer N, Gericke A. *Short-time Ocular Ischemia Induces Vascular Endothelial Dysfunction and Ganglion Cell Loss in the Pig Retina*. Int J Mol Sci 2019 Sep;20(19). PMID: 31546635.

III. **Zadeh JK**, Zhutdieva MB, Laspas P, Yuksel C, Musayeva A, Pfeiffer N, Brochhausen C, Oelze M, Daiber A, Xia N, Li H, Gericke A. *Apolipoprotein E Deficiency Causes Endothelial Dysfunction in the Mouse Retina.* Oxid Med Cell Longev 2019 Nov;2019:5181429. PMID: 31781340.

Inhaltsverzeichnis

1 Zusammenfassung

Die Retina besteht aus einem komplexen Netzwerk aus Nervenzellen, das für die Verarbeitung von visuellen Signalen und deren Weiterleitung in bestimmte Regionen des Gehirns verantwortlich ist. Als metabolisch aktivstes Gewebe im Körper können pathologische Veränderungen in der vaskulären Versorgung der Retina daher innerhalb kurzer Zeit irreversible Schäden und Erblindung zur Folge haben. Pathophysiologische Veränderungen des vaskulären Systems im Zusammenhang mit systemischen Erkrankungen zu untersuchen, stellt damit einen wichtigen Forschungsschwerpunkt dar, um mögliche pharmakologische Angriffspunkte zu entwickeln und irreversible Schäden erfolgreich vorzubeugen. Aufgrund der geringen Größe okulärer Gefäße, ihrer schweren Zugänglichkeit, und ihrer außerordentlich wichtigen Bedeutung für die Netzhaut besteht bei der Untersuchung der retinalen Perfusion großer Forschungsbedarf.

Das Ziel dieser Arbeit war es physiologische Auswirkungen systemischer Erkrankungen auf die Endothelfunktion retinaler Arteriolen am Ganztier-Modell zu untersuchen sowie die beteiligten Signalwege zu identifizieren. Dabei wurden *in vivo* drei klinisch relevante und mit hohen Mortalitätsraten verbundene Krankheits-Modelle etabliert: ein akuter Lungenschaden, eine transiente globale Ischämie und eine chronische Hypercholesterinämie. An diesen Modellen wurde das endothelabhängige und endothelunabhängige Vasodilatations- und konstriktionsverhalten retinaler Arteriolen sowie die Expression charakteristischer Marker bestimmt. In allen drei Modellen wurde eine endotheliale Dysfunktion und vermehrter oxidativer Stress festgestellt. Diese funktionelle Störung ging mit einer erhöhten Expression der Hypoxiemarker HIF-1α und VEGF-A und der prooxidativen Untereinheit der NADPH-Oxidase 2 auf mRNA- und Protein-Ebene einher. Des Weiteren weisen immunohistochemische Analysen auf eine Lokalisation dieser Marker in der Gefäßwand retinaler Arteriolen hin.

Die vorliegende Arbeit lässt auf eine wichtige Rolle dieser Marker in der Pathophysiologie einer endothelialen Dysfunktion von retinalen Arteriolen schließen und unterstreicht die hohe Relevanz retinaler Untersuchungen im Zusammenhang mit systemischen Erkrankungen.

Summary

The retina consists of a complex network of neural cells that is responsible for processing visual signals and transporting them to specific regions of the brain. As the most metabolically active tissue in the body, pathological changes in the vascular supply of the retina can therefore result in irreversible damage and blindness within a short period of time. Investigating pathophysiological changes of the vascular system in association with systemic diseases is therefore an important research focus in order to develop possible pharmacological targets and successfully prevent irreversible damage. Due to the small size of ocular vessels, their difficult accessibility, and their extraordinary importance for the retina, there is a great need for research in the investigation of retinal perfusion.

The aim of this work was to investigate the physiological effects of systemic diseases on the endothelial function of retinal arterioles in an animal model and to identify the signaling pathways involved. Three clinically relevant disease models associated with high mortality rates were established in vivo: acute lung injury, transient global ischemia and chronic hypercholesterolemia. These models were used to determine the endothelium-dependent and endothelium-independent vasodilation and constriction behavior of retinal arterioles and the expression of characteristic markers. In all three models, endothelial dysfunction and increased oxidative stress were observed. This functional disorder was associated with increased expression of the hypoxia markers HIF-1α and VEGF-A and the prooxidative subunit of NADPH oxidase 2 (NOX2) at mRNA- and proteinlevel. Furthermore, immunohistochemical analyses indicate a localization of these markers in the vessel wall of retinal arterioles.

The present work suggests an important role of these markers in the pathophysiology of endothelial dysfunction of retinal arterioles and underlines the high relevance of retinal studies in the context of systemic diseases.

2 Einleitung

2.1 Einführung in die Thematik

Die vaskuläre Versorgung der Retina erfolgt durch ein System von Endgefäßen, die keine Kollateralen untereinander oder mit anderen Gefäßsystemen bilden. Durch die essenzielle Rolle der Mikrozirkulation für die Sauerstoffversorgung der Retina und des Sehnervenkopfes sind Störungen der Durchblutung oftmals verbunden mit Sehstörungen [1]. Als Risikofaktoren retinaler Ischämien, die definiert sind durch eine Verminderung der Netzhautdurchblutung, sind kardiovaskuläre Erkrankungen, wie z.B. arterielle Hypertonie, Arteriosklerose und Diabetes mellitus identifiziert worden [2]. Diese haben pathophysiologische Veränderungen von retinalen Arteriolen und Venen zur Folge und können im späteren Verlauf durch ischämische Prozesse und das resultierende Absterben von neuronalen Zellen zu morphologischen und funktionellen Veränderungen der Retina führen. Netzhautischämien spiegeln sich in Abhängigkeit ihrer Ursachen in unterschiedlichen Krankheitsbildern wider. Die diabetische Retinopathie stellt einer der häufigsten Augenerkrankungen in Deutschland dar. So erkranken 38,2% der Typ 2-Diabetiker nach einer 20-jährigen Diabetesdauer daran [3]. Metabolisch bedingte mikrovaskuläre Veränderungen, wie eine gestörte endothelabhängige Gefäßregulation spielen eine wesentliche pathophysiologische Rolle bei retinalen Komplikationen, die im Zusammenhang mit ischämischen Folgen in der Retina diskutiert werden [4]. Die zweithäufigste Erblindungsursache weltweit stellt die Glaukomerkrankung dar, deren Entstehung unter anderem durch eine Perfusionsstörung der Retina begünstigt werden kann und sich in einem Verlust von retinalen Ganglienzellen (RGZ) widerspiegelt [5,6]. Trotz einer Prävalenz von 3,5% bei Menschen im Alter von 40-80 Jahren [7] beschränken sich aktuelle Therapiemöglichkeiten nur auf eine symptomatische Behandlung, da die Pathogenese bisher nicht hinreichend bekannt ist. Weitere Augenerkrankungen, wie z.B. retinale Arterienverschlüsse, die meistens im Rahmen einer Arteriosklerose entstehen [8], basieren ebenso auf einer Minderperfusion der Retina und daraus resultierenden Spätfolgen, für die es bis heute auch keine ursächliche Behandlungsgrundlage gibt [9]. Bedingt durch die Entwicklung hochauflösender optischer Verfahren wie der optischen Kohärenztomographie (engl. optical coherence tomography, OCT), der OCT-

Angiografie und dem Retinal Vessel Analyzer gewinnt die Messung der Gefäßreaktivität und der Gefäßmorphologie in der Retina im klinischen Alltag zunehmend an Bedeutung. Die OCT ermöglicht durch die Verwendung von Licht im nahen Infrarotbereich die mikroskopische Darstellung der retinalen und choroidalen Morphologie, was für eine frühe Diagnostik und die Evaluierung einer Schädigung von Netzhautschichten therapieentscheidend sein kann. Eine Weiterentwicklung der OCT ist die OCT-Angiographie, die mittels dreidimensionaler Darstellung von vaskulären Strukturen der Aderhaut und Netzhaut eine retinale und choroidale Perfusionsanalyse ermöglicht. Um die Fähigkeit der Gefäßerweiterung retinaler Arteriolen und Venolen dynamisch messen zu können, wird der Retinal Vessel Analyzer herangezogen. Nach Stimulation der Retina mit einem optoelektrischen Flickerlicht von 12,5 Hz wird am Augenhintergrund die Änderung des Gefäßdurchmessers beobachtet und ausgewertet. So liefern diese noninvasiven Untersuchungsmethoden zwar wichtige Informationen über bekannte Zusammenhänge zwischen retinalen Anomalien und internistischen Erkrankungen [10,11], jedoch ist bisher unbekannt, welche Erkrankungen zu einer Gefäßdysfunktion führen können und welche Rolle das Endothel dabei spielt. Derzeit existieren keine *in vivo* Methoden am Menschen, um die Endothelfunktion an der Retina zu bestimmen. Um die Mechanismen der Krankheitsentstehung besser zu verstehen, sind daher funktionelle Studien an isolierten Gefäßen und pathologischen Tiermodellen von großer Bedeutung. Die in dieser Arbeit verwendeten Methoden ermöglichen die Untersuchung zugrunde liegender lokaler Mechanismen, was *in vivo* nicht möglich ist.

2.2 Therapie

Das Therapieziel bei der Behandlung von retinalen Erkrankungen ist eine Progression des Krankheitsverlaufes zu verhindern und einem vollständigen Visusverlust durch symptomatische Behandlungen vorzubeugen. Der Grund hierfür liegt zum einen darin, dass das Bewusstsein um die Erkrankung bzw. die Auswirkungen systemischer Prozesse auf die retinale Funktion in der Bevölkerung kaum vorhanden ist [12], wodurch eine möglichst frühe Indikations-

und Therapieentscheidung nötig wird. Zum anderen sind pathologische Prozesse in der retinalen Gefäßversorgung, bedingt durch systemische Ereignisse, noch zu wenig erforscht, um effektive Therapieansätze bereits vor dem Voranschreiten der Erkrankung zu entwickeln. Charakteristisch für ischämisch-bedingte vaskuläre Veränderungen ist die Konstriktion von retinalen Arteriolen, erhöhter oxidativer Stress sowie entstehende Blutungen, die bedingt durch eine Schädigung der inneren Blut-Retina-Schranke in die Nervenfaserschicht der Netzhaut eindringen können. Maßnahmen, um einen normalen Blutfluss wiederherzustellen, oxidativen Stress zu minimieren oder die Produktion von Faktoren zu hemmen, die eine erhöhte Permeabilität der Gefäße und eine Neovaskularisation zur Folge haben (z.B. engl. vascular endothelial growth factor, VEGF) stellen eine der vielversprechendsten Strategien dar, sind jedoch in Leitlinien-gerechten Therapieoptionen aufgrund einer mangelnden Studienlage kaum vertreten. Neben der Verwendung von Kortikosteroid-Implantaten [13] (Dexamethason, Triamcinolonacetonid), die mit einigen Nebenwirkungen verbunden sind (Katarakt-Bildung, Erhöhung des Augeninnendrucks), bildet die intravitreale Injektion von VEGF-Inhibitoren (Aflibercept, Ranibizumab) bei fortgeschrittenem Stadium einer Retinopathie eine entscheidende Grundlage der medikamentösen symptomatischen Therapie. Der aktuelle Therapiestandard im Rahmen einer nicht-medikamentösen Therapie einer Gefäßleckage umfasst die Anwendung einer Laser- bzw. Photokoagulation und führt durch gezielte thermische Effekte zu einer Minderung des Sauerstoffbedarfs der Netzhaut und somit mittelbar zum Verschluss von Blutgefäßen. Zur Behandlung von okklusiven Augenerkrankungen konnte eine Reihe von randomisierten, multizentrischen Studien [9,14] die Wirksamkeit einer Lysetherapie z.B. mit gewebespezifischem Plasminogenaktivator, der die Blutgerinnung hemmt, im Vergleich zu konservativen Therapieansätzen mit Aspirin oder Bulbusmassagen nicht belegen. Weitere Therapieansätze in der Behandlung ischämischer Augenerkrankungen weisen aufgrund eines Mangels an prospektiven randomisierten Studien keinen hohen Evidenzgrad auf und bedürfen weiterer Forschung.

Die vorliegende Arbeit beschäftigt sich daher mit der Charakterisierung von ischämischen Prozessen an okulären Gefäßen in drei verschiedenen Modellen,

um pathologische Ansätze für die Entwicklung von vasoaktiven Substanzen zu ermöglichen.

2.3 Retinale und choroidale Zirkulation

Die arterielle Blutversorgung des Auges teilt sich in zwei verschiedene Systeme auf, die beide von einer gemeinsamen Arterie, der Arteria ophthalmica, stammen. Gekennzeichnet sind diese zwei Gefäßsysteme durch ihre unterschiedlichen Versorgungsbereiche der Retina. Die Arteria centralis retinae gelangt als Endarterie durch den Sehnerv in das Innere der Retina und versorgt etwa die Hälfte der inneren retinalen Schichten. Die Versorgung reicht hier bis zum äußeren Rand der inneren Körnerschicht [15]. Nach Eintritt in den Augapfel teilt sie sich im Zentrum der Papille in 4 retinale Arteriolen auf, die sich wiederum in ein Netzwerk von Kapillaren aufteilen und die Peripherie der Netzhaut versorgen. Das zweite Gefäßsystem umfasst Ziliararterien, die ebenso der Arteria ophthalmica entspringen. Im System der Ziliararterien unterscheidet man Arteriae ciliares posteriores breves und Arteriae ciliares posteriores longae, die beide entlang des Sehnerves lokalisiert sind und die Sklera des Auges durchdringen, um die Chorioidea (Aderhaut) mit Blut zu versorgen. Die Versorgung der restlichen Netzhautareale wird durch Diffusion von Sauerstoff und Nährstoffen aus der Chorioidea gewährleistet. Über die verschiedenen Versorgungsareale hinaus unterscheiden sich beide Gefäßsysteme in der Steuerung ihres Vasoregulationsverhaltens. Während retinale Arteriolen ihre extrinsische autonome Innervation verlieren, sobald diese durch den Sehnervenkopf in den Bulbus eindringen, wird die Steuerung der Perfusion von ziliaren Arterien von perivaskulären Nerven beeinflusst. So zeigte eine Studie zur Gefäßregulation am Rind eine Schlüsselrolle von Stickstoffmonoxid (NO) in der Vasodilatation, da diese durch eine Blockade der Stickstoffmonoxidsynthase (engl. nitric oxide synthase, NOS) aufgehoben werden konnte. Jedoch führte die Entfernung des Endothels zu keiner Veränderung dieses Verhaltens [16]. Diese Beobachtung und weitere Erkenntnisse geben Hinweise darauf, dass das choroidale Vasoregulationsverhalten durch die Aktivierung von benachbarten

sympathischen und parasympathischen Nerven gesteuert wird. Eine Vasokonstriktion kann hier aus der sympathischen Aktivierung von α_1-Adrenozeptoren in glatten Muskelzellen erfolgen [17], während eine Vasodilatation aus der Aktivierung von parasympathischen Nerven über NO-Signale resultieren kann [18]. Retinale Arteriolen hingegen sind umgeben von einem komplexen Netzwerk von Perizyten, Gliazellen und Neuronen, die durch die Ausschüttung von Transmittern ebenso einer komplexen Steuerung unterliegen. Bedingt durch die morphologische Heterogenität beider Systeme lassen sich nur beschränkt vergleichenden Rückschlüsse beider vaskulären Systeme im Hinblick auf pathologische systemische Zustände ziehen.

2.4 Physiologie retinaler Arteriolen

Retinale Arteriolen unterliegen physiologischen Vasoregulationsmechanismen [19,20], die bis heute noch weitgehend unerforscht sind. Das vaskuläre Endothel übernimmt als innere Auskleidung des arteriellen Gefäßbettes durch die Produktion von vasoaktiven Substanzen z.B. Bradykinin, EDHF (engl. endothelium-derived hyperpolarizing factor), Prostacyclin und Thromboxan A2 essenzielle Funktionen für die Steuerung der Gewebeperfusion. Besonders in der Retina, die das metabolisch aktivste Gewebe darstellt und mit einem hohen Bedarf an Sauerstoff verbunden ist, können Störungen der Endothelfunktion von retinalen Arteriolen zu irreversiblen Schäden und zum Verlust von Nervenzellen führen, die für eine visuelle Reizverarbeitung und Signalweiterleitung an das Gehirn verantwortlich sind [21,22]. So geht man heute davon aus, dass eine vaskuläre Dysregulation, neben anderen Risikofaktoren wie z.B. genetische Prädisposition und höheres Lebensalter zu den bedeutsamsten Risikofaktoren für die Entwicklung des Glaukoms verantwortlich sind [23-26] und einen Untergang von retinalen Ganglienzellen einhergehend mit einem Gesichtsfeldverlust mit sich bringt.

Als Widerstandsgefäße steuern retinale Arteriolen mit Hilfe einer endothelialen semipermeablen Schicht und einer darunterliegenden einfachen Schicht an glatten Muskelzellen das Vasoregulationsverhalten, das die Perfusion der Retina bestimmt. Es gibt nur wenige Arbeitsgruppen, die sich mit der

Erforschung retinaler Vasodilatationsmechanismen beschäftigen und Signalkaskaden in retinalen Arteriolen bisher charakterisieren konnten. Zum aktuellen Zeitpunkt der Forschung konnten Dalsgaard *et al.* am Schweine-Modell zeigen, dass eine Bradykinin-induzierte Vasodilatation in retinalen Arteriolen hauptsächlich auf der Ausschüttung von NO aus dem retinalen Endothel beruht. Als „endothelium-derived relaxing factor“ (EDRF) wurde NO bereits 1992 identifiziert [27] und moduliert die Gefäßregulation über vielfältige Funktionen, wie z.B. vasodilatierende, antiinflammatorische oder antiaggregatorische Wirkungen. Drei verschiedene Isoenzyme mit strukturellen Homologien und unterschiedlichen Expressionsorten synthetisieren NO aus L-Arginin nach Aktivierung durch verschiedenste Stimuli, die rezeptorabhängige Agonisten [z.B. Bradykinin, Acetylcholin, VEGF] oder auch physikalische Wirkungen (z.B. Scheerstress, Pulsatilität) sein können. Von grundlegender Bedeutung in der Regulation der retinalen Arteriolen ist die endotheliale Stickstoffmonoxidsynthase (eNOS, NOS3) identifiziert worden, wobei die Aktivität der neuronalen (nNOS, NOS1) und der induzierbaren NO-Synthase (iNOS, NOS2) unter pathologisch veränderten Bedingungen wie einer Ischämie [28], ebenso eine große Rolle spielt. In der Untersuchung weiterer Signalmechanismen für die Vasodilatation in retinalen Arteriolen wurde nachgewiesen, dass die Blockade Calcium-abhängiger Kaliumkanäle kleiner und mittlerer Leitfähigkeit durch einen spezifischen Kanalöffner mit Apamin und Charybdotoxin die Vasodilatation stark reduzierte [29], wobei der Calcium-Kanal großer Leitfähigkeit keinen Einfluss auf die Bradykinin-induzierte Vasoregulation hatte [30-32]. In einer weiteren Publikation konnte die Expression dieser zwei Kanäle mittels immunohistochemischen Untersuchungen in der Endothelzellschicht nachgewiesen werden. So geht man davon aus, dass eine retinale Vasodilatation durch die Ausschüttung von NO aus Endothelzellen über eine Aktivierung von Calcium-abhängigen Kaliumkanälen gesteuert wird. Es gibt jedoch keinerlei Erkenntnisse, ob und wie das retinale Vasoregulationsverhalten im Zusammenhang mit systemischen Erkrankungen verändert sein kann, inwieweit das Endothel retinaler Arteriolen betroffen ist und welche Mechanismen dabei eine Rolle spielen könnten.

2.5 Methodik

Da im Rahmen dieser Arbeit zwei verschiedene Spezies zur Etablierung der verschiedenen Tier-Modelle notwendig waren, gibt es einige wenige Unterschiede im experimentellen Aufbau, auf die nachfolgend eingegangen wird. Die funktionellen Messungen in Publikation I und II, welche die Auswirkungen eines akuten Lungenschadens und einer transienten globalen Ischämie untersuchten, sind an einem Schweine-Modell durchgeführt worden, während Publikation III die Auswirkungen einer Hypercholesterinämie auf retinale Arteriolen mit Hilfe eines Knock-out Modelles an der Maus darstellt, das sich in Schweinen nicht realisieren lässt.

Die in dieser Arbeit durchgeführten funktionellen Messungen der Gefäßreaktivität retinaler Arteriolen wurden mit Hilfe der Videomikroskopie *in vitro* durchgeführt. Dazu wurden in Publikation I und II nach Beendigung der *in vivo* etablierten Tier-Modelle, die zu untersuchenden Gefäße aus den entnommenen Bulbi mechanisch isoliert. In einer Perfusionskammer wurden diese Gefäßsegmente unmittelbar nach Isolation an beiden Enden mit Mikropipetten kanüliert und daran mit Hilfe von Fäden befestigt. Die Zufuhr von Flüssigkeit über die Mikropipetten ermöglichte den Aufbau eines definierten Druckes innerhalb des Blutgefäßes und die Darstellung des Gefäßes unter einem Lichtmikroskop. Nach Zugabe gefäßaktiver Substanzen in die Perfusionskammer ließ sich die endothelabhängige und endothelunabhängige Veränderung des Gefäßdurchmessers messen, wodurch die Gefäßreaktivität beurteilt werden konnte. Diese Methode ermöglicht die funktionelle Messungen an Gefäßen mit einem Innendurchmesser von 50-300 μm. Während Gefäße vom Schwein einen eigenen Tonus von 50-60% des Ausgangsdurchmessers nach einer Inkubationszeit von 30-45 Minuten unter nahezu physiologischen Bedingungen in der Perfusionskammer entwickeln, weisen retinale Arteriolen der Maus diesen Eigentonus nicht auf. Als Vasodilatator wurde in Publikation I und II Bradykinin verwendet, während in Publikation III Acetylcholin als Vasodilatator fungierte. Die Auswahl liegt darin begründet, dass die endothelabhängige Dilatation an Arteriolen vom Schwein nur mit Hilfe von Bradykinin beobachtet werden konnte, was im Einklang mit weiteren publizierten Arbeiten steht [30,33,34]. Acetylcholin zeigte dagegen eine nur sehr

schwache vasodilatative Wirkung an Schweinegewebe, weshalb die Substanz an der Schweinenetzhaut nicht verwendet wurde.
Die in der dritten Publikation untersuchten retinalen Arteriolen der Maus weisen einen Innendurchmesser von < 30 µm auf, wofür die Verwendung eines einzigartig neuen Systems erforderlich war, das in unserer Arbeitsgruppe etabliert worden ist [35]. Für die Messung der Gefäßreaktivität einer retinalen Arteriole wurde die Netzhaut und die Arteria ophthalmica einer Maus präpariert und in einer Perfusionskammer auf einer transparenten Plastikplattform ausgebreitet. Durch das Auflegen eines Stahlringes wurde die Netzhaut fixiert und die Arteria ophthalmica mittels einer Mikropipette kanüliert, die so wie im obigen Versuchsaufbau durch Flüssigkeitszufuhr für einen Gefäßinnendruck sorgte. Bedingt durch die Semitransparenz der Retina konnte somit die Veränderung des Gefäßdurchmessers durch die Zugabe vasoaktiver Substanzen mittels Durchlichtmikroskopie hochauflösend gemessen werden. Um eine standardisierte Messung der Vasodilatation aufgrund fehlendem Eigentonus zu ermöglichen, wurde mit dem Thromboxanmimetikum U46619 auf 50-70% des Ausgangsdurchmessers vorkontrahiert. Darauffolgende Konzentrations-Wirkungskurven wurden mit Acetylcholin durchgeführt, das für Gefäßmessungen an Mausgewebe bereits gut untersucht und etabliert ist [28,36]. In allen drei Publikationen wurde das endothelunabhängige Verhalten mit Hilfe des vasodilatativ wirkendenden NO-Donors Natriumnitroprussid und dem Vasokonstriktor, U46619, eines Thromboxan A2-Mimetikums, gemessen.

Zur Untersuchung veränderter Genexpressionen im Zusammenhang mit systemischen Erkrankungen wurde im Rahmen aller drei Publikationen die Echtzeit-PCR als weitere Methodik herangezogen. Die quantitative Bestimmung relativer Veränderungen auf mRNA-Ebene in isolierten retinalen Arteriolen ermöglicht es, charakteristische Systeme zu bestimmen, die mit einer Schädigung des funktionellen Verhaltens assoziiert sein könnten. Bedingt durch die kleinen Arteriolen und die damit verbundenen geringen Nukleinsäuremengen bietet die Echtzeit-PCR eine optimale Methode, durch Amplifikation geringster Mengen selektiv veränderte Marker bestimmen zu können. Um die Translation bestimmter charakteristisch veränderter Marker auf mRNA-Ebene in Protein-Ebene zu untersuchen, sind im Rahmen dieser Arbeit

immunohistochemische Verfahren herangezogen worden, mit denen nicht nur die Präsenz bestimmter Proteine mittels fluoreszierender Antikörper-Färbung, jedoch auch deren räumliche Verteilung in den Gefäßen nachgewiesen werden konnte.

Vor dem Hintergrund, dass reaktiven Sauerstoffverbindungen in einigen Arbeiten an okulären Arteriolen eine große Bedeutung für die Bildung von Vasospasmen und daraus resultierenden retinalen Komplikationen, wie z.B. diabetische Retinopathie und Glaukom zugesprochen wird [37,38], sind diese im Rahmen aller drei Publikationen mittels Dihydroethidium (DHE) quantifiziert worden. Als zellpermeable Substanz wird DHE von reaktiven Sauerstoffspezies oxidiert, wodurch das daraus entstehende reaktive Produkt 2-Hydroxyethidium mit der DNA interkaliert und im Zellkern angereichert wird. Mit Hilfe eines standardisierten Algorithmus, der über alle Messungen gelaufen ist, ließ sich die Emission der resultierenden roten Fluoreszenz mittels Fluoreszenzmikroskopie quantifizieren und der oxidative Stress in den untersuchten retinalen Arteriolen ermitteln.

3 Stand der Forschung

Durch das zunehmende Interesse an prädiktiven Markern für Allgemeinerkrankungen gewinnt die retinale Gefäßanalyse immer mehr an Bedeutung. Dank diagnostisch weit entwickelter Methoden und der Lokalisation retinaler Gefäße am optisch zugänglichen Augenhintergrund lässt sich die retinale Mikrozirkulation so gut abbilden, wie kein anderes mikrovaskuläres Gefäßbett im gesamten Körper. Zwar sind retinale Funktionseinschränkungen, wie oben erwähnt, im Zusammenhang mit kardiovaskulären Erkrankungen bekannt, doch bleibt die Rolle systemischer Ereignisse, sowie die strukturellen und funktionellen Veränderungen am retinalen Endothel, die weitere Spätfolgen mit sich ziehen können, weitestgehend unerforscht. Im klinischen Verlauf der Glaukomerkrankung konnte trotz einer Normalisierung des erhöhten Augeninnendruckes und der damit verbundenen Wiederherstellung der Blutversorgung gezeigt werden, dass sich das klinische Bild progredient

verschlechterte [39]. Eine verminderte Sauerstoffversorgung kann somit einen nachhaltigen physiologischen Schaden der Retina verursachen, der durch die räumliche Nähe zwischen Blutgefäßen und neuronalem Gewebe bedingt sein könnte. Welche diese sind, auf welche Zelltypen diese limitiert sind und wie die verschiedenen Zelltypen von retinalem Gewebe miteinander interagieren, ist Gegenstand aktueller Forschung. Eines der am häufigsten verwendeten Tier-Modelle zur Untersuchung Ischämie-bedingter Veränderungen ist die Verödung episkleraler Venen nach Shareef *et al* [40], durch die eine intraokuläre Druckerhöhung an Mäusen oder Ratten und eine daraus resultierende Minimierung der okulären Perfusion induziert wird [41,42]. Auch wenn dieses Model dem klinischen Bild einer Glaukom-Erkrankung sehr nahekommt, da das Model durch einen progressiven Verlust von retinalen Ganglienzellen und eine Schädigung des Sehnervenkopfes gekennzeichnet ist, wurden bisher mit Hilfe von diesem Modell primär die Veränderungen auf Proteinebene in retinalem Gewebe nach einer Minderversorgung mit Sauerstoff untersucht. Das saure Gliafaserprotein (GFAP) und Annexin A2, die im Zusammenhang mit dem Prozess der Gliose von Astrozyten und Müllerzellen der Retina gebildet werden [43-45] sowie die Proteinfamilie der Kristalline sind hier signifikant verändert nachgewiesen worden [46,47].

In klinischen Zuständen, in denen kein sofortiger Visusverlust eintritt, spielt jedoch die Reperfusion eines minderversorgten Gewebes in der Pathogenese ischämischer Folgen eine bedeutende Rolle. Mehrere Studien konnten zeigen, dass die erneute Durchblutung des ischämischen Gewebes mit erhöhten Konzentrationen von reaktiven Sauerstoffverbindungen, erhöhtem Calcium-Einstrom sowie inflammatorischen Prozessen assoziiert ist [48,49]. Daher gibt es neben der irreversiblen Methode der episkleralen Venenverödung auch Tier-Modelle, die einen Reperfusions-Schaden nach ischämischen Phasen in die Evaluierung physiologischer Veränderungen mit einbeziehen [50,51]. In bisher verwendeten experimentellen Modellen wird hierzu für eine definierte Zeitspanne der intraokuläre Druck durch die Injektion einer Kochsalzlösung in die Vorderkammer erhöht [42,52]. Morphologische und elektrophysiologische Untersuchungen zeigten hier, dass Zellen aus der retinalen Ganglienzellschicht und der inneren Körnerschicht, die über retinale Arteriolen versorgt werden, sensitiver auf einen Ischämie-Reperfusions (I/R) Schaden reagieren als

Bipolarzellen, die von der äußeren Retinaschicht mit Nährstoffen und Sauerstoff über die Aderhaut versorgt werden. Auch in dieser Studie konnte eine Aktivierung von Gliazellen über die erhöhte Expression von GFAP, aber auch die Induktion einer Apoptose, eine Reduktion der inneren Netzhautschichtdicke und der Verlust von Ganglienzellen nach einem I/R-Schaden festgestellt werden. Neben umfangreichen heterogenen Erkenntnissen über die Rolle extravasaler retinaler Zellen in verschiedenen Spezies [53] und experimentellen Modellen gibt es kaum Erkenntnisse zu pathophysiologischen Veränderungen von retinalen Arteriolen nach einem I/R-Schaden. Die Bedeutung physiologischer Integrität von retinalen Gefäßen für neuronales Gewebe wurde bereits 1993 von Veriac *et al* an Kaninchen nachgewiesen [54]. In einem Model der intraokularen Druckerhöhung, die zur verminderten Funktionalität retinaler Strukturen führte, konnte eine Erhöhung der Bioverfügbarkeit von NO und der daraus resultierenden wiederhergestellten okulären Perfusion die elektrophysiologische Funktionalität der Retina wiederherstellen.

Aufgrund des geringen Durchmessers retinaler Arteriolen und deren Lokalisation im Augeninneren beschränken sich aktuelle Forschungsarbeiten auf nur wenige funktionelle Gefäßuntersuchungen im Zusammenhang mit systemischen Erkrankungen. Die Rolle einer endothelialen Dysfunktion von retinalen Arteriolen am Schweine-Modell nach einem ischämischen Schaden, ohne darauffolgende Reperfusion, wurde mittels Erhöhung des intraokulären Druckes erstmalig von Hein *et al* beschrieben [55]. Nach einer 90-minütigen Ischämie-Phase ist sowohl das endothelabhängige Vasodilatationsverhalten nach Stimulation mit Bradykinin signifikant reduziert gewesen als auch erhöhte Konzentrationen von Sauerstoffradikalen in der Gefäßwand detektiert worden. Betrachtet man die Tatsache, dass ein komplexes Netzwerk aus Gliazellen und Neuronen im direkten Kontakt mit retinalen Gefäßen steht, stellt die Methode der intraokularen Druckerhöhung, die wie bereits beschrieben in den meisten Fällen verwendet wird, eine limitierte Methode dar, um den rein ischämischen Einfluss auf okuläre Gefäße zu messen. Vergleichbar mit cerebralen Arteriolen wird die Regulation von retinalen Arteriolen über zahlreiche Metabolite sowie über neuronale Aktivitäten gesteuert. Die Freisetzung von vasoaktiven Substanden, wie NO, Epoxyeicosatriensäuren und Prostaglandinen durch benachbarte Zellen kann über die Aktivierung von glatten Muskelzellen oder

Perizyten eine Veränderung des Gefäßlumens auslösen [56]. Ebenso können inflammatorische Prozesse oder die Bildung von reaktiven Sauerstoffverbindungen aus umliegenden Zellen eine wichtige Rolle in der Pathogenese der retinalen Gefäßregulation spielen. Bei der Auswahl von geeigneten Modellen zur Induktion eines I/R-Schadens war vor allem die primär systemisch induzierte Sauerstoffmangelversorgung von großer Bedeutung, die im Rahmen dieser Arbeit zur Untersuchung vasoregulatorischer und pathophysiologischer Veränderungen von retinalen Arteriolen etabliert worden ist. Der Fokus dieser Arbeit liegt daher auf der Untersuchung von Veränderungen im Vasodilatations- und Vasokonstriktionsverhalten in drei klinisch relevanten Krankheitsmodellen, die daraus resultierenden Veränderungen des Redox-Haushaltes auf mRNA Ebene sowie der Identifikation von spezifisch veränderten Markern mittels immunohistochemischen Messungen in okulären Gefäßen.

4 Vorstellung der einzelnen Publikationen

4.1 Vorstellung von Publikation I

Zadeh JK, Ruemmler R, Hartmann EK, Ziebart A, Ludwig M, Patzak A, Xia N, Li H, Pfeiffer N, Gericke A; Responses of retinal arterioles and ciliary arteries in pigs with acute respiratory distress syndrome (ARDS). Exp. Eye Res. 2019 Jul; 184:152-161.

Bei einem akuten Lungenversagen handelt es sich um eine multifaktorielle Komplikation, die insbesondere durch einen erniedrigten Sauerstoffgehalt im arteriellen Blut gekennzeichnet und mit hohen Mortalitätsraten verbunden ist [57]. Sind bestimmten Bedingungen im Krankheitsbild erfüllt, so bezeichnet man diesen Lungenschaden im klinischen Alltag als ARDS (engl. acute respiratory distress syndrome). Neben der Tatsache, dass eine resultierende Hypoxämie in Verbindung mit pulmonalen Entzündungsmechanismen in vielen Fällen zu einem Multiorganversagen führen kann, liefern Untersuchungen zu Langzeitfolgen des ARDS Hinweise darauf, dass erkrankte Patienten mit Einschränkungen in ihrer kognitiven Leistungsfähigkeit leben müssen [58]. Wenige klinische Studien an

kleinen Populationen deuten auf eine eingeschränkte Vasodilatation im Bereich der Mikrozirkulation hin [59,60]. Vor diesem Hintergrund dient die vorliegende Studie dazu, zum ersten Mal die Auswirkungen eines ARDS auf retinale und choroidale Gefäße zu untersuchen und mögliche pathologische Veränderungen im retinalen System zu identifizieren [61].

Für die Diagnose eines ARDS müssen nach der Berlin-Definition vier Kriterien erfüllt sein: der akute Beginn oder die akute Exazerbation des Lungenversagens innerhalb einer Woche, ein positiver endexpiratorischer Druck $\geq$10 cm H_20, der Ausschluss eines kardial bedingten Lungenödems und die Präsenz bilateraler Verdichtungen, die mittels Computertomographie oder Röntgenthoraxaufnahmen bestätigt werden [62]. Studien aus den USA berichten über 745.000 betroffene Patienten jährlich [63]. Die Ätiologie des ARDS lässt sich in direkte (pulmonale, z.B. Pneumonie, Aspiration von Magensaft) und indirekte (extrapulmonale, z.B. Sepsis, Verbrennungen) Ursachen unterteilen, wobei das Hauptcharakteristikum in allen Fällen die Schädigung der Blut-Luft-Schranke sowie ein erniedrigter Quotient aus Sauerstoffpartialdruck im arteriellen Blut (PaO_2) und Sauerstoffanteil der Atemluft (FiO_2) ist. Die Schädigung der Blut-Luft-Barriere entsteht durch eine akute Inflammation, die einen gesunden Gasaustausch zwischen Luft und Blut und die Diffusion von O_2 und CO_2 verhindert. Abhängig von der Ursache der ARDS-Induktion geht die Schädigung der mikrovaskulären Integration mit einer Ausschüttung proinflammatorischer Zytokine einher. In diesem experimentellen Model, das in der ersten Publikation näher beschrieben wird, bekamen die Tiere nach einer endotrachealen Intubation eine einmalige intratracheale Injektion einer Lipopolysaccharid (LPS)-haltigen Lösung. Das Endotoxin, das aus Gram-negativen Bakterien stammt, löst eine Entzündungsreaktion des Lungengewebes aus, das in einer weiteren Signalkaskade zu einer eingeschränkten Funktion des Surfactants auf der Alveolenoberfläche führt. Die Induktion eines moderaten ARDS durch die Applikation von LPS ist ein etabliertes Verfahren, das in einer Hypoxämie resultiert und das gleichzeitig alle oben beschriebenen Kriterien umfasst [64-66]. Die Reaktion des Schweines auf LPS wurde anhand von drei Parametern beurteilt: Verhältnis von intraarteriellem Sauerstoffpartialdruck und inspiratorischem Sauerstoffanteil (PaO2/FiO2), mittlerem pulmonalem arteriellem Druck (MPAP) und der Herzfrequenz. Während des 8-stündigen Experiments wurde eine volumengesteuerte Beatmung durchgeführt und die Tiere nach der

Verabreichung der LPS-Lösung oder einer Kontroll-Lösung intensivmedizinisch überwacht, bevor nach einer Enukleation der Augen retinale und ziliare Blutgefäße für weitere Untersuchungen isoliert wurden.
In dieser veröffentlichen Arbeit wurden erstmalig die endothelabhängige und die endothelunabhängige Gefäßreaktivität sowie pathologische Veränderungen auf mRNA- und Protein-Ebene in beiden Blutversorgungssystemen der Retina nach einem systemisch-ischämischen Zustand untersucht [61].
Die Ergebnisse dieser Studie weisen darauf hin, dass retinale Arteriolen eine verminderte Ansprechbarkeit auf die NO-vermittelte Vasodilatation mit Bradykinin zeigen, während es keine Unterschiede in der Vasodilatation mit Natriumnitroprussid zwischen der Kontroll- und ARDS-Gruppe in beiden Gefäßsystemen gab. Neben dieser beobachteten endothelialen Dysfunktion von retinalen Arteriolen beobachteten wir mittels Echtzeit-PCR die Hochregulation von spezifischen Markern: HIF-1α, VEGF-A, NOX2, was durch immunohistochemische Färbungen vor allem in der Endothelzellschicht retinaler Arteriolen bestätigt werden konnte. Untersuchungen zum oxidativen Stress mittels DHE-Färbung in beiden Gefäßsystemen weisen auf ein erhöhtes Level an reaktiven Sauerstoffverbindungen in retinalen Arteriolen hin, was im Einklang mit einer erhöhten Expression der prooxidativen NOX2-Einheit steht. Bei der Analyse bestimmter inflammatorischer Marker und weiterer prooxidativer und antioxidativer Enzyme haben wir weder signifikante Unterschiede im retinalen Gefäßbett noch in Ziliargefäßen gefunden. Hierfür untersuchten wir neben NOX2 ebenso zwei weitere Formen der NADPH-Oxidasen, NOX1 und NOX4 sowie die Xanthinoxidase und die induzierbare NO-Synthase. Während sich die prooxidative Wirkung der NOX1 und die Xanthinoxidase in der Produktion von Superoxidanionen widerspiegelt, generiert NOX4 Wasserstoffperoxid, welches über metallionenkatalysierte Prozesse ebenso Radikale entstehen lässt. Die induzierbare NOS hingegen führt aufgrund einer übermäßig hohen Produktion von NO über die Reaktion mit bestehenden Superoxidanionen zur Bildung von Peroxynitritanionen, die durch den Abbau bestimmter Cofaktoren in einer Entkopplung der NO-Synthase und zur Generation von Superoxidanionen resultieren. Um die antioxidative Kapazität retinaler Arteriolen in diesem Modell zu bestimmen, wurden die Expressionslevel der Katalase, Hämoxygenase 1, Glutathionperoxidase und aller drei Isoformen der Superoxiddismutase (SOD1-

SOD3) bestimmt. Letzteres entfaltet antioxidative Eigenschaften über das Abfangen gebildeter Sauerstoffradikale, die zu Sauerstoff und Wasserstoffperoxid umgewandelt werden, während die Katalase und die Glutathionperoxidase gebildete Peroxide in Sauerstoff und Wasser umwandelt. Obwohl die Aufgabe von Hämoxygenase darin besteht, den Abbau von Häm in Eisen, Biliverdin und Kohlenstoffmonoxid zu katalysieren, konnte in retinalen Untersuchungen gezeigt werden, dass ihre erhöhte Expression nach einem ischämischen Schaden und erhöhtem oxidativen Stress mit der Wiederherstellung retinaler Funktionen verbunden ist [67].
Auch wenn eine kompensatorische Hochregulation von antioxidativen Enzymen auf die vermehrte Produktion von oxidativem Stress in vielen Gewebetypen und Spezies gezeigt werden konnte, scheint solch eine protektive Rolle in retinalen Arteriolen des Schweines mit ARDS in diesem Modell nicht vorhanden zu sein.

Bedingt durch das enge Netzwerk von Arteriolen und neuronalen Zellen innerhalb der Retina war es von großem Interesse extravasale Effekte eines ARDS in der Retina zu untersuchen. Dabei war in histologischen Färbungen eine Schwellung der Nervenfaserschicht, die sich aus den Axonen retinaler Ganglienzellen zusammensetzt, zu sehen.
Als pathologische Quelle dieser ARDS-induzierten Veränderungen sind in dieser Arbeit sowohl verminderte Sauerstoffpartialdrücke sowie auch die im Blut zirkulierenden Zytokine TNF-α und IL-6 in der ARDS-Gruppe zu nennen, auf die eine erhöhte Expression der spezifisch hochregulierten Marker HIF-1α, VEGF-A und NOX2 in retinalen Arteriolen zurückzuführen sein könnte. So konnte man in einem Maus-Modell Assoziationen zwischen einer intravenösen TNF-α Injektion und strukturellen sowie funktionellen Veränderungen retinaler Arteriolen feststellen [68].
Publikation I konnte daher anhand einer ARDS-Erkrankung die bedeutende Beteiligung der retinalen Blutversorgung und neuronaler Strukturen unter hypoxämischen und inflammatorischen Bedingungen an einem *in vivo* Modell zeigen (siehe Abbildung 1).

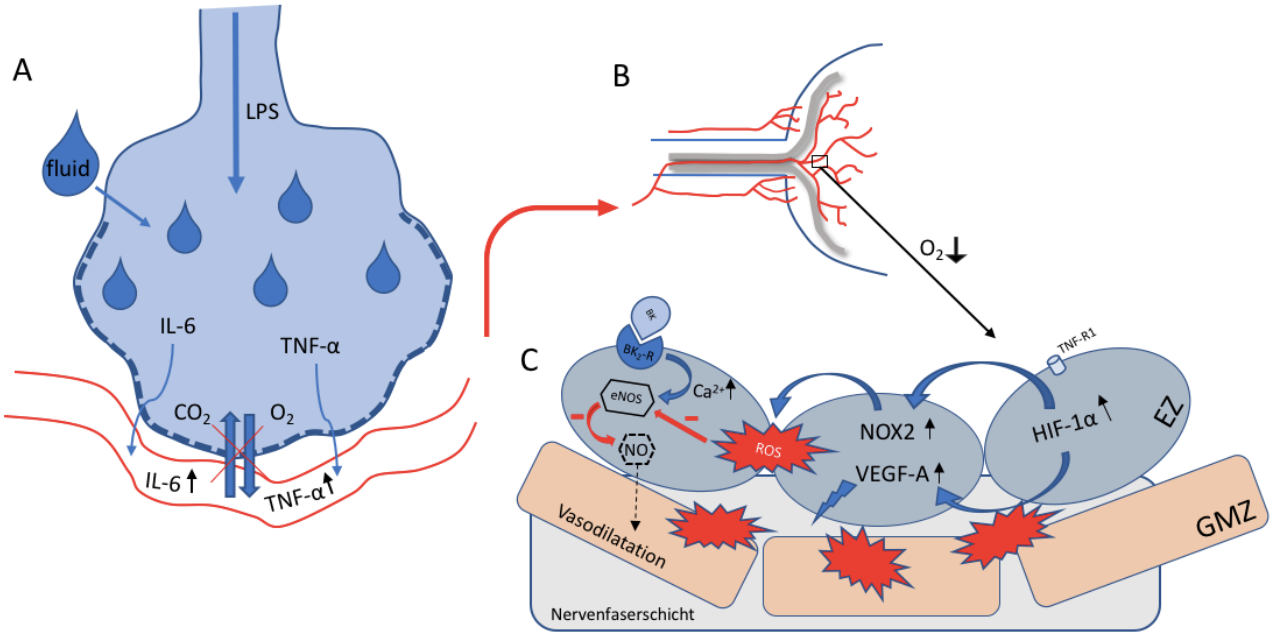

Abbildung 1 – Schematische Darstellung einer ARDS-Erkrankung und ihren Auswirkungen auf retinale Gefäßendothelzellen. **A** Die intratracheale Applikation einer LPS-haltigen Lösung resultiert in einer alveolaren Schädigung und einer Störung der mikrovaskulären Integrität. Die Inaktivierung von Surfactant geht mit einem Einströmen alveolarer Flüssigkeiten und der Aktivierung von neutrophilen Granulozyten einher. Proinflammatorische Prozesse, wie die Ausschüttung von Zytokinen aus alveolaren Makrophagen und der reduzierte Sauerstoffgehalt im Blut führen zu pathophysiologischen Prozessen in der Mikrozirkulation. **B** Darstellung der retinalen Blutversorgung, die sich aus Ziliararterien und retinalen Arteriolen zusammensetzt. **C** Übersicht zellulärer Veränderungen in retinalen Arteriolen, die mit einer verringerten Ansprechbarkeit auf den endothelabhängigen Vasodilatator Bradykinin (BK) einhergehen. EZ=Endothelzelle, GMZ=Glatte Muskelzelle, BK_2-R=Bradykinin-Rezeptor

4.2 Vorstellung von Publikation II

Zadeh JK, Garcia-Bardon A, Hartmann EK, Patzak A, Ludwig M, Xia N, Li H, Pfeiffer N, Gericke A. Short-time ocular ischemia induces vascular endothelial dysfunction and ganglion cell loss in the pig retina. Int J Mol Sci 2019 Sep;20(19).

Während Publikation I ischämisch- aber auch inflammatorisch bedingte Folgen für die retinale Blutversorgung nach einer ARDS-Erkrankung behandelte, geht es in Publikation II um pathologische Veränderungen, die auf rein ischämischen Prozessen basieren [69]. Bisherige Studien konnten zeigen, dass eine Mangelversorgung von retinaler Strukturen mit Sauerstoff mit visusschädigenden Folgen einhergeht und zu Mikroaneurysmen, Neovaskularisationen oder Einblutungen in den Glaskörper führen können. So stellt ein Ischämie-Reperfusionsschaden eine Ursache vieler retinaler Dysfunktionen dar. Obwohl bisherige Studien pathologische Veränderungen in der Retina festhalten und in Verbindung mit Ischämien bringen konnten, gibt es keine Untersuchungen, die auf die endothelabhängige und endothelunabhängige Gefäßreaktivität retinaler Arteriolen und die zugrundeliegenden Mechanismen bereits nach kürzester Zeit einer Ischämie eingehen. Daher wird in Publikation II die Fragestellung bearbeitet, welche Gefäßschichten der retinalen Blutversorgung und welche retinale Strukturen unter ischämischen Zuständen pathologische Veränderungen aufweisen und welche Signalmechanismen diesen Veränderungen zugrunde liegen könnten.

Im zweiten Krankheitsmodell wurden die zum Gehirn führenden Arterien mechanisch abgeklemmt, wodurch auch in retinalen Strukturen eine Mangelversorgung mit Sauerstoff induziert wurde [69]. So wie bei allen etablierten Modellen bestehen zu den bereits existierenden Modellen Vorteile, aber auch Nachteile. Um frühzeitig einsetzende rein vaskuläre Veränderungen in der retinalen Blutversorgung untersuchen zu können, war es nötig, ein Modell zu etablieren, dass nicht von anderen Parametern am okulären System beeinflusst wird, wie es bisher der Fall war. Zum Beispiel wird oft die Technik einer intraokulären Druckerhöhung mittels Applikation einer Salzlösung in die Vorderkammer des Auges verwendet. So praktikabel diese Methodik scheint, könnten für die Untersuchung vaskulärer Veränderungen jedoch auch

mechanische Einflüsse eine Rolle spielen, die durch die Verletzung von neuronalen Zellen komplexe pathologische Mechanismen auslösen könnten. Demnach wurde im Rahmen dieser Publikation zum ersten Mal die Okklusion zentraler Gefäße etabliert, welche für die Blutversorgung der Retina essenziell sind. Zahlreiche retinale Erkrankungen haben ihren Ursprung nicht nur in einem kontinuierlichen Zustand einer Sauerstoffmangelversorgung, sondern auch in einer transienten ischämischen Phase, die gefolgt ist von einer Reperfusion des ischämischen Gewebes [70,71]. So konnten wir hier nicht nur die zeitlich begrenzte Hypoperfusion der Retina untersuchen, sondern ebenso den mit einer Wiederherstellung des Blutflusses verbundenen Schaden, wie es klinisch betrachtet auch bei behandelten Zentralarterienverschlüssen oder Embolien der Fall ist.

Die Klemmung der Arteria innominata, von der die rechte und linke Halsschlagader und die rechte Arteria subclavia entspringen sowie die Klemmung der linken Arteria subclavia ermöglichte eine vollständige Blockade der okulären Blutversorgung. Bestätigt wurde die effektive Klemmung und die resultierende zerebrale Ischämie mit Hilfe intensivmedizinischer Parameter, wie der Beobachtung der regionalen Sauerstoffsättigung im Gehirn, der Erhöhung von Blutdruck und Herzfrequenz sowie durch erweiterte nicht reaktive Pupillen. Nach 12 Minuten wurde die Klemmung gelöst und der Blutfluss wiederhergestellt. Nach einer anfänglichen Stabilisierung wurden die Schweine hämodynamisch überwacht und die Normwerte für die nächsten 20 Stunden aufrechterhalten. Der operative Einfluss auf darauffolgende Ergebnisse wurde durch eine Scheinoperation auch an Kontrolltieren durchgeführt. In dieser Gruppe wurden, abgesehen vom Verschluss der Arterien, die gleichen chirurgischen und intensivmedizinischen Eingriffe wie in der abgeklemmten Gruppe durchgeführt.

Nachdem wir im Rahmen der ersten Publikation höhere Resistenzeigenschaften des zilliaren Gefäßbettes auf ischämische und inflammatorische Zustände bestätigen konnten [61], sollten für Publikation II und III das retinale Blutversorgungssystem im Fokus stehen. Die *in vitro* Messungen des endothelabhängigen und endothelunabhängigen Vasoregulationsverhaltens von retinalen Arteriolen nach Beendigung der Versuchsreihe zeigten eine endotheliale Dysfunktion, die sich durch eine

verminderte Ansprechbarkeit auf Bradykinin äußerte. Bei der Untersuchung zugrundeliegender Mechanismen beobachteten wir auch in diesem Modell die vermehrte Expression der Hypoxiemarker HIF-1α, VEGF-A, aber auch der prooxidativen Gene für NOX2 und induzierbare NOS (iNOS). Auf Proteinebene konnte man die Expression dieser vier Marker vorwiegend im retinalen Endothel beobachten. Die Aktivierung von iNOS, wie sie in bisherigen Studien unter ischämischen Bedingungen in der Retina beobachtet worden ist [60], löst die Produktion von drastisch hoher NO-Konzentrationen aus, die über die Bildung von Peroxynitrit eine Dysfunktion der eNOS und oxidativen Stress auslösen kann [72,73]. Im Einklang mit hochregulierten Markern sind mittels DHE-Färbung eine signifikant höhere Fluoreszenz in ischämischen Arteriolen der Retina detektiert worden als in der scheinoperierten Gruppe. Um auch in diesem Modell, das eine endotheliale Dysfunktion verursacht hat, die neuronale Beteiligung an pathologischen Prozessen zu untersuchen sind sowohl histologische Färbungen als auch Immunofluoreszenz Färbungen durchgeführt worden. Dabei weisen die Ergebnisse auf eine verminderte Anzahl von retinalen Ganglienzellen und auf einen Verlust der vaskulären Integrität hin, die durch ödematöse Einlagerungen in der retinalen Nervenfaserschicht gekennzeichnet sind.

Damit wurde im Rahmen von Publikation II ein Modell etabliert, das frühzeitig aktivierte Mechanismen und Signalwege als Antwort auf einen ischämischen Schaden aufdeckt. Bereits nach einer 12-minütigen Ischämie ist dieser Schaden gekennzeichnet durch die Entwicklung einer endothelialen Dysfunktion, erhöhten oxidativen Stress und erhöhte Expressionen von HIF-1α, VEGF-A, NOX2 und iNOS. Der Verlust von retinalen Ganglienzellen deutet auf eine neuronale Beteiligung hin. In Abbildung 2 sind die in dieser Publikation beobachteten Ergebnisse zusammenfassend dargestellt.

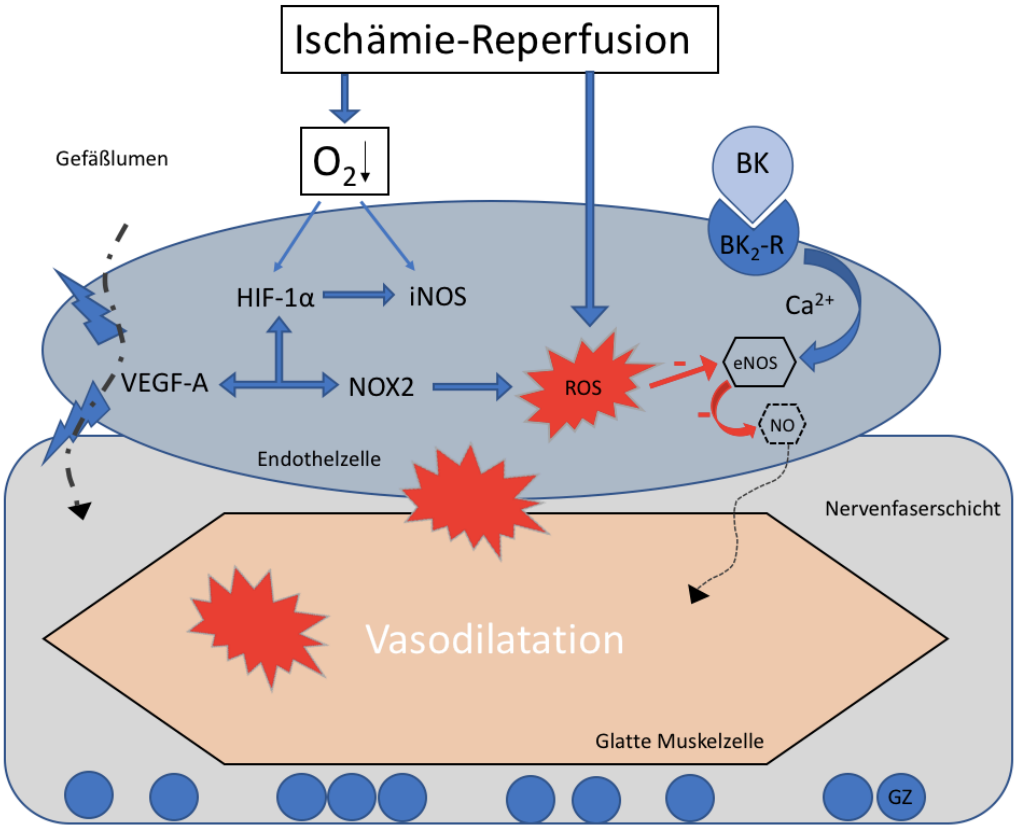

Abbildung 2 – Darstellung veränderter Signalwege nach der Induktion eines Ischämie-Reperfusionsschadens mit möglichen Hinweisen auf Interaktionen. Eine temporäre Sauerstoffmangelversorgung und eine Reperfusionsphase von retinalen Arteriolen resultierte in einer erhöhten Expression von hypoxischen und prooxidativen Markern in der Endothelzellschicht, die zu einer Störung der vaskulären Integrität und zu einer erhöhten Produktion von reaktiven Sauerstoffverbindungen führten. Auch in diesem Model ist eine endotheliale Dysfunktion zu beobachten, die durch eine reduzierte endothelabhängige Vasodilatation nach Stimulation mit Bradykinin gemessen wurde. GZ=Ganglienzelle.

4.3 Vorstellung von Publikation III

Zadeh JK, Zhutdieva MB, Laspas P, Yuksel C, Musayeva A, Pfeiffer N, Brochhausen C, Oelze M, Daiber A, Xia N, Li H, Gericke A. *Apolipoprotein E Deficiency Causes Endothelial Dysfunction in the Mouse Retina*. Oxidative Medicine and Cellular Longevity, 2019.

Eines der größten Risikofaktoren für die Entwicklung einer koronaren Herzkrankheit stellt die Hypercholesterinämie dar. Bedingt durch oxidative Veränderungen von zirkulierenden Lipoproteinen und Phospholipiden sowie inflammatorische Prozesse in den Blutgefäßen kann die Hypercholesterinämie zu arteriosklerotischen Ablagerungen in der Gefäßwand führen. Eine erst kürzlich veröffentlichte Metaanalyse konnte eine klare Verbindung zwischen erhöhten Blutfettwerten und dem Glaukom aufzeigen, die die zweithäufigste Erblindungsursache weltweit darstellt [74]. Das Glaukom ist gekennzeichnet durch den Verlust retinaler Ganglienzellen und deren Axone, was mit einem Gesichtsfeldverlust einhergeht. Neben der Tatsache, dass die Ursachen und auch die Pathogenese eines Glaukoms bis heute unverstanden sind, gehören okuläre Perfusionsstörungen und eine endotheliale Dysfunktion zu den am häufigsten diskutierten Hypothesen bei der Pathophysiologie des Glaukoms. Obwohl es ebenso Studien gibt, die einen Zusammenhang zwischen der Ätiologie okklusiver Retinaerkrankungen oder eingeschränktem Vasodilatationsverhalten retinaler Arteriolen und einer Fettstoffwechselstörung nachweisen [7,75-79], ist bis heute unbekannt, über welchen Mechanismen erhöhte Cholesterinwerte zu Veränderungen in der retinalen Blutversorgung führen, und ob diese Veränderungen mit einem Glaukom einhergehen könnten. Damit bearbeitet Publikation III erstmalig die Fragestellung, ob ein erhöhter Cholesterinspiegel zu einer endothelialen Dysregulation retinaler Arteriolen führt, welche Mechanismen in der retinalen Blutversorgung aktiviert werden und ob ein Verlust retinaler Ganglienzellen zu beobachten ist, der charakteristisch für das Glaukom sein würde [80]. Da retinale Arteriolen der Maus einen Innendurchmesser von weniger als 30 μm aufweisen, ist die Methode zur Darstellung des Arteriolendurchmessers eine aufwendige aber einzigartige Methode, die den Ergebnissen einen besonderen Stellenwert gibt.

Für die Induktion von erhöhten Cholesterinwerten im Blut wurden in der dritten Veröffentlichung genetisch modifizierte Mäuse verwendet, denen das Apolipoprotein E (ApoE) fehlt. Da Lipide, wie Cholesterin, Cholesterinester und Triacylglycerine hydrophobe Eigenschaften aufweisen, ist die Bildung von Komplexen mit ApoE (Lipoproteine) für den Abtransport aus dem Blut notwendig. Somit ermöglicht ApoE als Strukturprotein in der Phospholipidmembran von Lipoproteinen die Versorgung peripherer Organe mit Lipiden über das Blut. Durch eine gestörte Aufnahme von Lipoproteinen und Chylomikronen aus dem Plasma entstehen erhöhte LDL- und Cholesterin-Werte, dessen Auswirkungen auf die retinale Blutversorgung in dieser Arbeit untersucht werden. Das Knockout-Modell des ApoE-Gens (ApoE -/-) stellt ein etabliertes Verfahren dar, um *in vivo* Untersuchungen über zugrunde liegende Mechanismen der Hypercholesterinämie durchzuführen [81,82]. Obwohl die Pathophysiologie der Hypercholesterinämie ein multifaktorielles Geschehen darstellt, bilden oxidative Veränderungen an Lipoproteinen einen wichtigen Grundbaustein für das klinische Krankheitsbild von atherosklerotischen Plaques. Oxidativ modifizierte Lipoproteine niederer Dichte (engl. oxidized low density lipoproteins, ox-LDL), die durch ein Ungleichgewicht von reaktiven Sauerstoffverbindungen auf der einen Seite und antioxidativen Enzymen auf der anderen Seite durch eine schädigende Oxidation entstehen, werden in Endothelzellen aufgenommen, wo sie sich in Schaumzellen umwandeln. Diese Aufnahme wird über einen endothelialen Lectin-like oxLDL-Rezeptor (LOX-1) vermittelt, den wir erstmalig an retinalen Arteriolen an der Maus im Rahmen dieser Publikation immunohistochemisch nachweisen konnten. Studien zeigen, dass die Aktivierung von LOX-1 durch ox-LDL zu erhöhtem oxidativem Stress, zur Steigerung der Leukozytenadhäsion und zu einer endothelialen Dysfunktion führen können. Übereinstimmend mit diesen Ergebnissen beobachteten wir eine verminderte Reaktionsfähigkeit retinaler Arteriolen auf den endothelabhängigen Vasodilatator Acetylcholin und eine erhöhte DHE-Fluoreszenzintensität in der ApoE-defizienten Gruppe [80]. Diese Ergebnisse stehen im Einklang mit Forschungsarbeiten an Koronararterien und cerebralen Arterien, die ebenso ein vermindertes endotheliales Vasodilatationsvermögen aufwiesen, was mit einer verringerten Bioverfügbarkeit von NO und einem erhöhten Level an reaktiven Sauerstoffverbindungen einherging [83-85].

An humanem Gewebe konnten mittels Flickerlicht Veränderungen der Gefäßreaktivität aufgezeigt werden. Diese könnten darauf hindeuten, dass pathogene Prozesse im Rahmen der Hypercholesterinämie auf eine Dysfunktion der Endothelzellschicht zurückzuführen sein könnten [86]. Jedoch ist unklar, ob durch Flickerlicht die reine Funktion des Endothels untersucht wird oder ob hierbei nicht auch neuronale Prozesse involviert sind. Die erhöhten Cholesterinwerte lösten vielfältig erhöhte Expressionslevel verschiedenster Inflammations-, Hypoxie- und Redox-Marker aus, die wir auch in dieser Studie mittels Echtzeit-PCR detektierten. Darunter fallen die induzierbare und neuronale NO-Synthase, HIF-1α, VEGF-A, NOX1, NOX2 und bedeutsame antioxidativ wirkende Enzyme wie die Catalase, Glutathion-Peroxidase, Hämoxygenase und die drei Enzymklassen der Superoxiddismutase (SOD1, SOD2, SOD3), was vermutlich mit einer kompensatorischen Reaktion auf pathologische Veränderungen begründet werden kann. Basierend auf einer Studie, die die vaskuläre Dysregulation cerebraler Gefäße in einem ApoE-/- Modell untersucht, ist die Quelle von erhöhten Konzentrationen von Sauerstoffverbindungen der erhöhten Expression von NOX2 zugesprochen worden, dessen Expression auf Proteinebene auch in dieser Studie in retinalen Arteriolen bestätigt werden konnte, wohingegen eine erhöhte NOX1-Expression mittels Immunofluoreszenz Färbung in retinalen Arteriolen nicht sichtbar war. Der Hochregulation von antioxidativen Enzymen als Protektion vor schädigenden Mechanismen, wie der Lipidperoxidation könnte eine wichtige Rolle in der neuronalen Beteiligung zukommen. Diese wurde mittels Quantifizierung retinaler Ganglienzellen und deren Axonen ermittelt, wobei im Vergleich zu beiden vorangegangen Publikationen in diesem Modell keine Unterschiede in der gesunden und kranken Gruppe festzustellen waren. Die in dieser Arbeit diskutieren Ergebnisse sind in Abbildung 3 dargestellt und werden von einer Reihe von Untersuchungen bestätigt. Auch wenn funktionelle Störungen in klinischen, aber auch in tierexperimentellen Studien nachgewiesen werden konnte, ist eine ApoE Defizienz bisher nicht mit strukturellen Veränderungen neuronaler Strukturen in der Retina beobachtet worden [87,88].

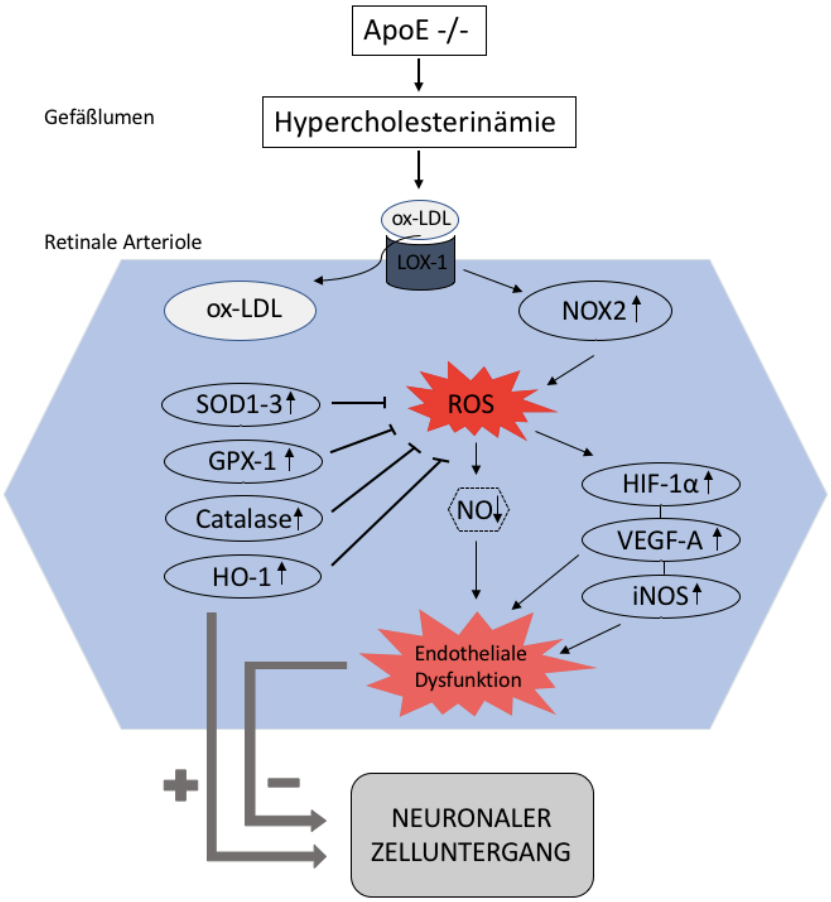

Abbildung 3 – Übersicht zellulärer Veränderungen in retinalen Arteriolen der Maus, deren Expression durch die Induktion einer Hypercholesterinämie erhöht worden sind. Im Zusammenhang mit der Detektion von LOX-1- Rezeptoren in retinalen Arteriolen, die die Aufnahme von prooxidativ veränderten Lipiden in die Endothelzelle ermöglichen, ist ebenso eine erhöhte Expression von Hypoxie-Markern, prooxidativen- und antioxidativen Enzymen induziert worden. Die Aufrechterhaltung der neuronalen Integrität von retinalem Gewebe könnte auf eine kompensatorische und protektive Wirkung der antioxidativen Enzyme zurückgeführt werden (+).

5 Diskussion (aller Publikationen)

Das Ziel dieser Forschungsarbeit war, die pathophysiologischen Veränderungen in retinalen Arteriolen nach an drei etablierten Krankheitsmodellen zu identifizieren sowie endotheliale Dilatationsmechanismen zu untersuchen, aus denen neue mögliche Therapieoptionen für die Behandlung der vaskulären Dysfunktion im retinalen Gefäßbett abgeleitet werden könnten.

Die in allen Publikationen etablierten Tiermodelle am Schwein und an der Maus konnten eine entscheidende Perfusionsstörung der Retina abbilden, die sich in einer endothelialen Dysfunktion von retinalen Arteriolen widerspiegelt. Diese physiologische Veränderung ermöglichte es spezifische Veränderungen auf mRNA- und Proteinebene zu analysieren, Veränderungen im ROS-Haushalt zu identifizieren sowie die neuronale Beteiligung in Abhängigkeit von diesen Parametern zu bestimmen. Eine übergeordnete Rolle ließ sich dabei in allen Publikationen den Hypoxie-Markern HIF-1α, VEGF-A und NOX2 (als einem Vertreter der NADPH-Oxidasen, die mit oxidativem Stress assoziiert sind) zuschreiben. Diese erhöhten Expressionen schienen in allen drei Publikationen mit erhöhten Konzentrationen von reaktiven Sauerstoffverbindungen assoziiert zu sein. Im Hinblick auf Untersuchungen zu neuronalen Effekten konnten wir in den drei etablierten Modellen Unterschiede feststellen. Diese beinhalteten strukturelle Veränderungen in Publikation I und II, welche anhand histologischer Färbungen detektiert worden sind. Im Rahmen der zweiten Publikation war es möglich, die Dichte der retinalen Ganglienzellen zu bestimmen, die als Folge eines Ischämie-Reperfusionsschadens signifikant niedriger war als in der Kontrollgruppe. Antioxidative Enzymklassen waren in diesen beiden Kontrollgruppen nicht kompensatorisch hochreguliert laut Echtzeit-PCR Analysen. Im Gegensatz dazu zeigte das ApoE-Modell in Publikation III, dass protektiv hochregulierte antioxidative Enzyme mit dem Erhalt der neuronalen Integrität, gemessen an der Anzahl retinaler Ganglienzellen und deren Axonen einhergehen. Zu den bereits existierenden Kenntnissen im Bereich der retinalen Beeinträchtigung im Zusammenhang mit systemischen Erkrankungen stellen diese gewonnenen Daten eine Erweiterung der Grundlagenkenntnisse auf physiologischer und molekularer Ebene dar.

In zwei der drei Veröffentlichungen wurde das Hausschwein (*sus scrofa domesticus*) als tierexperimentelles Modell gewählt, da es elementare ophthalmologische Charakteristika mitbringt, die mit dem menschlichen Auge vergleichbar sind. Eine Vielzahl von Studien berichtet über hohe Analogien zwischen der menschlichen Netzhaut und der von Schweinen [89,90] hinsichtlich Vaskularisierung, Anatomie und Fotorezeptorenverteilung. Eine weitere Studie beschreibt die Morphologie retinaler Ganglienzellen und stellt nach Untersuchungen der neuronalen Pathogenese einer Glaukomerkrankung vergleichbare Ergebnisse zwischen Mensch und Schwein fest [91]. Somit ermöglicht die Wahl des Schweines als Tier-Modell den Ansatz einer Translation auf das Krankheitsbild des Menschen und bietet eine solide Grundlage für die ophthalmologische Forschung, um ein besseres Verständnis von retinalen Erkrankungen zu gewinnen und neue Therapieansätze zu finden. Die Entnahme von menschlichem Retinagewebe, vor allem im Rahmen dieser spezifischen Krankheitsbilder, ist unter praktischen Bedingungen nahezu unmöglich, und in seltenen Fällen nur *post mortem* durchführbar, wobei auch hier mögliche weitere Veränderungen aufgrund der fortschreitenden Zeit bis zur Isolierung des Gewebes einen großen Einfluss auf die daraus gewonnene Erkenntnisse hätte.

Betrachtet man die Ergebnisse der in dieser Arbeit diskutierten Veröffentlichungen legen alle Erkenntnisse eine verminderte Bioverfügbarkeit von NO in retinalen Arteriolen, gekennzeichnet durch eine verminderte Reaktion auf endothel-abhängigen Vasodilatatoren, nahe [61,69,80]. In der hier vorgestellten ersten Publikation war es von großem Interesse, ischämische und inflammatorische Auswirkungen auf beide Blutversorgungssysteme der Retina zu untersuchen. Messungen des Sauerstoffpartialdruckes im arteriellen Blut nach Induktion des Lungenschadens konnten Rückschlüsse darauf geben, dass die Retina mit weniger Sauerstoff versorgt wird als in der Kontrollgruppe [61]. Die darauffolgenden funktionellen und pathophysiologischen Ergebnisse deuteten auf höhere Resistenzeigenschaften des ziliaren Gefäßbettes im Vergleich zu retinalen Arteriolen hin. Bisherige Studien bestätigen, dass ziliare Gefäße, die die Retina über die Aderhaut versorgen über parasympathische und sympathische Nervenfasern gesteuert werden. Eine Aktivierung des Parasympathikus hat sich als vasodilatierend und die Aktivierung des

Sympathikus als vasokonstriktiv erwiesen [20]. Einhergehend mit dieser protektiven Eigenschaft zur Aufrechterhaltung der Vasoregulation fanden wir in Hinsicht auf die Produktion von Hypoxiemarkern, trotz erniedrigten Sauerstoffpartialdrücken im ARDS-Model, in zilliaren Gefäßen keine reduzierte Gefäßansprechbarkeit. Während retinale Arteriolen eine erhöhte Expression von HIF-1α, VEGF-A und NOX2 auf mRNA- und Proteinebene zeigten, beobachteten wir keine Unterschiede zwischen ziliaren Gefäßen der LPS- und Kontrollgruppe. Wie in der ersten Publikation, beobachteten wir auch in der zweiten und dritten Publikation die Veränderung dieser spezifischen Marker in retinalen Arteriolen. Der Sauerstoffmangel in Publikation II wurde durch die Messung der zerebralen Sauerstoffsättigung bestätigt, die im Vergleich zur Kontrollgruppe während der Klemmphase stark herrunterreguliert war [69]. Analog zur ersten Publikation blieb der mittlere arterielle Blutdruck, abgesehen von der Klemmphase, über die Dauer des Experimentes konstant aufrecht. Auch in diesem zweiten Modell, das durch eine vollständige Okklusion der zerebralen Gefäße gekennzeichnet ist, gefolgt von einer Reperfusions-Phase von 20 Stunden, beobachteten wir den Anstieg von HIF-1α, VEGF-A und NOX2 auf mRNA- und Protein- Ebene im Endothel der retinalen Arteriolen. Die in Publikation III verursachte endotheliale Dysfunktion, verursacht durch die vaskuläre Pathogenese einer Hypercholesterinämie, löst eine Perfusionsstörung und Hypoxie von retinalem Gewebe aus, was sich erstaunlicherweise ebenso in einer Hochregulation von HIF-1α, VEGF-A und NOX2 in retinalen Gefäßen bemerkbar macht [80]. In allen Publikationen wurden erhöhte Level reaktiver Sauerstoffverbindungen in der Gefäßwand nachgewiesen, die bereits in einer Vielzahl von Studien im Zusammenhang mit erhöhten Expressionen von NOX2 und pathologischen Veränderungen beschrieben worden sind [92-94]. Als Transmembranproteine gehört der Transport von Elektronen über die Membran zu den Hauptaufgaben der NOX-Familie. Für diesen Prozess werden durch die Reduktion von Sauerstoff reaktive Sauerstoffspezies, insbesondere das Superoxidanion O_2^-, produziert, das in der Pathophysiologie verschiedenster vaskulärer Erkrankungen involviert ist. Im basalen, gesunden Zustand weisen NOX-Enzyme eine geringe Aktivität auf, können jedoch durch pathologische Zustände aktiviert werden, indem eine

Translokation der zytosolischen Komponenten induziert wird und eine Erhöhung der katalytischen Aktivität erfolgt [95,96]. Diese Beobachtung der erhöhten NOX2-Expression steht in Einklang mit der Detektion erhöhter Konzentrationen reaktiver Sauerstoffverbindungen mittels DHE-Färbung in allen drei Publikationen. Eine Vielzahl von Studien berichtete über die essenzielle Rolle von ROS bei der Entstehung neurodegenerativer Erkrankungen der Retina, wie z.B. im Rahmen des Glaukoms, der diabetischen Retinopathie und der altersbedingten Makuladegeneration [97], was die Ergebnisse aus Publikationen II, wo ein erhöhtes Expressionsniveau dieser Marker zugleich mit einem Untergang von retinalen Ganglienzellen assoziiert ist, bestätigt. Die Hochregulation antioxidativer Mechanismen, die wir im Rahmen der dritten Publikation beobachtet haben, insbesondere Catalase, Glutathion-Peroxidase (GPx-1), Hämoxygenase (HO-1) sowie die drei Subtypen der Superoxiddismutasen (SOD 1-3) könnten in diesem Zusammenhang protektive Eigenschaften auf den neuronalen Zelluntergang gehabt haben, da trotz einer endothelialen Dysfunktion und der hochregulierten Marker keine Unterschiede in der retinalen Ganglienzellzahl im ApoE-Model festzustellen waren. Dieser Hypothese folgend konnten unsere Ergebnisse durch Masuda *et al* bestätigt werden, die die Effekte einer antioxidativen Therapie durch den Einsatz eines Radikalfängers auf neurodegenerativen Erkrankungen der Retina untersucht haben. Nicht nur der Untergang an retinalen Ganglienzellen konnte hierdurch inhibiert werden, sondern auch apoptotische Zellprozesse und oxidative Schäden der DNA und Lipide, die auf erhöhten oxidativen Stress zurückzuführen sind, wurden herrunterreguliert [98]. Im Kontext mit ischämischen Zuständen ist die Synthese des proangiogenen Wachstumsfaktors VEGF-A sowie der direkte Zusammenhang zum Transkriptionsfaktor HIF-1α, der dessen Expression mit dem Ziel der Wiederherstellung der Sauerstoffversorgung in ischämischen Geweben steuert, bereits vielfach beschrieben worden [99]. Zwar bewirkt die VEGF-Expression die Ausbildung neuer Blutgefäße und eine Proliferation von retinalen Endothelzellen [100], doch ist sie bedingt durch die erhöhte Permeabilität der Gefäße mit pathologischen Zuständen in der Retina verbunden. Aus diesem Grund hat sich die Blockade der VEGF-Aktivität zum Therapiestandard retinaler Erkrankungen entwickelt, mit dem Ziel, die Progression des Krankheitsbildes zu

minimieren. Neben der Tatsache, dass HIF-1α die Expression von VEGF-A induzieren kann, gibt es Studien, die eine direkte Korrelation zwischen NOX2 und VEGF-A, sowie NOX2 und HIF-1α mit Hilfe eines Knockout-Modells an der Maus nachgewiesen haben. Hier war die mRNA-Expression von VEGF-A in der Retina und die damit verbundene Neovaskularisation im Rahmen einer hypoxie-induzierten Retinopathie durch einen Knockout des NOX2-Gens vollständig herrunterreguliert und vergleichbar mit der Kontroll-Gruppe, die nicht unter einer Hypoxie-induzierten Retinopathie litt [93]. Ein weiteres Knockout-Experiment stellte heraus, dass die HIF-1α-abhängige Angiogenese durch den Einsatz von Antioxidantien aber auch durch eine Defizienz des NOX2-Gens an der Maus verhindert werden konnte und in einer Herabregulierung von HIF-1α resultierte [101]. Dass es sich hierbei um kein NOX2 spezifisches Phänomen handelt, sondern es mehr um die entstehenden pathogenen Sauerstoffradikale geht, die eine HIF-1α-VEGFA Achse aktivieren können, zeigen Studien, die die Rolle anderer NOX-Subtypen oder auch den Einsatz von Antioxidantien untersuchten [102,103]. In retinalen Arteriolen konnten wir jedoch speziell die essenzielle Rolle der NOX2 in der Entstehung von Sauerstoffradikalen feststellen und erstmalig auch im retinalen Gewebe des Schweines im Zusammenhang mit systemischen Erkrankungen beobachten.

Betrachtet man nun die Parallelen der hochregulierten Marker in allen 3 Krankheitsmodellen, liegt die Tatsache nahe, dass diese im direkten Zusammenhang zur Pathogenese retinaler Dysfunktion beitragen könnten und frühe Signalmechanismen als Folge von systemischen Erkrankungen repräsentieren, die mit Perfusionsstörung von retinalen Arteriolen einhergehen könnten.

6 Schlussfolgerung, Limitierung und Ausblick

Die Ergebnisse aus den in dieser Arbeit zusammengefassten Studien zeigen, dass drei verschiedene Krankheitsmodelle in einer endothelialen Dysfunktion retinaler Arteriolen resultieren, die von der erhöhten Expression drei gleicher charakteristischer Marker begleitet worden ist. Zudem unterstreichen die übereinstimmenden Ergebnisse des erhöhten oxidativen Stresses in allen drei Modellen die wichtige Rolle frühzeitiger Untersuchungen im Zusammenhang mit systemischen Erkrankungen, da erhöhte Sauerstoffradikale in zahlreichen Gewebetypen, Spezies oder auch Krankheitsbilder eine pathogene Rolle einnehmen.

Trotz bereits vorher aufgeführten Parallelen zwischen dem menschlichen okulären System und dem des Schweines ist eine Translation dieser wissenschaftlichen Ergebnisse auf den Menschen nur bedingt möglich und kann nur als Ansatz neuer Forschungsansätze verwendet werden. Genauso verhält es sich auch mit der Spezies Maus, die zwar ein gut erforschtes und etabliertes Tiermodell repräsentiert, jedoch noch einige Schritte von der Translation auf menschliches Gewebe entfernt ist. Auch wenn die Hochregulierung einer HIF-1α-VEGFA-NOX2- Achse charakteristisch in allen 3 Modellen zu beobachten war, handelt es sich bei der Verwendung von systemischen Ganztier-Modellen um ein komplexes Phänomen, das die Analyse von spezifisch veränderten zellulären Faktoren schwierig gestaltet, nicht zuletzt bedingt durch die Heterogenität von retinalem Gewebe. Dazu kommt, dass wir uns im Rahmen dieser Arbeit nur auf die Analyse von bestimmten Markern in retinalen Arteriolen und im Blutserum fokussieren konnten, die die Effekte weiterer Mediatoren sowie weiterer Signalwege außer Betracht lässt. Zum Beispiel ging im Rahmen der ersten Publikation auch eine Hochregulation von inflammatorischen Markern, wie TNFα und Interleukin-6 im Blutserum mit einem Lungenschaden einher. Zwar konnten wir keine Veränderung dieser Zytokine auf mRNA- und Protein Ebene im retinalen Gewebe feststellen, jedoch könnte ihnen eine Rolle in der Induktion der beobachteten Veränderungen zukommen, die nicht Gegenstand dieser Arbeit sind, aber noch weiter erforscht werden sollten. So zeigte eine kürzlich veröffentliche Studie an Aorten der Maus, dass TNFα durch die Bindung an TNFα-Rezeptoren eine Aktivierung von NOX2 induziert und entstehende

Sauerstoffradikale mit einer endothelialen Dysfunktion einhergingen [104]. Im Hinblick auf die selektive Beeinflussung der retinalen Perfusion sollten weiterhin Therapieansätze erforscht werden, die die Entwicklung einer endothelialen Dysfunktion vorbeugen oder regenerieren. So könnte sich trotz kleinster Gefäße, die gute Erreichbarkeit retinaler Strukturen am Auge durch beispielsweise intravitreale Injektionen als erfolgversprechend für die Entwicklung neuer Therapieansätze darstellen.

Dem Thema des komplexen Netzwerks aus arteriellen und venösen Gefäßen, die im direkten Kontakt stehen mit retinalen Neuronen wird zunehmend Aufmerksamkeit geschenkt. So rücken vaskuläre Dysfunktionen in der Pathogenese neurodegenerativer Erkrankungen immer mehr in den Mittelpunkt der Forschung, weshalb zukünftige Untersuchungen retinaler Erkrankungen die Pathogenese retinaler Gefäße nicht außer Betracht lassen sollten. So konnte diese Arbeit erstmalig an zwei verschiedenen Spezies die bedeutsame Rolle einer endothelialen Dysfunktion retinaler Arteriolen in inflammatorischen, hypoxischen und ischämischen Zuständen nachweisen, die unter anderem mit strukturellen Defiziten der Retina in Zusammenhang gebracht werden konnten.

7 Literaturverzeichnis

1. Stitt AW, O'Neill CL, O'Doherty MT, Archer DB, Gardiner TA, Medina RJ: **Vascular stem cells and ischaemic retinopathies.** *Prog Retin Eye Res* (2011) **30**(3):149-166 doi: 10.1016/j.preteyeres.2011.02.001.

2. McClintic BR, McClintic JI, Bisognano JD, Block RC: **The relationship between retinal microvascular abnormalities and coronary heart disease: A review.** *Am J Med* (2010) **123**(4):374 e371-377 doi: 10.1016/j.amjmed.2009.05.030.

3. Hammes HP, Welp R, Kempe HP, Wagner C, Siegel E, Holl RW, Mellitus DPVI-GBCND: **Risk factors for retinopathy and dme in type 2 diabetes-results from the german/austrian dpv database.** *PLoS One* (2015) **10**(7):e0132492 doi: 10.1371/journal.pone.0132492.

4. Sorrentino FS, Matteini S, Bonifazzi C, Sebastiani A, Parmeggiani F: **Diabetic retinopathy and endothelin system: Microangiopathy versus endothelial dysfunction.** *Eye (Lond)* (2018) **32**(7):1157-1163 doi: 10.1038/s41433-018-0032-4.

5. Grieshaber MC, Flammer J: **Blood flow in glaucoma.** *Curr Opin Ophthalmol* (2005) **16**(2):79-83 doi: 10.1097/01.icu.0000156134.38495.0b.

6. Resch H, Garhofer G, Fuchsjager-Mayrl G, Hommer A, Schmetterer L: **Endothelial dysfunction in glaucoma.** *Acta Ophthalmol* (2009) **87**(1):4-12 doi: 10.1111/j.1755-3768.2007.01167.x.

7. Tham YC, Li X, Wong TY, Quigley HA, Aung T, Cheng CY: **Global prevalence of glaucoma and projections of glaucoma burden through 2040: A systematic review and meta-analysis.** *Ophthalmology* (2014) **121**(11):2081-2090 doi: 10.1016/j.ophtha.2014.05.013.

8. Feltgen N, Schmidt D, Hansen L: **[occlusion of the retinal artery].** *Ophthalmologe* (2003) **100**(8):651-665; quiz 666-657 doi: 10.1007/s00347-003-0845-8.

9. Feltgen N, Neubauer A, Jurklies B, Schmoor C, Schmidt D, Wanke J, Maier-Lenz H, Schumacher M, Group EA-S: **Multicenter study of the european assessment group for lysis in the eye (eagle) for the treatment of central retinal artery occlusion: Design issues and implications. Eagle study report no. 1 : Eagle study report no. 1.** *Graefes Arch Clin Exp Ophthalmol* (2006) **244**(8):950-956 doi: 10.1007/s00417-005-0140-2.

10. Querques G, Borrelli E, Sacconi R, De Vitis L, Leocani L, Santangelo R, Magnani G, Comi G, Bandello F: **Functional and morphological changes of the retinal vessels in alzheimer's disease and mild cognitive impairment.** *Sci Rep* (2019) **9**(1):63 doi: 10.1038/s41598-018-37271-6.

11. Seidelmann SB, Claggett B, Bravo PE, Gupta A, Farhad H, Klein BE, Klein R, Di Carli M, Solomon SD: **Retinal vessel calibers in predicting long-term cardiovascular outcomes: The atherosclerosis risk in communities study.** *Circulation* (2016) **134**(18):1328-1338 doi: 10.1161/CIRCULATIONAHA.116.023425.

12. Uhr JH, Mishra K, Wei C, Wu AY: **Awareness and knowledge of emergent ophthalmic disease among patients in an internal medicine clinic.** *JAMA Ophthalmol* (2016) **134**(4):424-431 doi: 10.1001/jamaophthalmol.2015.6212.

13. Hayashi K, Hayashi H: **Intravitreal versus retrobulbar injections of triamcinolone for macular edema associated with branch retinal vein occlusion.** *Am J Ophthalmol* (2005) **139**(6):972-982 doi: 10.1016/j.ajo.2004.12.087.

14. Schumacher M, Schmidt D, Jurklies B, Gall C, Wanke I, Schmoor C, Maier-Lenz H, Solymosi L, Brueckmann H, Neubauer AS, Wolf A *et al*: **Central retinal artery occlusion: Local intra-arterial fibrinolysis versus conservative treatment, a multicenter randomized trial.** *Ophthalmology* (2010) **117**(7):1367-1375 e1361 doi: 10.1016/j.ophtha.2010.03.061.

15. Kuwabara T, Cogan DG: **Studies of retinal vascular patterns. I. Normal architecture.** *Arch Ophthalmol* (1960) **64**(904-911 doi: 10.1001/archopht.1960.01840010906012.

16. Wiencke AK, Nilsson H, Nielsen PJ, Nyborg NC: **Nonadrenergic noncholinergic vasodilation in bovine ciliary artery involves cgrp and neurogenic nitric oxide.** *Invest Ophthalmol Vis Sci* (1994) **35**(8):3268-3277.

17. Kawarai M, Koss MC: **Sympathetic vasoconstriction in the rat anterior choroid is mediated by alpha1-adrenoceptors.** *Eur J Pharmacol* (1998) **363**(1):35-40 doi: 10.1016/s0014-2999(98)00790-0.

18. Nilsson SF: **Nitric oxide as a mediator of parasympathetic vasodilation in ocular and extraocular tissues in the rabbit.** *Invest Ophthalmol Vis Sci* (1996) **37**(10):2110-2119.

19. Laties AM: **Central retinal artery innervation. Absence of adrenergic innervation to the intraocular branches.** *Arch Ophthalmol* (1967) **77**(3):405-409 doi: 10.1001/archopht.1967.00980020407021.

20. Reiner A, Fitzgerald MEC, Del Mar N, Li C: **Neural control of choroidal blood flow.** *Prog Retin Eye Res* (2018) **64**(96-130 doi: 10.1016/j.preteyeres.2017.12.001.

21. Sickel W: **Electrical and metabolic manifestations of receptor and higher-order neuron activity in vertebrate retina.** *Adv Exp Med Biol* (1972) **24**(0):101-118 doi: 10.1007/978-1-4684-8231-7_11.

22. Yu DY, Cringle SJ: **Oxygen distribution and consumption within the retina in vascularised and avascular retinas and in animal models of retinal disease.** *Prog Retin Eye Res* (2001) **20**(2):175-208 doi: 10.1016/s1350-9462(00)00027-6.

23. Flammer J, Haefliger IO, Orgul S, Resink T: **Vascular dysregulation: A principal risk factor for glaucomatous damage?** *J Glaucoma* (1999) **8**(3):212-219.

24. Flammer J, Mozaffarieh M: **What is the present pathogenetic concept of glaucomatous optic neuropathy?** *Surv Ophthalmol* (2007) **52 Suppl 2**(S162-173 doi: 10.1016/j.survophthal.2007.08.012.

25. Venkataraman ST, Flanagan JG, Hudson C: **Vascular reactivity of optic nerve head and retinal blood vessels in glaucoma--a review.** *Microcirculation* (2010) **17**(7):568-581 doi: 10.1111/j.1549-8719.2010.00045.x.

26. Ster AM, Popp RA, Petrisor FM, Stan C, Pop VI: **The role of oxidative stress and vascular insufficiency in primary open angle glaucoma.** *Clujul Med* (2014) **87**(3):143-146 doi: 10.15386/cjmed-295.

27. Schreiber V: **[edrf-no. The endothelium-derived relaxing factor is nitric oxide].** *Cas Lek Cesk* (1992) **131**(13):388-390.

28. Gericke A, Wolff I, Musayeva A, Zadeh JK, Manicam C, Pfeiffer N, Li H, Xia N: **Retinal arteriole reactivity in mice lacking the endothelial nitric oxide synthase (enos) gene.** *Exp Eye Res* (2019) **181**(150-156 doi: 10.1016/j.exer.2019.01.022.

29. Dalsgaard T, Kroigaard C, Misfeldt M, Bek T, Simonsen U: **Openers of small conductance calcium-activated potassium channels selectively enhance no-mediated bradykinin vasodilatation in porcine retinal arterioles.** *Br J Pharmacol* (2010) **160**(6):1496-1508 doi: 10.1111/j.1476-5381.2010.00803.x.

30. Dalsgaard T, Kroigaard C, Bek T, Simonsen U: **Role of calcium-activated potassium channels with small conductance in bradykinin-induced vasodilation of porcine retinal arterioles.** *Invest Ophthalmol Vis Sci* (2009) **50**(8):3819-3825 doi: 10.1167/iovs.08-3168.

31. Jeppesen P, Aalkjaer C, Bek T: **Bradykinin relaxation in small porcine retinal arterioles.** *Invest Ophthalmol Vis Sci* (2002) **43**(6):1891-1896.

32. Simonsen U, Winther AK, Olivan-Viguera A, Comerma-Steffensen S, Kohler R, Bek T: **Extracellular l-arginine enhances relaxations induced by opening of calcium-activated skca channels in porcine retinal arteriole.** *Int J Mol Sci* (2019) **20**(8): doi: 10.3390/ijms20082032.

33. Potts LB, Bradley PD, Xu W, Kuo L, Hein TW: **Role of endothelium in vasomotor responses to endothelin system and protein kinase c activation in porcine retinal arterioles.** *Invest Ophthalmol Vis Sci* (2013) **54**(12):7587-7594 doi: 10.1167/iovs13-13178.

34. Haefliger IO, Flammer J, Luscher TF: **Heterogeneity of endothelium-dependent regulation in ophthalmic and ciliary arteries.** *Invest Ophthalmol Vis Sci* (1993) **34**(5):1722-1730.

35. Gericke A, Sniatecki JJ, Goloborodko E, Steege A, Zavaritskaya O, Vetter JM, Grus FH, Patzak A, Wess J, Pfeiffer N: **Identification of the muscarinic acetylcholine receptor subtype mediating cholinergic vasodilation in murine retinal arterioles.** *Invest Ophthalmol Vis Sci* (2011) **52**(10):7479-7484 doi: 10.1167/iovs.11-7370.

36. Gericke A, Mayer VG, Steege A, Patzak A, Neumann U, Grus FH, Joachim SC, Choritz L, Wess J, Pfeiffer N: **Cholinergic responses of ophthalmic arteries in m3 and m5 muscarinic acetylcholine receptor knockout mice.** *Invest Ophthalmol Vis Sci* (2009) **50**(10):4822-4827 doi: 10.1167/iovs.09-3600.

37. Yamagishi S, Ueda S, Matsui T, Nakamura K, Okuda S: **Role of advanced glycation end products (ages) and oxidative stress in diabetic retinopathy.** *Curr Pharm Des* (2008) **14**(10):962-968 doi: 10.2174/138161208784139729.

38. Delaney Y, Walshe TE, O'Brien C: **Vasospasm in glaucoma: Clinical and laboratory aspects.** *Optom Vis Sci* (2006) **83**(7):406-414 doi: 10.1097/01.opx.0000225877.13217.01.

39. Leske MC, Heijl A, Hyman L, Bengtsson B, Komaroff E: **Factors for progression and glaucoma treatment: The early manifest glaucoma trial.** *Curr Opin Ophthalmol* (2004) **15**(2):102-106 doi: 10.1097/00055735-200404000-00008.

40. Shareef SR, Garcia-Valenzuela E, Salierno A, Walsh J, Sharma SC: **Chronic ocular hypertension following episcleral venous occlusion in rats.** *Exp Eye Res* (1995) **61**(3):379-382 doi: 10.1016/s0014-4835(05)80131-9.

41. Renner M, Stute G, Alzureiqi M, Reinhard J, Wiemann S, Schmid H, Faissner A, Dick HB, Joachim SC: **Optic nerve degeneration after retinal ischemia/reperfusion in a rodent model.** *Front Cell Neurosci* (2017) **11**(254 doi: 10.3389/fncel.2017.00254.

42. Schmid H, Renner M, Dick HB, Joachim SC: **Loss of inner retinal neurons after retinal ischemia in rats.** *Invest Ophthalmol Vis Sci* (2014) **55**(4):2777-2787 doi: 10.1167/iovs.13-13372.

43. Tanihara H, Hangai M, Sawaguchi S, Abe H, Kageyama M, Nakazawa F, Shirasawa E, Honda Y: **Up-regulation of glial fibrillary acidic protein in the retina of primate eyes with experimental glaucoma.** *Arch Ophthalmol* (1997) **115**(6):752-756 doi: 10.1001/archopht.1997.01100150754011.

44. Yang Z, Wang KK: **Glial fibrillary acidic protein: From intermediate filament assembly and gliosis to neurobiomarker.** *Trends Neurosci* (2015) **38**(6):364-374 doi: 10.1016/j.tins.2015.04.003.

45. Gunther A, Luczak V, Abel T, Baumann A: **Caspase-3 and gfap as early markers for apoptosis and astrogliosis in shrna-induced hippocampal cytotoxicity.** *J Exp Biol* (2017) **220**(Pt 8):1400-1404 doi: 10.1242/jeb.154583.

46. Anders F, Teister J, Liu A, Funke S, Grus FH, Thanos S, von Pein HD, Pfeiffer N, Prokosch V: **Intravitreal injection of beta-crystallin b2 improves retinal ganglion cell survival in an experimental animal model of glaucoma.** *PLoS One* (2017) **12**(4):e0175451 doi: 10.1371/journal.pone.0175451.

47. Piri N, Song M, Kwong JM, Caprioli J: **Modulation of alpha and beta crystallin expression in rat retinas with ocular hypertension-induced ganglion cell degeneration.** *Brain Res* (2007) **1141**(1-9 doi: 10.1016/j.brainres.2006.11.095.

48. Kalogeris T, Baines CP, Krenz M, Korthuis RJ: **Cell biology of ischemia/reperfusion injury.** *Int Rev Cell Mol Biol* (2012) **298**(229-317 doi: 10.1016/B978-0-12-394309-5.00006-7.

49. Bonne C, Muller A, Villain M: **Free radicals in retinal ischemia.** *Gen Pharmacol* (1998) **30**(3):275-280 doi: 10.1016/s0306-3623(97)00357-1.

50. Dollery CT, Henkind P, Kohner EM, Paterson JW: **Effect of raised intraocular pressure on the retinal and choroidal circulation.** *Invest Ophthalmol* (1968) **7**(2):191-198.

51. Buchi ER, Suivaizdis I, Fu J: **Pressure-induced retinal ischemia in rats: An experimental model for quantitative study.** *Ophthalmologica* (1991) **203**(3):138-147 doi: 10.1159/000310240.

52. Kim BJ, Braun TA, Wordinger RJ, Clark AF: **Progressive morphological changes and impaired retinal function associated with temporal regulation of gene expression after retinal ischemia/reperfusion injury in mice.** *Mol Neurodegener* (2013) **8**(21 doi: 10.1186/1750-1326-8-21.

53. Wurm A, Iandiev I, Uhlmann S, Wiedemann P, Reichenbach A, Bringmann A, Pannicke T: **Effects of ischemia-reperfusion on physiological properties of muller glial cells in the porcine retina.** *Invest Ophthalmol Vis Sci* (2011) **52**(6):3360-3367 doi: 10.1167/iovs.10-6901.

54. Veriac S, Tissie G, Bonne C: **Oxygen free radicals adversely affect the regulation of vascular tone by nitric oxide in the rabbit retina under high intraocular pressure.** *Exp Eye Res* (1993) **56**(1):85-88 doi: 10.1006/exer.1993.1012.

55. Hein TW, Ren Y, Potts LB, Yuan Z, Kuo E, Rosa RH, Jr., Kuo L: **Acute retinal ischemia inhibits endothelium-dependent nitric oxide-mediated dilation of retinal arterioles via enhanced superoxide production.** *Invest Ophthalmol Vis Sci* (2012) **53**(1):30-36 doi: 10.1167/iovs.11-8753.

56. Ravi Teja KV, Tos Berendschot T, Steinbusch H, Carroll Webers AB, Praveen Murthy R, Mathuranath PS: **Cerebral and retinal neurovascular changes: A biomarker for alzheimer's disease.** *J Gerontol Geriatr Res* (2017) **6**(4): doi: 10.4172/2167-7182.1000447.

57. Chinh LQ, Manabe T, Son DN, Chi NV, Fujikura Y, Binh NG, Co DX, Tuan DQ, Ton MD, Dai KQ, Thach PT *et al*: **Clinical epidemiology and mortality on patients with acute respiratory distress syndrome (ards) in vietnam.** *PLoS One* (2019) **14**(8):e0221114 doi: 10.1371/journal.pone.0221114.

58. Sasannejad C, Ely EW, Lahiri S: **Long-term cognitive impairment after acute respiratory distress syndrome: A review of clinical impact and pathophysiological mechanisms.** *Crit Care* (2019) **23**(1):352 doi: 10.1186/s13054-019-2626-z.

59. Troiani S, Cardona A, Milioni M, Monacelli D, Verrotti A, Gehring M, Ambrosio G: **Evidence of impaired microvascular dilatation in preterms with acute respiratory distress syndrome.** *Int J Cardiol* (2017) **241**(83-86 doi: 10.1016/j.ijcard.2017.04.018.

60. Orbegozo Cortes D, Rahmania L, Irazabal M, Santacruz C, Fontana V, De Backer D, Creteur J, Vincent JL: **Microvascular reactivity is altered early in patients with acute respiratory distress syndrome.** *Respir Res* (2016) **17**(1):59 doi: 10.1186/s12931-016-0375-y.

61. Zadeh JK, Ruemmler R, Hartmann EK, Ziebart A, Ludwig M, Patzak A, Xia N, Li H, Pfeiffer N, Gericke A: **Responses of retinal arterioles and ciliary arteries in pigs with acute respiratory distress syndrome (ards).** *Exp Eye Res* (2019) **184**(152-161 doi: 10.1016/j.exer.2019.04.021.

62. Force ADT, Ranieri VM, Rubenfeld GD, Thompson BT, Ferguson ND, Caldwell E, Fan E, Camporota L, Slutsky AS: **Acute respiratory distress syndrome: The berlin definition.** *JAMA* (2012) **307**(23):2526-2533 doi: 10.1001/jama.2012.5669.

63. Sweeney RM, Griffiths M, McAuley D: **Treatment of acute lung injury: Current and emerging pharmacological therapies.** *Semin Respir Crit Care Med* (2013) **34**(4):487-498 doi: 10.1055/s-0033-1351119.

64. de Souza Xavier Costa N, Ribeiro Junior G, Dos Santos Alemany AA, Belotti L, Zati DH, Frota Cavalcante M, Matera Veras M, Ribeiro S, Kallas EG, Nascimento Saldiva PH, Dolhnikoff M *et al*: **Early and late pulmonary effects of nebulized lps in mice: An acute lung injury model.** *PLoS One* (2017) **12**(9):e0185474 doi: 10.1371/journal.pone.0185474.

65. An X, Sun X, Hou Y, Yang X, Chen H, Zhang P, Wu J: **Protective effect of oxytocin on lps-induced acute lung injury in mice.** *Sci Rep* (2019) **9**(1):2836 doi: 10.1038/s41598-019-39349-1.

66. Tian L, Li W, Wang T: **Therapeutic effects of silibinin on lps-induced acute lung injury by inhibiting nlrp3 and nf-kappab signaling pathways.** *Microb Pathog* (2017) **108**(104-108 doi: 10.1016/j.micpath.2017.05.011.

67. He M, Pan H, Chang RC, So KF, Brecha NC, Pu M: **Activation of the nrf2/ho-1 antioxidant pathway contributes to the protective effects of lycium barbarum polysaccharides in the rodent retina after ischemia-reperfusion-induced damage.** *PLoS One* (2014) **9**(1):e84800 doi: 10.1371/journal.pone.0084800.

68. Robinson R, Ho CE, Tan QS, Luu CD, Moe KT, Cheung CY, Wong TY, Barathi VA: **Fluvastatin downregulates vegf-a expression in tnf-alpha-induced retinal vessel tortuosity.** *Invest Ophthalmol Vis Sci* (2011) **52**(10):7423-7431 doi: 10.1167/iovs.11-7912.

69. Zadeh JK, Garcia-Bardon A, Hartmann EK, Pfeiffer N, Omran W, Ludwig M, Patzak A, Xia N, Li H, Gericke A: **Short-time ocular ischemia induces vascular endothelial dysfunction and ganglion cell loss in the pig retina.** *Int J Mol Sci* (2019) **20**(19): doi: 10.3390/ijms20194685.

70. Osborne NN, Casson RJ, Wood JP, Chidlow G, Graham M, Melena J: **Retinal ischemia: Mechanisms of damage and potential therapeutic**

strategies. *Prog Retin Eye Res* (2004) **23**(1):91-147 doi: 10.1016/j.preteyeres.2003.12.001.

71. Gao S, Andreeva K, Cooper NG: **Ischemia-reperfusion injury of the retina is linked to necroptosis via the erk1/2-rip3 pathway.** *Mol Vis* (2014) **20**(1374-1387.

72. Sennlaub F, Courtois Y, Goureau O: **Inducible nitric oxide synthase mediates retinal apoptosis in ischemic proliferative retinopathy.** *J Neurosci* (2002) **22**(10):3987-3993 doi: 20026405.

73. Chauhan SD, Seggara G, Vo PA, Macallister RJ, Hobbs AJ, Ahluwalia A: **Protection against lipopolysaccharide-induced endothelial dysfunction in resistance and conduit vasculature of inos knockout mice.** *FASEB J* (2003) **17**(6):773-775 doi: 10.1096/fj.02-0668fje.

74. Chuaiphichai S, Starr A, Nandi M, Channon KM, McNeill E: **Endothelial cell tetrahydrobiopterin deficiency attenuates lps-induced vascular dysfunction and hypotension.** *Vascul Pharmacol* (2016) **77**(69-79 doi: 10.1016/j.vph.2015.08.009.

75. Gundogan FC, Ilhan A, Yolcu U, Altun S: **Measurement of retinal function with flash electroretinography in chinese patients with hyperlipidemia.** *Graefes Arch Clin Exp Ophthalmol* (2015) **253**(5):821 doi: 10.1007/s00417-014-2855-4.

76. Sharifizad M, Witkowska KJ, Aschinger GC, Sapeta S, Rauch A, Schmidl D, Werkmeister RM, Garhofer G, Schmetterer L: **Factors determining flicker-induced retinal vasodilation in healthy subjects.** *Invest Ophthalmol Vis Sci* (2016) **57**(7):3306-3312 doi: 10.1167/iovs.16-19261.

77. Leung H, Wang JJ, Rochtchina E, Wong TY, Klein R, Mitchell P: **Dyslipidaemia and microvascular disease in the retina.** *Eye (Lond)* (2005) **19**(8):861-868 doi: 10.1038/sj.eye.6701668.

78. Montgomery CL, Johnson HM, Johnston TP, Koulen P: **Mechanisms underlying early-stage changes in visual performance and retina function after experimental induction of sustained dyslipidemia.** *Neurochem Res* (2018) **43**(8):1500-1510 doi: 10.1007/s11064-018-2563-2.

79. Stojakovic T, Scharnagl H, Marz W, Winkelmann BR, Boehm BO, Schmut O: **Low density lipoprotein triglycerides and lipoprotein(a) are risk factors for retinal vascular occlusion.** *Clin Chim Acta* (2007) **382**(1-2):77-81 doi: 10.1016/j.cca.2007.03.024.

80. Zadeh JK, Zhutdieva MB, Laspas P, Yuksel C, Musayeva A, Pfeiffer N, Brochhausen C, Oelze M, Daiber A, Xia N, Li H *et al*: **Apolipoprotein e**

deficiency causes endothelial dysfunction in the mouse retina. *Oxid Med Cell Longev* (2019) **2019**(5181429 doi: 10.1155/2019/5181429.

81. Jawien J: **The role of an experimental model of atherosclerosis: Apoe-knockout mice in developing new drugs against atherogenesis.** *Curr Pharm Biotechnol* (2012) **13**(13):2435-2439.

82. Jawien J, Nastalek P, Korbut R: **Mouse models of experimental atherosclerosis.** *J Physiol Pharmacol* (2004) **55**(3):503-517.

83. Henderson KK, Turk JR, Rush JW, Laughlin MH: **Endothelial function in coronary arterioles from pigs with early-stage coronary disease induced by high-fat, high-cholesterol diet: Effect of exercise.** *J Appl Physiol (1985)* (2004) **97**(3):1159-1168 doi: 10.1152/japplphysiol.00261.2004.

84. Xia N, Horke S, Habermeier A, Closs EI, Reifenberg G, Gericke A, Mikhed Y, Munzel T, Daiber A, Forstermann U, Li H: **Uncoupling of endothelial nitric oxide synthase in perivascular adipose tissue of diet-induced obese mice.** *Arterioscler Thromb Vasc Biol* (2016) **36**(1):78-85 doi: 10.1161/ATVBAHA.115.306263.

85. Yamashiro K, Milsom AB, Duchene J, Panayiotou C, Urabe T, Hattori N, Ahluwalia A: **Alterations in nitric oxide and endothelin-1 bioactivity underlie cerebrovascular dysfunction in apoe-deficient mice.** *J Cereb Blood Flow Metab* (2010) **30**(8):1494-1503 doi: 10.1038/jcbfm.2010.34.

86. Marcucci R, Sodi A, Giambene B, Liotta AA, Poli D, Mannini L, Falciani M, Abbate R, Menchini U, Prisco D: **Cardiovascular and thrombophilic risk factors in patients with retinal artery occlusion.** *Blood Coagul Fibrinolysis* (2007) **18**(4):321-326 doi: 10.1097/MBC.0b013e32809cc922.

87. Saadane A, Petrov A, Mast N, El-Darzi N, Dao T, Alnemri A, Song Y, Dunaief JL, Pikuleva IA: **Mechanisms that minimize retinal impact of apolipoprotein e absence.** *J Lipid Res* (2018) **59**(12):2368-2382 doi: 10.1194/jlr.M090043.

88. Mak AC, Pullinger CR, Tang LF, Wong JS, Deo RC, Schwarz JM, Gugliucci A, Movsesyan I, Ishida BY, Chu C, Poon A *et al*: **Effects of the absence of apolipoprotein e on lipoproteins, neurocognitive function, and retinal function.** *JAMA Neurol* (2014) **71**(10):1228-1236 doi: 10.1001/jamaneurol.2014.2011.

89. Guduric-Fuchs J, Ringland LJ, Gu P, Dellett M, Archer DB, Cogliati T: **Immunohistochemical study of pig retinal development.** *Mol Vis* (2009) **15**(1915-1928.

90. Garca M, Ruiz-Ederra J, Hernandez-Barbachano H, Vecino E: **Topography of pig retinal ganglion cells.** *J Comp Neurol* (2005) **486**(4):361-372 doi: 10.1002/cne.20516.

91. Ruiz-Ederra J, Garcia M, Hernandez M, Urcola H, Hernandez-Barbachano E, Araiz J, Vecino E: **The pig eye as a novel model of glaucoma.** *Exp Eye Res* (2005) **81**(5):561-569 doi: 10.1016/j.exer.2005.03.014.

92. Sena CM, Leandro A, Azul L, Seica R, Perry G: **Vascular oxidative stress: Impact and therapeutic approaches.** *Front Physiol* (2018) **9**(1668 doi: 10.3389/fphys.2018.01668.

93. Chan EC, van Wijngaarden P, Liu GS, Jiang F, Peshavariya H, Dusting GJ: **Involvement of nox2 nadph oxidase in retinal neovascularization.** *Invest Ophthalmol Vis Sci* (2013) **54**(10):7061-7067 doi: 10.1167/iovs.13-12883.

94. Song H, Vijayasarathy C, Zeng Y, Marangoni D, Bush RA, Wu Z, Sieving PA: **Nadph oxidase contributes to photoreceptor degeneration in constitutively active rac1 mice.** *Invest Ophthalmol Vis Sci* (2016) **57**(6):2864-2875 doi: 10.1167/iovs.15-18974.

95. Chanock SJ, el Benna J, Smith RM, Babior BM: **The respiratory burst oxidase.** *J Biol Chem* (1994) **269**(40):24519-24522.

96. Di Meo S, Reed TT, Venditti P, Victor VM: **Role of ros and rns sources in physiological and pathological conditions.** *Oxid Med Cell Longev* (2016) **2016**(1245049 doi: 10.1155/2016/1245049.

97. Rohowetz LJ, Kraus JG, Koulen P: **Reactive oxygen species-mediated damage of retinal neurons: Drug development targets for therapies of chronic neurodegeneration of the retina.** *Int J Mol Sci* (2018) **19**(11): doi: 10.3390/ijms19113362.

98. Masuda T, Shimazawa M, Hara H: **Retinal diseases associated with oxidative stress and the effects of a free radical scavenger (edaravone).** *Oxid Med Cell Longev* (2017) **2017**(9208489 doi: 10.1155/2017/9208489.

99. Xia XB, Xiong SQ, Xu HZ, Jiang J, Li Y: **Suppression of retinal neovascularization by shrna targeting hif-1alpha.** *Curr Eye Res* (2008) **33**(10):892-902 doi: 10.1080/02713680802416670.

100. Aiello LP, Northrup JM, Keyt BA, Takagi H, Iwamoto MA: **Hypoxic regulation of vascular endothelial growth factor in retinal cells.** *Arch Ophthalmol* (1995) **113**(12):1538-1544 doi: 10.1001/archopht.1995.01100120068012.

101. Diebold I, Petry A, Sabrane K, Djordjevic T, Hess J, Gorlach A: **The hif1 target gene nox2 promotes angiogenesis through urotensin-ii.** *J Cell Sci* (2012) **125**(Pt 4):956-964 doi: 10.1242/jcs.094060.

102. Irwin DC, McCord JM, Nozik-Grayck E, Beckly G, Foreman B, Sullivan T, White M, T. Crossno J J, Bailey D, Flores SC, Majka S *et al*: **A potential role for reactive oxygen species and the hif-1alpha-vegf pathway in hypoxia-induced pulmonary vascular leak.** *Free Radic Biol Med* (2009) **47**(1):55-61 doi: 10.1016/j.freeradbiomed.2009.03.027.

103. Li J, Wang JJ, Yu Q, Chen K, Mahadev K, Zhang SX: **Inhibition of reactive oxygen species by lovastatin downregulates vascular endothelial growth factor expression and ameliorates blood-retinal barrier breakdown in db/db mice: Role of nadph oxidase 4.** *Diabetes* (2010) **59**(6):1528-1538 doi: 10.2337/db09-1057.

104. Li Y, Cifuentes-Pagano E, DeVallance ER, de Jesus DS, Sahoo S, Meijles DN, Koes D, Camacho CJ, Ross M, St Croix C, Pagano PJ: **Nadph oxidase 2 inhibitors cpp11g and cpp11h attenuate endothelial cell inflammation & vessel dysfunction and restore mouse hind-limb flow.** *Redox Biol* (2019) **22**(101143 doi: 10.1016/j.redox.2019.101143.

8 Anhang

8.1 Abkürzungsverzeichnis

Acetylcholin	Ach
Bradykinin	BK
Cyclooxygenase	COX
Endothelium-derived Relaxing Factor	EDRF
Endotheliale NO-Synthase	eNOS
G-Protein gekoppelter Rezeptor	GPCR
Hypoxia-inducible Factor-1α	HIF-1α
Inducible NO-Synthase	iNOS
Lipopolysaccharid LPS	LPS
Nicotinamid-Adenin-Dinucleotide Phosphat Oxidase	NOX
Neuronale NO-Synthase	nNOS
Mittlerer Pulmonal Arterieller Druck	MPAP
Retinale Ganglienzelle	RGC

Sauerstoffpartialdruck im arteriellen Blut	PaO_2
Sauerstoffanteil der Atemluft	FiO_2
Saures Gliafaserprotein	GFAP
Stickstoffmonoxid	NO
Reactive Oxygen Species	ROS
Vascular Endothelial Growth Factor	VEGF
Xanthinoxidase	XO

8.2 Erklärung zum Eigenanteil

Die Forschungsergebnisse dieser Dissertationsschrift sind in Form von drei Einzelarbeiten veröffentlicht worden. Auch wenn jede dieser Publikationen einen Abschnitt zu den jeweiligen Verantwortungsbereichen aller Autoren beinhaltet, sollen im Folgenden meine eigenverantwortlichen und wissenschaftlichen Beiträge zu diesen Publikationen nochmals detailliert dargelegt werden. Bei allen drei Publikationen wirkte ich maßgeblich bei der Konzeptualisierung und der Methodikbestimmung sowie der Erhebung und Visualisierung der Daten mit. Alle Gefäßexperimente, die die Messung des Vasoregulationsverhaltens der retinalen Blutversorgung unter bestimmten pathologischen Bedingungen beinhalten und einen Schwerpunkt jeder einzelnen Veröffentlichung darstellen, wurden sowohl von mir durchgeführt als auch analysiert. Ebenso verhält es sich mit allen immunohistochemischen Untersuchungen zu Veränderungen von charakteristischen Markern auf Proteinebene und histologischen Veränderungen von retinalen Strukturen. Die Erstellung des Manuskriptes ist in allen drei Veröffentlichungen von mir durchgeführt, von Herrn Dr. Adrian Gericke korrigiert sowie von allen Koautoren vor Veröffentlichung überprüft worden.

8.3 In der Dissertation zusammengefasste Arbeiten

Experimental Eye Research 184 (2019) 152–161

Contents lists available at ScienceDirect

Experimental Eye Research

journal homepage: www.elsevier.com/locate/yexer

Responses of retinal arterioles and ciliary arteries in pigs with acute respiratory distress syndrome (ARDS)

Jenia Kouchek Zadeh[a,*], Robert Ruemmler[b], Erik Kristoffer Hartmann[b], Alexander Ziebart[b], Marion Ludwig[c], Andreas Patzak[c], Ning Xia[d], Huige Li[d], Norbert Pfeiffer[a], Adrian Gericke[a]

[a] Department of Ophthalmology, University Medical Center, Johannes Gutenberg University Mainz, Langenbeckstr. 1, 55131, Mainz, Germany
[b] Department of Anesthesiology, University Medical Center, Johannes Gutenberg University Mainz, Langenbeckstr. 1, 55131, Mainz, Germany
[c] Institute of Vegetative Physiology, Charité-Universitätsmedizin Berlin, Charitéplatz 1, 10117, Berlin, Germany
[d] Department of Pharmacology, University Medical Center, Johannes Gutenberg University Mainz, Obere Zahlbacher Str. 67, 55131, Mainz, Germany

ARTICLE INFO

Keywords:
ARDS
Retinal arterioles
Ciliary arteries
Endothelial dysfunction

ABSTRACT

Acute respiratory distress syndrome (ARDS) is a clinical syndrome of acute lung failure in critically sick patients, which severely compromises the function of multiple organs, including the brain. Although, the optic nerve and the retina are a part of the central nervous system, the effects of ARDS on these ocular structures are completely unknown. Thus, the major goal of this study was to test the hypothesis that ARDS affects vascular function in the eye. ARDS was induced in anesthetized pigs by intratracheal injection of lipopolysaccharide (LPS). Sham-treated animals served as controls. Pigs were monitored for 8 h and then sacrificed. Subsequently, retinal arterioles and short posterior ciliary arteries were isolated and cannulated with micropipettes to measure vascular responses by videomicroscopy. Levels of reactive oxygen species (ROS) were quantified in isolated vessels using dihydroethidium (DHE). Messenger RNA expression of hypoxic, inflammatory, prooxidative, and antioxidative genes was assessed by real-time PCR. When group-dependent differences in mRNA expression levels were found for a particular gene, immunostainings were conducted. Strikingly, responses to the endothelium-dependent vasodilator, bradykinin, were markedly impaired in retinal arterioles of LPS-treated pigs, but no differences were seen between ciliary arteries of LPS- and sham-treated animals. ROS levels were increased in retinal arterioles but not in ciliary arteries of LPS-treated pigs. Messenger RNA levels for HIF-1α, VEGF-A and NOX2 were markedly increased in retinal arterioles of LPS-treated pigs, whereas ciliary arteries had only negligible mRNA level changes. Pronounced immunoreactivity for HIF-1α, VEGF-A and NOX2 was seen in the endothelium of retinal arterioles from LPS-treated pigs. Histologically, massive edema was seen especially in the retinal nerve fiber layer of pigs treated with LPS. Our study provides the first evidence that ARDS induced by intratracheal LPS application evokes endothelial dysfunction in porcine retinal arterioles together with retinal edema, indicative of vascular leakage. In contrast, ciliary arteries appear to be resistant to intratracheal LPS application.

1. Introduction

Acute respiratory distress syndrome (ARDS), also known as acute lung injury (ALI), is a type of respiratory failure characterized by rapid onset of widespread lung inflammation (Fioretto and Carvalho, 2013; Lucas et al., 2009; Ragaller and Richter, 2010). It is widely known as a trigger of systemic inflammation or sepsis as well as of long-term physical and neuropsychological impairment leading to cognitive deficits (Pandharipande et al., 2013). The incidence of ARDS varies between 10.1 per 100,000 person-years in South America and 78.9 per 100,000 person-years in the USA (Caser et al., 2014; Rezoagli et al., 2017; Rubenfeld et al., 2005). A prospective cohort study reported mortality rates of 40% among patients with moderate ARDS and of 46% for patients with severe ARDS (Bellani et al., 2016). The syndrome is characterized by damage of the alveolar epithelium and the microvascular endothelial barrier due to locally released cytokines and proinflammatory mediators, which in turn results in severe hypoxia (Johnson and Matthay, 2010). Pulmonary injury is often followed by systemic inflammation as a direct response of upregulated cytokines, an increase in vascular permeability and oxidative stress (Rezoagli et al., 2017). Furthermore, there is emerging evidence suggesting a cross-talk between the lung and distal organs, such as the brain (Pelosi and Rocco, 2011) and the kidneys (Donoso et al., 2015), by still unrevealed mechanisms. The aim of this study was to examine the hypothesis that

* Corresponding author.
E-mail address: jenia.kouchekzadeh@unimedizin-mainz.de (J.K. Zadeh).

https://doi.org/10.1016/j.exer.2019.04.021
Received 21 December 2018; Received in revised form 29 March 2019; Accepted 17 April 2019
Available online 22 April 2019

Abbreviations

ALI	acute lung injury
ARDS	acute respiratory distress syndrome
BL	baseline
CAT	catalase
DAPI	4′,6-diamidino-2-phenylindole
DHE	dihydroethidium
DMSO	dimethyl sulfoxide
ELISA	enzyme-linked immunosorbent assay
$etCO_2$	end tidal CO_2
FiO_2	fraction of inspired oxygen
GPx1	glutathione peroxidase 1
HIF-1α	hypoxia-inducible factior-1α
HO-1	heme oxygenase-1
IL	interleukin
iNOS	inducible nitric oxide synthase
LPS	lipopolysaccharide
MAP	mean arterial pressure
MPAP	mean pulmonary arterial pressure
NOX	nicotinamide adenine dinucleotide phosphate oxidase
PaO_2/FiO_2	ratio of intra-arterial partial oxygen pressure and inspiratory oxygen fraction
PBS	phosphate buffered saline
PEEP	positive end-expiratory pressure
ROS	reactive oxygen species
SNP	sodium nitroprusside
SOD	superoxide dismutase
TNF-α	tumor necrosis factor alpha
U46619	9,11-dideoxy-9α,11α-methanoepoxy prostaglandin F2α
VEGF-A	vascular endothelial growth factor A
Vt	tidal volume
XO	xanthine oxidase

ARDS induced by intratracheal application of lipopolysaccharide (LPS), an endotoxin of gram-negative bacteria, affects function of the vasculature supplying the optic nerve and the retina. Our experiments were conducted in short posterior ciliary arteries, which supply a large part of the optic nerve head and, via the choroidal vascular network, the outer retina with blood. Further, we studied retinal arterioles, which supply the inner retina and the anterior part of the optic nerve head with blood. Both vascular beds differ anatomically and functionally, e.g., with regard to their endothelial barrier and autonomic innervation (Bill, 1975; Bill and Nilsson, 1985).

2. Materials and methods

2.1. Animals

All studies were performed in accordance with the guidelines of EU Directive 2010/63/EU for animal experiments and were approved by the Animal Care Committee of Rhineland-Palatinate, Germany. Male pigs (Sus scrofa domesticus) at the age of 3 months (body weight 27–30 kg) were randomly assigned to one of two groups (LPS-treated group or sham-treated group, respectively) and examined in an investigator-blinded study.

2.2. Treatment of animals to induce ARDS

Animals were anesthetized by intravenous propofol/fentanyl administration ($4\,mg\,kg^{-1}/4\,\mu g\,kg^{-1}$**)**. During the experiment, anesthesia was maintained by continuous infusion of propofol ($5–10\,mg\,kg^{-1}\,h^{-1}$), fentanyl ($8–12\,\mu g\,kg^{-1}\,h^{-1}$) and balanced salt solution (BSS, $5\,ml\,kg^{-1}\,h^{-1}$). A secure airway was established by endotracheal intubation after a single dose of atracurium ($0{,}5\,mg\,kg^{-1}$). During the experiment, volume-controlled ventilation was conducted and monitored (Engström care station, GE healthcare, Munich): tidal volume (Vt) 6–7 $ml\,kg^{-1}$, positive end-expiratory pressure (PEEP) 5 mbar, fraction of inspired oxygen (FiO_2) 0.4, variable respiratory rate to guarantee an end tidal CO_2 ($etCO_2$) < 6 kPa and pH 7.4. Thirty minutes after endotracheal intubation, baseline (BL) measurements were recorded and blood collected. Subsequently, LPS was administered intratracheally by a single injection of 20 mg of LPS (E.coli Serotype O111:B4, Sigma-Aldrich, Buchs, Switzerland) dissolved in 200 ml BSS (Sterofundin iso, B. Braun, Germany) containing $Na^+ = 145.0$ mmol/l, $K^+ = 4.0$ mmol/l, $Mg^{2+} = 1.0$ mmol/l, $Ca^{2+} = 2.5$ mmol/l, pH = 5.1–5.9, osmolarity = 309 mosm/l. The sham group received 200 ml of the vehicle (Sterofundin iso) intratracheally only. Pigs were monitored for 8 h after administration of LPS or vehicle. In particular, the response to LPS or vehicle administration was evaluated by the analysis of three parameters: ratio of intra-arterial partial oxygen pressure and inspiratory oxygen fraction (PaO_2/FiO_2), mean pulmonary arterial pressure (MPAP) and heart rate.

2.3. Determination of inflammatory cytokine levels in blood plasma

Plasma levels of the pro-inflammatory cytokines, tumor necrosis factor alpha (TNF-α) and interleukin-6 (IL-6), were determined by the use of enzyme-linked immunosorbent assay (ELISA) according to the manufacturer-provided instruction (Porcine TNF-alpha Quantikine ELISA and Porcine IL-6 Quantikine ELISA; R&D Systems, Germany) from blood samples collected 30 min after endotracheal intubation and before vehicle or LPS administration as well as 4 and 8 h after vehicle or LPS administration.

2.4. Measurement of vascular reactivity in ocular blood vessels

Eight hours after vehicle or LPS administration, the anesthetized pigs were killed by an overdose of intravenous administration of potassium chloride (1 M, 20 ml, Fresenius, Bad Homburg, Germany), which resulted in cardiac arrest. The eyes were enucleated and transferred into cold Krebs' buffer with the following ionic composition (in mM): 118.3 NaCl, 4.7 KCl, 2.5 $CaCl_2$, 1.2 $MgSO_4$, 1.2 KH_2PO_4, 25 $NaHCO_3$, 11 glucose. Next, arteries were isolated under a dissecting microscope using micro-scissors and fine-point tweezers. For retinal arteriole isolation, the eye was opened along the limbus using eye scissors, and the vitreous body was removed with tweezers. Then, Krebs buffer was injected under the retina to detach it from the pigment epithelium. Next, the detached retina was excised near the pars plana and removed from the eye globe to isolate retinal arterioles of the first order (Fig. 1A) with micro-scissors and fine-point tweezers. Short posterior ciliary arteries (Fig. 1B) were visualized by gently dissecting fat and connective tissue around the optic nerve close to the eye ball and then isolated using micro-scissors and fine-point tweezers. After cannulation onto two micropipettes in a perfusion chamber, blood vessels were sutured with 10-0 nylon monofilament suture and pressurized to 40 mm Hg under no-flow conditions by two single reservoirs filled with Krebs buffer. The chamber solution was maintained at 37 °C and continuously perfused by oxygenated (95%) and carbonated (5%) Krebs buffer at pH 7.4. Vascular responses were recorded by videomicroscopy. Vessels were used for experiments when at least 50% constriction from initial diameter to 100 mM of KCl was obtained. All retinal arterioles and ciliary arteries were equilibrated for 45 min. Concentration-response curves were first conducted for the thromboxane mimetic, 9,11-dideoxy-9α,11α-methanoepoxy prostaglandin F2α (U46619, 10^{-11}-10^{-6} M, Cayman Chemical, Ann Arbor, MI, USA).

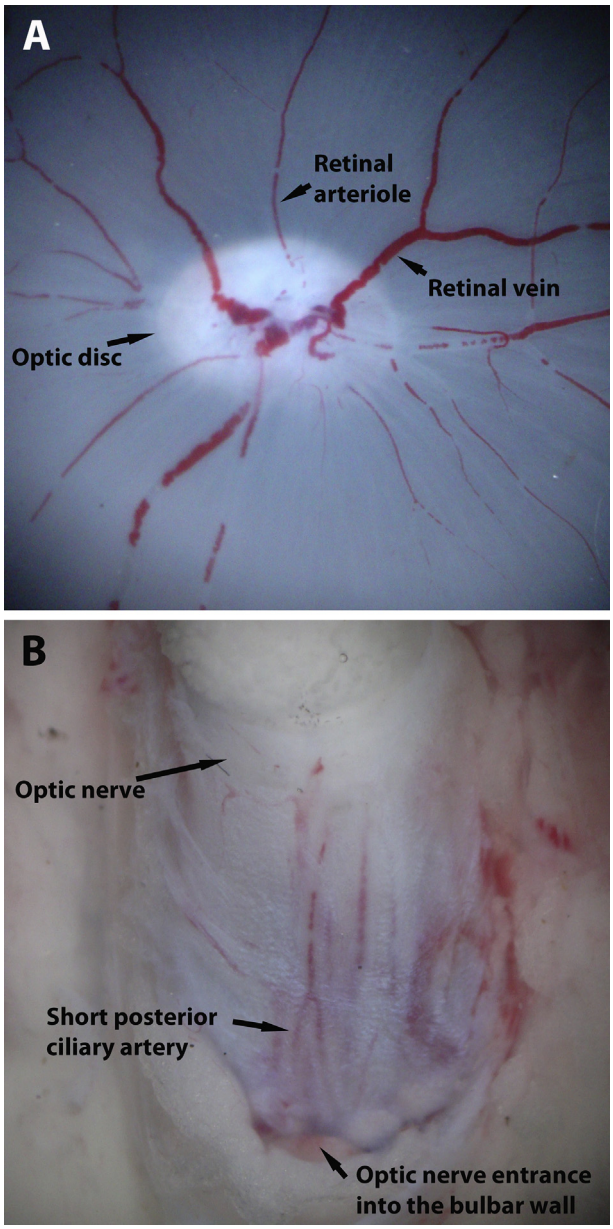

Fig. 1. (A) Photograph of the porcine ocular fundus showing first order retinal arterioles that have been used for the experiments. **(B)** Photograph of the optic nerve depicting the short posterior ciliary arteries that have been used for the experiments.

After U46619 had been washed out, vessels were again equilibrated for 45 min. When luminal diameter had reduced to 40–60% of the initial diameter by spontaneous tone, concentration response curves to the endothelium-dependent vasodilator, bradykinin (10^{-12}-10^{-7} M, Sigma-Aldrich Chemie GmbH), or the endothelium-independent vasodilator, sodium nitroprusside (SNP, 10^{-9}-10^{-4} M, Sigma-Aldrich Chemie GmbH), were conducted. Bradykinin was previously shown to induce endothelium-dependent vasodilation in both porcine retinal arterioles and ciliary arteries mainly via involvement of nitric oxide synthase metabolites (Dalsgaard et al., 2009; Jeppesen et al., 2002; Zhu et al., 1997). In vessels with weak intrinsic tone, luminal diameter was reduced to 40–60% of the initial diameter by titration of U46619 in order to ensure a similar level of preconstriction in all blood vessels before administration of bradykinin or SNP, respectively. Stock solutions of U46619 were dissolved in dimethyl sulfoxide (DMSO), whereas stock solutions of bradykinin and SNP were dissolved in PBS.

2.5. Detection of ROS in retinal arterioles and ciliary arteries

After pigs had been killed, blood vessels were rapidly isolated, fixed in Tissue-Tek O.C.T. Compound (Sakura Finetek Europe, Alphen aan den Rijn, Netherlands), snap frozen in liquid nitrogen, and stored at −80 °C until use. Freshly prepared cryostat sections (10 µm thickness, Leica Reichert Jung, 2030; Leica, Rijswijk, Netherlands) were incubated with 1 µM of dihydroethidium (DHE, Thermo Fischer Scientific, Waltham, USA) for 30 min at 37 °C. Fluorescence intensity was visualized by an Eclipse TS 100 microscope (Nikon, Yurakucho, Tokyo, Japan) with a DS – Fi1-U2 digital microscope camera (Nikon) and an ELWD 20x/0.45 S Plan Fluor Ph1 ADM objective (Nikon), recorded by the imaging software NIS Elements (Nikon, Version 1.10 64 bit) and quantified using ImageJ software.

2.6. Real-time PCR analysis

Once eyes had been enucleated, vessels were immediately isolated by using fine-point tweezers and microscissors, added into a 1,5 ml tube and snap-frozen. Tissue homogenization was conducted in lysis buffer (1,0% NP40, 0.5% sodium deoxycholate, 0.1% SDS, 10 mmol/l NaF, 80 mmol/l TRIS, pH 7.5). Using a light cycler (LC480, Roche Diagnostics, Mannheim, Germany) and StepOnePlus device (Applied Biosystems, Foster City, CA, United States) quantitative PCR was performed according to the manufacturer's protocol. SYBR Green was used for fluorescent detection of generated DNA during PCR. Primer sequences are listed in Table 1. Relative mRNA levels of target genes were quantified using comparative threshold (CT) normalized to the β-actin gene.

2.7. Immunostainings

Pieces of the retina containing segments of first-order retinal

Table 1
Primer sequences for mRNA expression studies.

Gene name	Primer sequence
NOX1	F: TCAGTTTTATTTCTGGCTGCTTGG
	R: CTTTCTCAGGGTGCGCCTAC
NOX2	F: CACTTCACGCCACGATTCAC
	R: TTGACTCGGGCGTTCACAC
NOX4	F: GTCCCAGTGTGTCTGCGTTAG
	R: TCTCGAAATCGTTCTGTCCAGTC
XO	F: TTTGCCATCAAGGACGCCAT
	R: CAGTGACACACAGGGAGGTG
CAT	F: GCTTCAACAGTGCCAACGAA
	R: ACTGAAGTTCTTGACCGCTTTC
GPx1	F: AGTTTGGACATCAGGAAAATGCC
	R: AGCATGAAGTTGGGCTCGAA
HO-1	F: GATGGCGTCCTTGTACCAC
	R: GACCGGGTTCTCCTTGTTGT
SOD1	F: GGGCACCATCTACTTCGAGC
	R: CTGCACTGGTACAGCCTTGT
SOD2	F: GGCCTACGTGAACAACCTGA
	R: AATTCCCCTTTGGGTTCCCC
SOD3	F: GAAGAGCTGGAAAGGTGCCC
	R: ATCTCCGTCACTTTGGCCTG
iNOS	F: ACTATTTCTTCCAGCTTAAGAGCC
	R: CTCGTAGGGAAATACAGCACCA
TNF-α	F: TTCTGCCTACTGCACTTCGAG
	R: TGAGACGATGATCTGAGTCCTT
IL-1β	F:ATAGTACCTGAACCCGCCAAG
	R: GTGCAGCACTTCATCTCTTTGG
HIF-1α	F: CGTGCGACCATGAGGAAATG
	R: GTGAAGTACTTTCCATGTTGCAG
VEGF-A	F: ATAGAGCGAGGCAAGAAAATCCC
	R: ACACGTCTGCGGATCTTGTA
β-actin	F:TGGACTACCTCCTGTCTGCT
	R:CCTAGGGGTGGGTTTCTGTG

arterioles were dissected, embedded in Tissue-Tek O.C.T. Compound (Sakura Finetek Europe) and snap frozen. Cross sections (10 μm thickness) were incubated with a rabbit polyclonal antibody directed either against HIF-1α (Novus Biologicals, Centennial, CO, USA; catalog number: NB 100-654; dilution 1:100; incubation time: 2 h at RT), vascular endothelial growth factor A (VEGF-A, Abcam, Waltham, MA, USA; catalog number: ab9570, dilution 1:100, incubation time: 2 h at RT) or nicotinamide adenine dinucleotide phosphate oxidase 2 (NOX2, Abcam; catalog number: ab80508, dilution 1:100, incubation time: 2 h at RT). A Rhodamine Red-X-coupled, goat anti-rabbit polyclonal secondary antibody (dianova GmbH, Hamburg, Germany; catalog number: 111-295-003; dilution 1:200, incubation time: 1 h at RT) was used. Negative control sections were incubated with blocking media and the secondary antibody. Slides were mounted using VECTASHIELD® Mounting Medium with 4′,6-diamidino-2-phenylindole (DAPI) (BIOZOL Diagnostica Vertrieb GmbH, Eching, Germany) and cover-slipped.

2.8. Histology

Pieces of the retina containing segments of first-order retinal arterioles were dissected, placed in cryomolds containing embedding medium (Tissue-Tek O.C.T. Compound; Sakura Finetek Germany, Staufen, Germany) and snap frozen in liquid nitrogen. Retinal cross-sections (10 μm) were cut, transferred onto glass slides, dried at room temperature, fixed for 20 min in 4% paraformaldehyde and washed twice for 5 min in purified water. Next, the cryosections were immersed in hematoxylin for 3 min and washed in purified water for 5 min. Subsequently, the slides were placed for 1 min into 95% ethanol and were stained for 1 min in eosin solution. After an ascending ethanol series (70, 96, and 100%), the slides were bathed for 10 min in xylene. Finally, the glass slides were mounted with Eukitt quick-hardening mounting medium (Sigma-Aldrich Chemie, Munich, Germany).

2.9. Statistical analysis

Time courses of PaO_2/FiO_2, pO_2, pCO_2, MAP, MPAP, heart rate, TNF-α and IL-6 levels as well as vascular concentration response curves were compared by two-way ANOVA for repeated measurements. Responses to U46619, bradykinin, SNP are presented as relative change in luminal diameter. For comparison of ROS and mRNA expression levels, an unpaired *t*-test was used. The significance level was set at 0.05, and n represents the number of pigs per group.

3. Results

3.1. Respiratory and cardiovascular characteristics

The PaO_2/FiO_2, which is a clinical indicator of hypoxemia due to pulmonary injury, was markedly reduced in LPS-treated compared to sham-treated pigs (n = 7 per group, *P < 0.05, Fig. 2A). The definition of ARDS requires a PaO_2/FiO_2 of < 300 and is categorized as mild ($PaO_2/FiO_2 \leq 300$), moderate ($PaO_2/FiO_2 \leq 200$) and severe $PaO_2/FiO_2 \leq 100$). According to this categorization, LPS-treated pigs developed moderate ARDS, whereas sham-treated developed mild ARDS. Intra-arterial partial oxygen pressure was also markedly reduced in LPS-treated pigs (n = 7 per group, *P < 0.05, Fig. 2B), whereas partial carbon dioxide pressure did not differ between the two groups (n = 7 per group, P > 0.05, Fig. 2C). Also, mean arterial pressure was similar in sham- and LPS-treated pigs (n = 7 per group, P > 0.05, Fig. 2D), whereas LPS-treated pigs developed severe pulmonary hypertension (mPAP ≥ 35 mmHg), indicative of increased vascular resistance in the pulmonary circulation, due to loss of microvascular endothelial function and hypoxia as typical characteristics of ARDS (n = 7 per group, ****P < 0.0001, Fig. 2E). Likewise, heart rate was increased in LPS- compared to sham-treated pigs (n = 7 per group, *P < 0.05, Fig. 2F). Moderate hypoxia and impairment of blood flow in the lung lead to reduced oxygen availability, which may result in increased heart rate, to compensate for the loss of oxygen supply.

3.2. Plasma cytokine levels

Levels of TNF-α remained constant during the experimental time of 8 h in sham-treated pigs, whereas they were elevated after 4 and 8 h in LPS-treated pigs (n = 7 per group, *P < 0.05, Fig. 3A). Similarly, levels of IL-6 remained constant throughout the experiment in the sham group, while they increased markedly over time in the LPS group

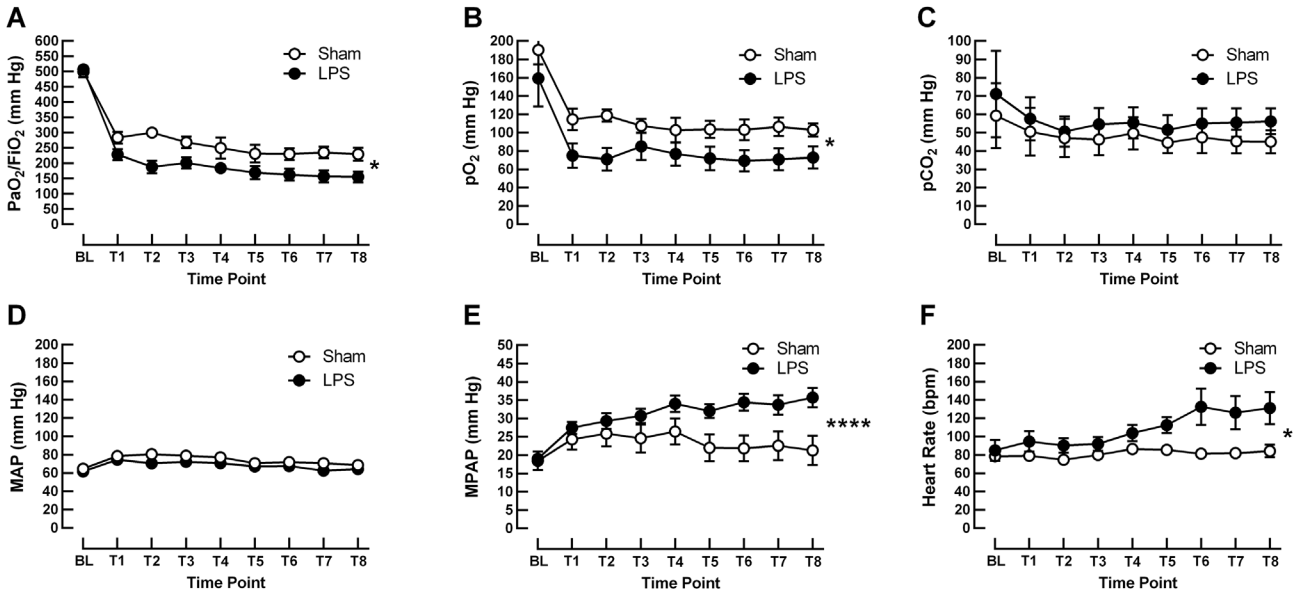

Fig. 2. Time courses of monitoring parameters in sham- and LPS-treated pigs for the experimental time of 8 h. The baseline (BL) measurement was done directly before application of LPS or vehicle (sham). **(A)** Ratio of intra-arterial partial oxygen pressure (PaO_2) and inspiratory oxygen fraction (FiO_2) (PaO_2/FiO_2). The definition of ARDS requires a PaO_2/FiO_2 of < 300 and is categorized as mild ($PaO_2/FiO_2 \leq 300$), moderate ($PaO_2/FiO_2 \leq 200$) and severe ($PaO_2/FiO_2 \leq 100$). **(B)** Partial oxygen pressure (pO_2). **(C)** Partial carbon dioxide pressure (pCO_2). **(D)** Mean arterial pressure (MAP). **(E)** Mean pulmonary arterial pressure (MPAP). **(F)** Heart rate. Data are presented as mean ± SE (n = 7 per group, *P < 0.05, ****P < 0.0001).

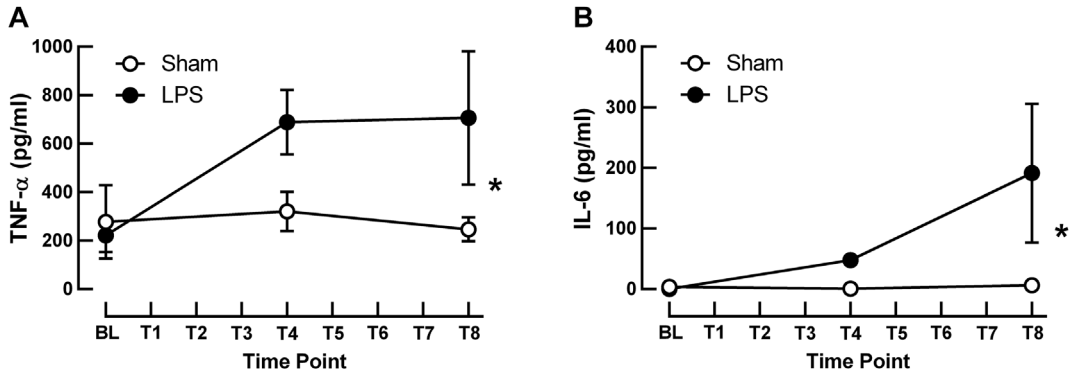

Fig. 3. Plasma levels of TNF-α **(A)** and IL-6 **(B)** at baseline (BL) as well as 4 and 8 h after LPS or vehicle (sham) application (n = 7 per group, *P < 0.05).

(n = 7 per group, *P < 0.05, Fig. 3B).

3.3. Responses of retinal arterioles and ciliary arteries

The initial luminal vessel diameter, measured 5 min after cannulation, was 78.97 ± 10.30 μm, 89.75 ± 9.091 μm, 105.5 ± 12.04 μm and 113.9 ± 16.91 μm in retinal arterioles from sham-treated pigs, retinal arterioles from LPS-treated pigs, ciliary arteries from sham-treated pigs and ciliary arteries from LPS-treated pigs, respectively (p > 0.05, one-way ANOVA and Tukey's multiple comparisons test). After development of spontaneous myogenic tone, mean luminal vessel diameter was 53.23 ± 11.44 μm, 58.93 ± 10.37 μm, 80.78 ± 12.65 μm and 88.39 ± 10.16 μm in retinal arterioles from sham-treated pigs, retinal arterioles from LPS-treated pigs, ciliary arteries from sham-treated pigs and ciliary arteries from LPS-treated pigs, respectively (p > 0.05, one-way ANOVA and Tukey's multiple comparisons test). The thromboxane mimetic, U46619, elicited concentration-dependent vasoconstrictor responses that were similar in retinal arterioles from sham- and LPS-treated pigs. For example, in response to 10^{-6} M of U46619, luminal diameter decreased by 39.44 ± 7.346% (n = 7) and by 43.57 ± 6.488% (n = 7) in sham- and LPS-treated pigs, respectively (Fig. 4A). The endothelium-independent vasodilator, SNP, elicited similar vasodilation responses in retinal arterioles of both sham-treated and LPS-treated pigs, which were 43.98 ± 7.215%

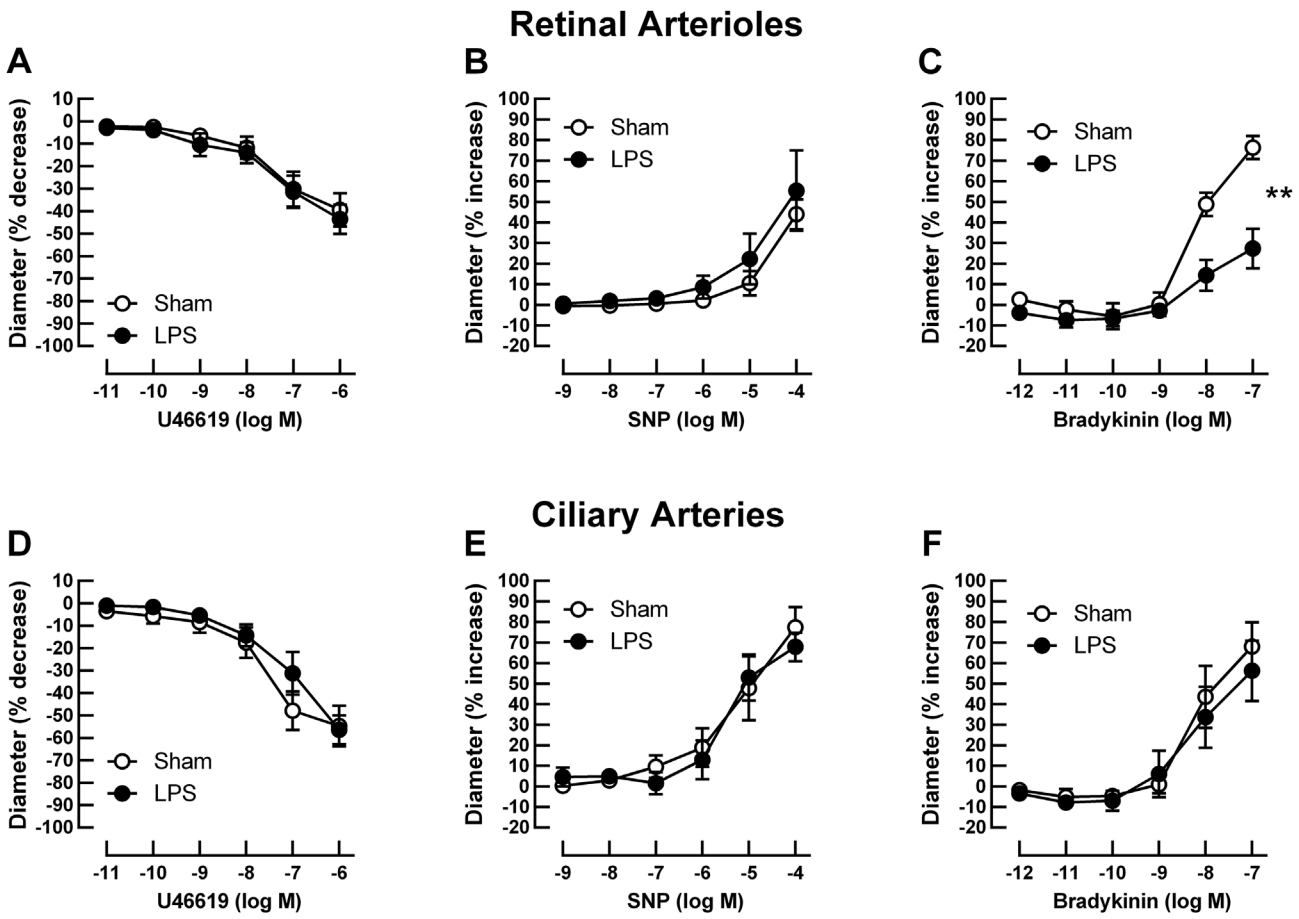

Fig. 4. Vascular responses of retinal arterioles to the vasoconstrictor, U46619 **(A)** and to the endothelium-independent vasodilator, SNP **(B)**, were similar in sham- and LPS-treated pigs. In contrast, reactivity to the endothelium-dependent vasodilator, bradykinin **(C)**, was reduced in retinal arterioles of LPS-treated pigs. Responses of ciliary arteries to U46619 **(D)**, SNP **(E)**, and bradykinin **(F)** were similar in both groups. Data are presented as mean ± SE (n = 7 per group, **P < 0.01).

(n = 7) and 55.43 ± 19.48% (n = 7), respectively (Fig. 4B). Of note, responses to the endothelium-dependent vasodilator, bradykinin, were markedly reduced in LPS-treated pigs (76.36 ± 5.557% versus 27.37 ± 9.597%, sham versus LPS at 10^{-7} M, n = 7 per group, Fig. 4C). In short posterior ciliary arteries, vasoconstrictor responses to U46619 did not differ between sham- and LPS-treated pigs (54.71 ± 9.107% versus 56.41 ± 6.463% at 10^{-6} M, n = 7 per group, Fig. 4D). Also, vasodilator responses to SNP (77.43 ± 9.882% versus 67.90 ± 6.960% at 10^{-4} M, n = 7 per group, Fig. 4E) and to bradykinin (68.00 ± 11.82% versus 56.27 ± 14.63% at 10^{-4} M, n = 7 per group, Fig. 4F) were similar in sham- and LPS-treated pigs.

3.4. Levels of reactive oxygen species

In cross-sections of retinal arterioles from LPS-treated pigs, a higher DHE fluorescence signal intensity was measured compared to those from sham-treated pigs (Fig. 5A), whereas no differences in fluorescence intensity were detected in cross-sections of short posterior ciliary arteries from both groups (Fig. 5B).

3.5. Expression of hypoxic, redox and inflammatory genes in retinal arterioles and ciliary arteries

In retinal arterioles, LPS-treatment resulted in markedly increased mRNA expression of two hypoxic markers, HIF-1α (≈125-fold; ***p < 0.001) and VEGF-A (≈9-fold; *p < 0.05), compared to the sham group (Fig. 6A). Also, mRNA expression for the prooxidative redox enzyme, NOX2 (≈12-fold; *p < 0.05), was markedly increased in retinal arterioles from LPS-treated pigs (Fig. 6A). In contrast, mRNA expression levels of the antioxidative enzymes catalase (CAT), glutathione peroxidase 1 (GPx1), heme oxygenase-1 (HO-1), superoxide dismutase 1, 2 and 3 (SOD 1, 2 and 3) and of the inflammatory markers, TNF-α, interleukin-1β (IL-1β) and inducible nitric oxide synthase (iNOS), did not differ between retinal arterioles of LPS- and sham-treated pigs (Fig. 6A). Interestingly, in short posterior ciliary arteries, mRNA expression levels did not differ for any of the tested genes between LPS- and sham-treated pigs (Fig. 6B).

3.6. Expression of HIF-1α, VEGF-A and NOX2 in retinal arterioles

In retinal arterioles from sham-treated pigs, immunoreactivity to the hypoxia marker, HIF-1α, was weak, diffuse and comparable in endothelium, smooth muscle layer and the surrounding retinal tissue (Fig. 7A). In contrast, retinal arterioles from LPS-treated pigs, displayed strong immunoreactivity in the endothelium (Fig. 7B). Immunoreactivity to the hypoxia and angiogenesis marker, VEGF-A, was faint in retinal arterioles from pigs of the sham group (Fig. 7C), whereas it was pronounced in the endothelium of pigs treated with LPS (Fig. 7D). Also, immunoreactivity to the prooxidative redox enzyme, NOX2, was weak in retinal arterioles from pigs of the sham group (Fig. 7E), while strong staining was seen in the endothelium of LPS-treated pigs (Fig. 7F).

3.7. Histological findings in the retina

Compared to retinal cross-sections of sham-treated pigs (Fig. 8A), cross-sections of LPS-treated pigs (Fig. 8B) displayed massive edematous thickening of the nerve fiber layer. Moreover, slight derangement

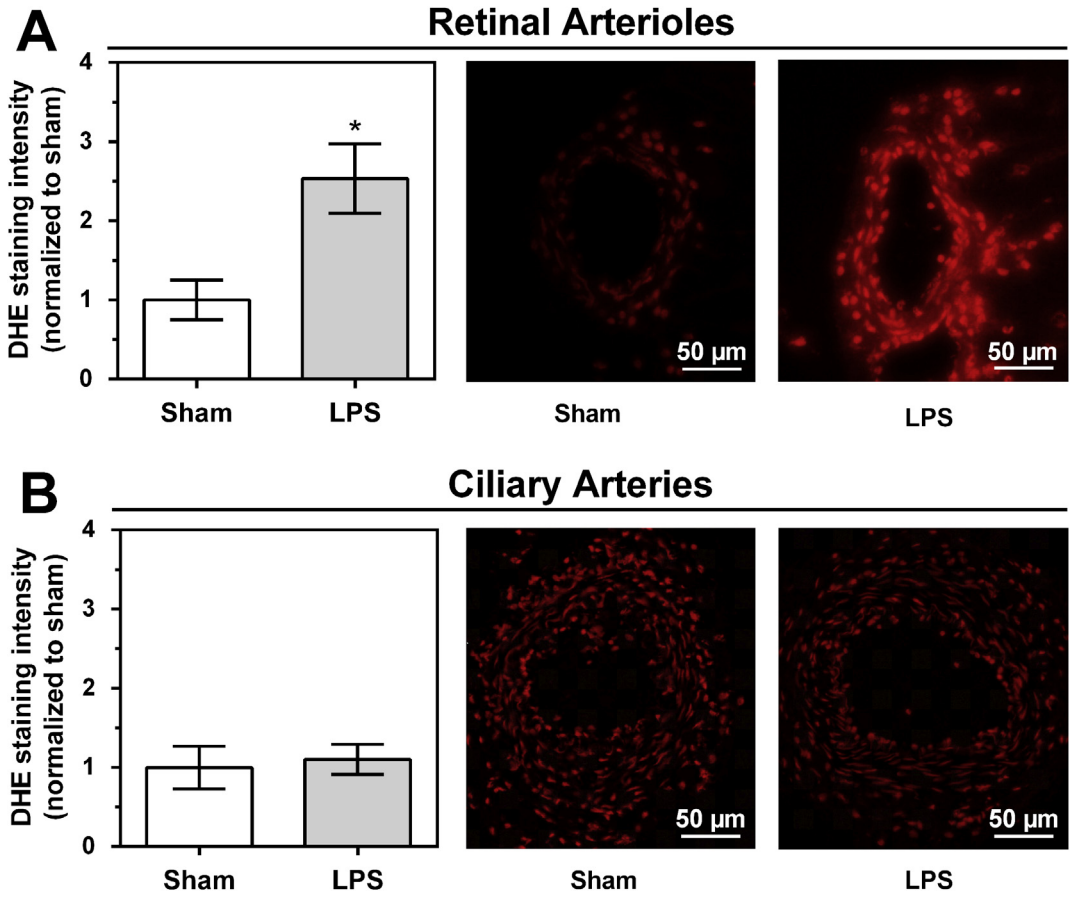

Fig. 5. DHE fluorescence intensity in cross-sections of retinal arterioles **(A)** and ciliary arteries **(B)** from sham- and LPS-treated pigs. Retinal arterioles of LPS-treated pigs showed a higher intensity of DHE fluorescence than retinal arterioles of the sham-treated group. In contrast, no differences in DHE fluorescence intensity were found between ciliary arteries of both groups. Data are presented as mean ± SE (n = 7 per group, *P < 0.05). Scale bar = 50 µm.

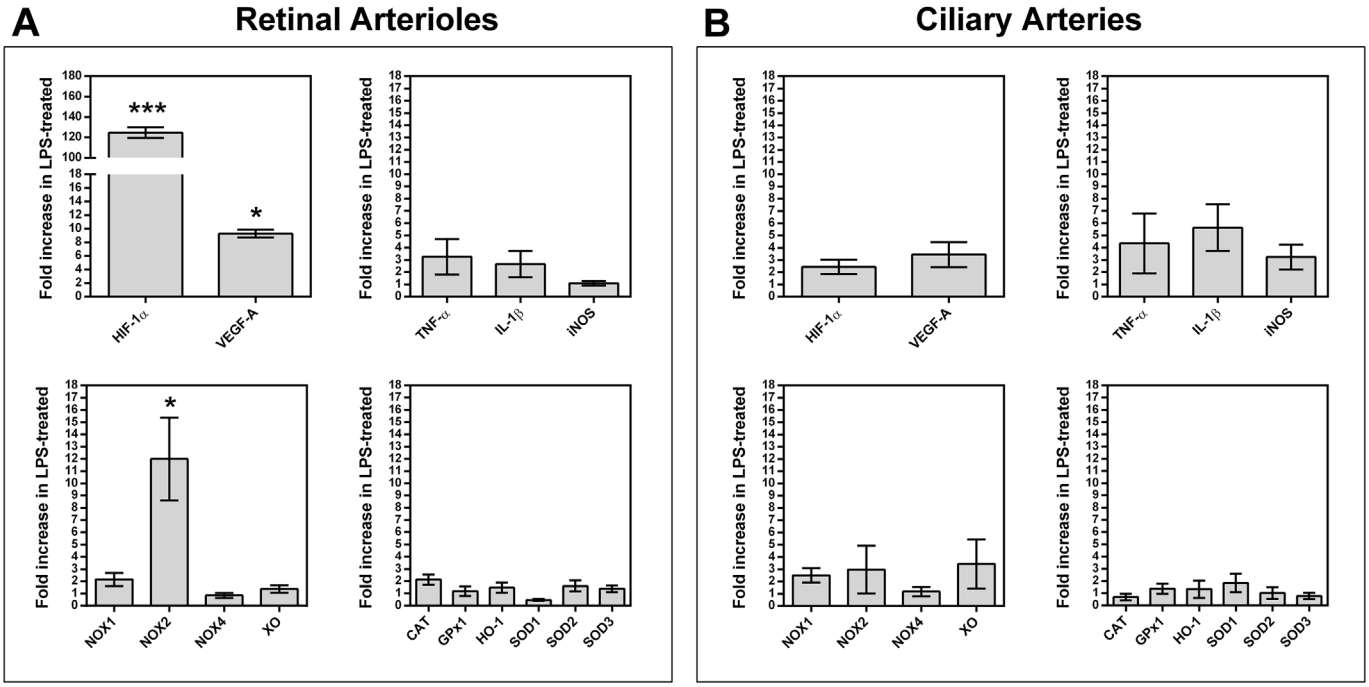

Fig. 6. Messenger RNA expression of hypoxia markers (HIF-1α, VEGF-A), inflammatory markers (TNFα, IL-1β, iNOS), prooxidative (NOX1, NOX2, NOX4, XO) and antioxidative redox enzymes (CAT, GPx1, HO-1, SOD1, SOD2, SOD3) in retinal arterioles **(A)** and in short posterior ciliary arteries **(B)**. Data are presented as the fold-change (mean ± SE) in LPS-treated pigs versus sham-treated pigs (n = 7 per group, *P < 0.05, ***P < 0.001).

of the arterial wall architecture was observed in retinal arterioles of LPS-treated pigs. In the other retinal layers, only minor changes were visible.

4. Discussion

There are several major new findings in the present study. First, intratracheal LPS administration induced moderate ARDS and sham-treatment mild ARDS in pigs. The development of mild ARDS in sham-treated pigs may be explained by distortion of pulmonary function by the administered vehicle volume of 200 ml. Remarkably, LPS-treated pigs had elevated serum levels of TNF-α and IL-6 and developed endothelial dysfunction in retinal arterioles but not in short posterior ciliary arteries compared to sham-treated pigs. Second, ROS levels were elevated in retinal arterioles, however, not in short posterior ciliary arteries of LPS-treated pigs. Third, mRNA expression for the hypoxic markers, HIF-1α and VEGF-A, as well as for the prooxidative redox enzyme, NOX2, was substantially increased in retinal arterioles of LPS-treated pigs. These findings were confirmed on the protein level by immunohistochemistry, where pronounced expression of HIF-1α, VEGF-A and NOX2 was visible in the endothelium. In contrast, mRNA expression was similar in short posterior ciliary arteries of sham- and LPS-treated pigs. Moreover, LPS-treated pigs displayed remarkable edema of the retinal nerve fiber layer, indicative of breakdown of the inner blood-retina barrier and vascular leakage.

The present study is the first to report the effects of ARDS on ocular vascular function. The syndrome was shown to be associated with high morbidity and mortality and bears a high risk for developing cognitive impairment (Mikkelsen et al., 2012; Pandharipande et al., 2013). Hence, it is reasonable to assume that ARDS may also affect ocular structures, such as the retina and optic nerve, which are parts of the central nervous system. Of note, retinal vessel abnormalities have been associated with reduced cognitive function, progression of brain microvascular disease and risk of stroke (Baker et al., 2007; Hanff et al., 2014; Wong et al., 2002). ARDS can experimentally be induced by either intravenous, intraperitoneal or intratracheal administration of LPS or other agents (Cheng et al., 2007; de Souza Xavier Costa et al., 2017; Everhart et al., 2006; Hartmann et al., 2015; Rittirsch et al., 2008; Ziebart et al., 2014). To examine the impact of a compromised respiratory function on ocular blood vessels, we have chosen to apply LPS intratracheally in order to minimize direct effects of the agent on extrapulmonary blood vessels, since previous clinical and experimental findings suggest that sepsis and systemic inflammation itself compromise ocular vascular function via direct effects of LPS or other toxins (Erikson et al., 2017).

Remarkably, we observed an increase of plasma levels for the cytokines, TNF-α and IL-6, indicative of substantial systemic inflammation. However, we did not observe any changes of the inflammatory markers, TNF-α, IL-1β, and iNOS, in ocular blood vessels of LPS-treated pigs, suggesting that intratracheally administered LPS induced only negligible inflammation in retinal and short posterior ciliary arteries. LPS-treated pigs developed a reduced PaO_2/FiO_2 and hypoxemia together with an increased pulmonary arterial pressure, which is consistent with other models of ARDS (Kamuf et al., 2017; Wang et al., 2010). Hypoxemia, a key pathogenic factor of ARDS, develops by disruption of alveolar-capillary membrane integrity, leading to an influx of protein-rich edema fluid into the alveolus leading to inactivation of surfactant (Johnson and Matthay, 2010). We found that the hypoxia markers, HIF-1α and VEGF-A, were markedly increased in the retinal arteriole endothelium of LPS-treated pigs indicating that moderate ARDS may have induced hypoxia in the retinal circulation. Hypoxia activates HIF-1α, which in turn promotes vascular leakage and angiogenesis by transcriptionally activating many angiogenic genes, such as VEGF-A (Kurihara et al., 2014; Lin et al., 2011; Yamakawa et al., 2003). However, it is also possible that circulating inflammatory cytokines directly triggered HIF-1α expression in the endothelium of retinal arterioles. For example, TNF-α, IL-6 and LPS were shown to induce HIF-1α expression in various cells also under normoxic conditions (Kuschel et al., 2012; Middleton et al., 2014). Remarkably, NOX2 expression was also substantially increased in the endothelium of retinal arterioles, which is in line with previous studies reporting on a pathogenic link between increased HIF-1α expression, subsequent upregulation of NOX2 and generation of ROS (Yuan et al., 2011). Excessive ROS accumulation in the vascular wall is well known to induce endothelial

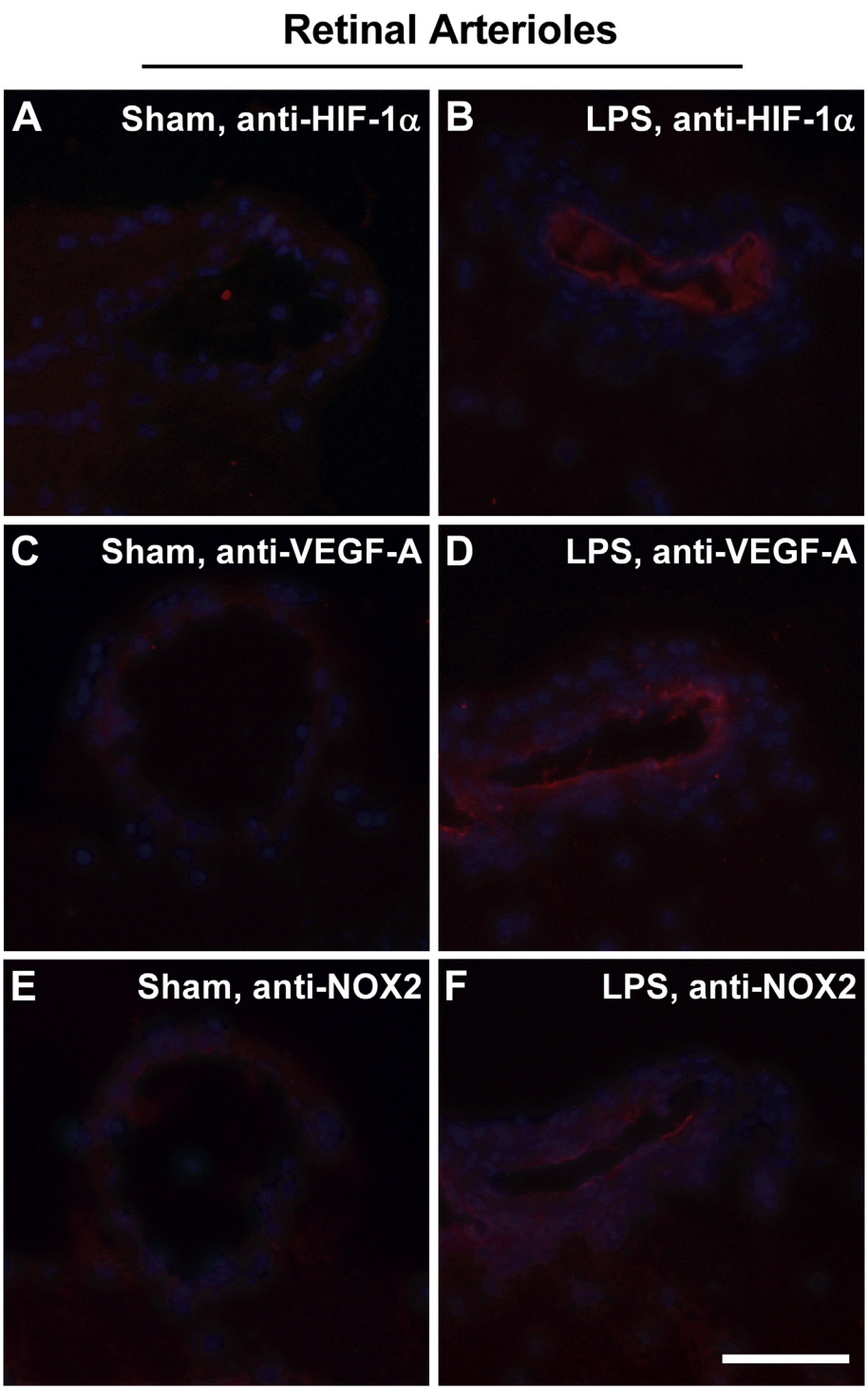

Fig. 7. Immunostainings with primary antibodies directed against HIF-1α, VEGF-A and NOX2 and a secondary antibody coupled with Rhodamine Red-X (red color) are presented as merged pictures with nucleic acid stain using DAPI (blue color). In retinal arterioles from vehicle-treated pigs (sham), immunoreactivity to the hypoxic marker, HIF-1α, was weak, diffuse and comparable in endothelial cells, the smooth muscle layer and the surrounding retinal tissue (A). In contrast, in retinal arterioles from LPS-treated pigs (LPS), strong immunoreactivity was seen in the endothelium (B). Immunoreactivity to the angiogenesis marker, VEGF-A, was faint in retinal arterioles from pigs of the sham group (C), whereas it was pronounced in the endothelium of pigs treated with LPS (D). Also, NOX2 immunoreactivity was weak and diffuse in retinal arterioles from pigs of the sham group (E), while marked staining was seen in the endothelium of LPS-treated pigs (F). Scale bar = 50 μm. (For interpretation of the references to color in this figure legend, the reader is referred to the Web version of this article.)

dysfunction as found in retinal arterioles of the present study (Forstermann et al., 2017; Ismaeel et al., 2018). Moreover, there is already strong evidence that NOX-derived reactive oxygen species play an important role in retinal neovascularization and ischemia-induced angiogenesis (Chan et al., 2013; Wei et al., 2016). Interestingly, mRNA for none of the tested inflammatory markers or antioxidative enzymes was altered in retinal arterioles. This is surprising, because these factors were previously shown to be upregulated in various models of brain or retinal hypoxia/ischemia (Agardh et al., 2006; Berger et al., 2008; Danielisova et al., 2005; Feuerstein et al., 1994; He et al., 2007; Yoneda et al., 2001). A plausible explanation for these results is that the time period of 8 h was too short to induce any inflammatory and antioxidative response in ocular blood vessels of our ARDS model, and we cannot rule out the possibility that such changes may occur in chronic stages of the disease. In contrast to retinal arterioles, short posterior ciliary arteries of LPS-treated pigs displayed neither endothelial dysfunction nor increased ROS levels suggesting that these vessels are more resistant to the effects of ARDS compared to retinal arterioles. Interestingly, neither mRNA for the hypoxia markers, HIF-1α and VEGF-A, nor for any of the inflammatory, prooxidative or antioxidative markers was altered in this vascular bed, suggesting that the threshold for inducing molecular and functional changes by ARDS is higher in short posterior ciliary arteries than in retinal arterioles. Already many differences between retinal arterioles and retrobulbar

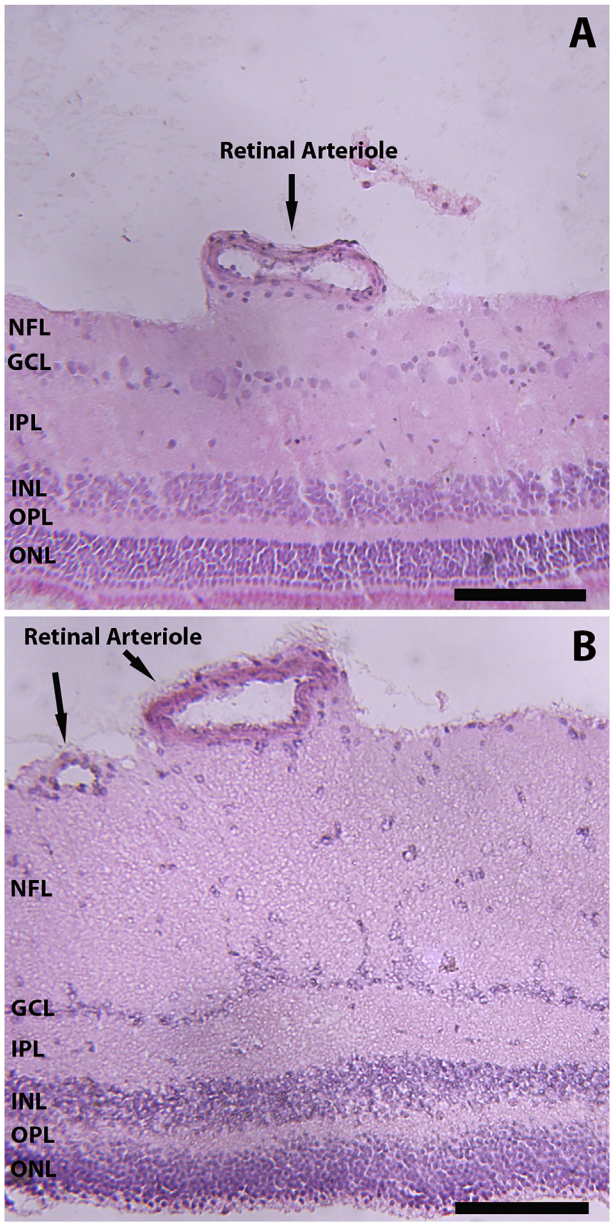

Fig. 8. Retinal cross-sections (H&E stain) of sham-treated (A) and LPS-treated pigs (B). Of note, remarkable edema was seen especially in the nerve fiber layer (NFL) of LPS-treated pigs, indicative of inner blood-retinal barrier breakdown. NFL: nerve fiber layer, GCL: ganglion cell layer, IPL: inner plexiform layer, INL: inner nuclear layer, OPL: outer plexiform layer, ONL: outer nuclear layer. Scale bar = 100 μm.

blood vessels have been reported with regard to their endothelial barrier function, autonomic innervation, and autoregulation (Bill, 1975; Bill and Nilsson, 1985; McDougal and Gamlin, 2015; Pournaras et al., 2008). Moreover, retinal arterioles and retrobulbar blood vessels differ with respect to their mechanisms of vascular reactivity under normal and pathophysiological conditions (Bohmer et al., 2014; Gericke et al., 2011, 2013, 2019; Manicam et al., 2016, 2017; Reimann et al., 2009; Senn et al., 1999). However, a different susceptibility of retinal arterioles and short posterior ciliary arteries to pathological changes induced by ARDS, such as hypoxemia and elevated circulating cytokine levels, has not been reported before. The underlying mechanisms should be pursued further in order to better understand the disease pathophysiology and to develop effective treatment strategies.

In conclusion, the findings of the present study provide evidence that LPS-induced ARDS evokes endothelial dysfunction in porcine retinal arterioles possibly via involvement of a HIF-1α – NOX2 – ROS pathway. Moreover, increased VEGF-A expression was observed in retinal arterioles together with pronounced edema in the retinal nerve fiber layer, indicative of increased vascular permeability, which may have been triggered by VEGF-A and ROS. In contrast to retinal arterioles, ciliary arteries appear to be resistant to LPS-induced ARDS.

Authors contributions statement

J.K.Z. conducted the experiments, analyzed the data and wrote the manuscript. Part of this study will be presented in the PhD thesis of J.K.Z. R.R. and E.H. have been involved in the design of the study and monitored the experiments. A.Z. contributed essential reagents and analysis tools and N.P. contributed essential materials. A.P. and M.L. performed measurements and contributed analysis tools. N.X. and H.L. contributed essential reagents. A.G. designed the study, analyzed and interpreted the data and contributed in writing the manuscript.

Declarations of interest

None.

Appendix A. Supplementary data

Supplementary data to this article can be found online at https://doi.org/10.1016/j.exer.2019.04.021.

References

Agardh, C.D., Gustavsson, C., Hagert, P., Nilsson, M., Agardh, E., 2006. Expression of antioxidant enzymes in rat retinal ischemia followed by reperfusion. Metab. Clin. Exp. 55, 892–898.
Baker, M.L., Marino Larsen, E.K., Kuller, L.H., Klein, R., Klein, B.E., Siscovick, D.S., Bernick, C., Manolio, T.A., Wong, T.Y., 2007. Retinal microvascular signs, cognitive function, and dementia in older persons: the Cardiovascular Health Study. Stroke 38, 2041–2047.
Bellani, G., Laffey, J.G., Pham, T., Fan, E., Brochard, L., Esteban, A., Gattinoni, L., van Haren, F., Larsson, A., McAuley, D.F., Ranieri, M., Rubenfeld, G., Thompson, B.T., Wrigge, H., Slutsky, A.S., Pesenti, A., Investigators, L.S., Group, E.T., 2016. Epidemiology, patterns of care, and mortality for patients with acute respiratory distress syndrome in intensive care units in 50 countries. Jama 315, 788–800.
Berger, S., Savitz, S.I., Nijhawan, S., Singh, M., David, J., Rosenbaum, P.S., Rosenbaum, D.M., 2008. Deleterious role of TNF-alpha in retinal ischemia-reperfusion injury. Investig. Ophthalmol. Vis. Sci. 49, 3605–3610.
Bill, A., 1975. Blood circulation and fluid dynamics in the eye. Physiol. Rev. 55, 383–417.
Bill, A., Nilsson, S.F., 1985. Control of ocular blood flow. J. Cardiovasc. Pharmacol. 7 (Suppl. 3), S96–S102.
Bohmer, T., Manicam, C., Steege, A., Michel, M.C., Pfeiffer, N., Gericke, A., 2014. The alpha(1)B -adrenoceptor subtype mediates adrenergic vasoconstriction in mouse retinal arterioles with damaged endothelium. Br. J. Pharmacol. 171, 3858–3867.
Caser, E.B., Zandonade, E., Pereira, E., Gama, A.M., Barbas, C.S., 2014. Impact of distinct definitions of acute lung injury on its incidence and outcomes in Brazilian ICUs: prospective evaluation of 7,133 patients*. Crit. Care Med. 42, 574–582.
Chan, E.C., van Wijngaarden, P., Liu, G.S., Jiang, F., Peshavariya, H., Dusting, G.J., 2013. Involvement of Nox2 NADPH oxidase in retinal neovascularization. Investig. Ophthalmol. Vis. Sci. 54, 7061–7067.
Cheng, D.S., Han, W., Chen, S.M., Sherrill, T.P., Chont, M., Park, G.Y., Sheller, J.R., Polosukhin, V.V., Christman, J.W., Yull, F.E., Blackwell, T.S., 2007. Airway epithelium controls lung inflammation and injury through the NF-kappa B pathway. J. Immunol. 178, 6504–6513.
Dalsgaard, T., Kroigaard, C., Bek, T., Simonsen, U., 2009. Role of calcium-activated potassium channels with small conductance in bradykinin-induced vasodilation of porcine retinal arterioles. Investig. Ophthalmol. Vis. Sci. 50, 3819–3825.
Danielisova, V., Nemethova, M., Gottlieb, M., Burda, J., 2005. Changes of endogenous antioxidant enzymes during ischemic tolerance acquisition. Neurochem. Res. 30, 559–565.
de Souza Xavier Costa, N., Ribeiro Junior, G., Dos Santos Alemany, A.A., Belotti, L., Zati, D.H., Frota Cavalcante, M., Matera Veras, M., Ribeiro, S., Kallas, E.G., Nascimento Saldiva, P.H., Dolhnikoff, M., Ferraz da Silva, L.F., 2017. Early and late pulmonary effects of nebulized LPS in mice: an acute lung injury model. PLoS One 12, e0185474.
Donoso, F.A., Arriagada, S.D., Cruces, R.P., 2015. [Pulmonary-renal crosstalk in the critically ill patient]. Rev. Chil. Pediatr. 86, 309–317.
Erikson, K., Liisanantti, J.H., Hautala, N., Koskenkari, J., Kamakura, R., Herzig, K.H., Syrjala, H., Ala-Kokko, T.I., 2017. Retinal arterial blood flow and retinal changes in patients with sepsis: preliminary study using fluorescein angiography. Crit. Care

21, 86.
Everhart, M.B., Han, W., Sherrill, T.P., Arutiunov, M., Polosukhin, V.V., Burke, J.R., Sadikot, R.T., Christman, J.W., Yull, F.E., Blackwell, T.S., 2006. Duration and intensity of NF-kappaB activity determine the severity of endotoxin-induced acute lung injury. J. Immunol. 176, 4995–5005.
Feuerstein, G.Z., Liu, T., Barone, F.C., 1994. Cytokines, inflammation, and brain injury: role of tumor necrosis factor-alpha. Cerebrovasc. Brain Metab. Rev. 6, 341–360.
Fioretto, J.R., Carvalho, W.B., 2013. Temporal evolution of acute respiratory distress syndrome definitions. J. Pediatr. 89, 523–530.
Forstermann, U., Xia, N., Li, H., 2017. Roles of vascular oxidative stress and nitric oxide in the pathogenesis of atherosclerosis. Circ. Res. 120, 713–735.
Gericke, A., Goloborodko, E., Sniatecki, J.J., Steege, A., Wojnowski, L., Pfeiffer, N., 2013. Contribution of nitric oxide synthase isoforms to cholinergic vasodilation in murine retinal arterioles. Exp. Eye Res. 109, 60–66.
Gericke, A., Kordasz, M.L., Steege, A., Sanbe, A., Goloborodko, E., Vetter, J.M., Patzak, A., Pfeiffer, N., 2011. Functional role of alpha1-adrenoceptor subtypes in murine ophthalmic arteries. Investig. Ophthalmol. Vis. Sci. 52, 4795–4799.
Gericke, A., Wolff, I., Musayeva, A., Zadeh, J.K., Manicam, C., Pfeiffer, N., Li, H., Xia, N., 2019. Retinal arteriole reactivity in mice lacking the endothelial nitric oxide synthase (eNOS) gene. Exp. Eye Res. 181, 150–156.
Hanff, T.C., Sharrett, A.R., Mosley, T.H., Shibata, D., Knopman, D.S., Klein, R., Klein, B.E., Gottesman, R.F., 2014. Retinal microvascular abnormalities predict progression of brain microvascular disease: an atherosclerosis risk in communities magnetic resonance imaging study. Stroke 45, 1012–1017.
Hartmann, E.K., Ziebart, A., Thomas, R., Liu, T., Schad, A., Tews, M., Moosmann, B., Kamuf, J., Duenges, B., Thal, S.C., David, M., 2015. Inhalation therapy with the synthetic TIP-like peptide AP318 attenuates pulmonary inflammation in a porcine sepsis model. BMC Pulm. Med. 15, 7.
He, T., Ai, M., Zhao, X.H., Xing, Y.Q., 2007. Inducible nitric oxide synthase mediates hypoxia-induced hypoxia-inducible factor-1 alpha activation and vascular endothelial growth factor expression in oxygen-induced retinopathy. Pathobiology: J. Immunopathol. Mol. Cell. Biol. 74, 336–343.
Ismaeel, A., Brumberg, R.S., Kirk, J.S., Papoutsi, E., Farmer, P.J., Bohannon, W.T., Smith, R.S., Eidson, J.L., Sawicki, I., Koutakis, P., 2018. Oxidative stress and arterial dysfunction in peripheral artery disease. Antioxidants 7.
Jeppesen, P., Aalkjaer, C., Bek, T., 2002. Bradykinin relaxation in small porcine retinal arterioles. Investig. Ophthalmol. Vis. Sci. 43, 1891–1896.
Johnson, E.R., Matthay, M.A., 2010. Acute lung injury: epidemiology, pathogenesis, and treatment. J. Aerosol Med. Pulm. Drug Deliv. 23, 243–252.
Kamuf, J., Garcia-Bardon, A., Duenges, B., Liu, T., Jahn-Eimermacher, A., Heid, F., David, M., Hartmann, E.K., 2017. Endexpiratory lung volume measurement correlates with the ventilation/perfusion mismatch in lung injured pigs. Respir. Res. 18, 101.
Kurihara, T., Westenskow, P.D., Friedlander, M., 2014. Hypoxia-inducible factor (HIF)/vascular endothelial growth factor (VEGF) signaling in the retina. Adv. Exp. Med. Biol. 801, 275–281.
Kuschel, A., Simon, P., Tug, S., 2012. Functional regulation of HIF-1 alpha under normoxia–is there more than post-translational regulation? J. Cell. Physiol. 227, 514–524.
Lin, M., Chen, Y., Jin, J., Hu, Y., Zhou, K.K., Zhu, M., Le, Y.Z., Ge, J., Johnson, R.S., Ma, J.X., 2011. Ischaemia-induced retinal neovascularisation and diabetic retinopathy in mice with conditional knockout of hypoxia-inducible factor-1 in retinal Muller cells. Diabetologia 54, 1554–1566.
Lucas, R., Verin, A.D., Black, S.M., Catravas, J.D., 2009. Regulators of endothelial and epithelial barrier integrity and function in acute lung injury. Biochem. Pharmacol. 77, 1763–1772.
Manicam, C., Ginter, N., Li, H., Xia, N., Goloborodko, E., Zadeh, J.K., Musayeva, A., Pfeiffer, N., Gericke, A., 2017. Compensatory vasodilator mechanisms in the ophthalmic artery of endothelial nitric oxide synthase gene knockout mice. Sci. Rep. 7, 7111.
Manicam, C., Staubitz, J., Brochhausen, C., Grus, F.H., Pfeiffer, N., Gericke, A., 2016. The gatekeepers in the mouse ophthalmic artery: endothelium-dependent mechanisms of cholinergic vasodilation. Sci. Rep. 6, 20322.
McDougal, D.H., Gamlin, P.D., 2015. Autonomic control of the eye. Compr. Physiol. 5, 439–473.
Middleton, K., Jones, J., Lwin, Z., Coward, J.I., 2014. Interleukin-6: an angiogenic target in solid tumours. Crit. Rev. Oncol.-Hematol. 89, 129–139.
Mikkelsen, M.E., Christie, J.D., Lanken, P.N., Biester, R.C., Thompson, B.T., Bellamy, S.L., Localio, A.R., Demissie, E., Hopkins, R.O., Angus, D.C., 2012. The adult respiratory distress syndrome cognitive outcomes study: long-term neuropsychological function in survivors of acute lung injury. Am. J. Respir. Crit. Care Med. 185, 1307–1315.
Pandharipande, P.P., Girard, T.D., Jackson, J.C., Morandi, A., Thompson, J.L., Pun, B.T., Brummel, N.E., Hughes, C.G., Vasilevskis, E.E., Shintani, A.K., Moons, K.G., Geevarghese, S.K., Canonico, A., Hopkins, R.O., Bernard, G.R., Dittus, R.S., Ely, E.W., Investigators, B.-I.S., 2013. Long-term cognitive impairment after critical illness. N. Engl. J. Med. 369, 1306–1316.
Pelosi, P., Rocco, P.R., 2011. The lung and the brain: a dangerous cross-talk. Crit. Care 15, 168.
Pournaras, C.J., Rungger-Brandle, E., Riva, C.E., Hardarson, S.H., Stefansson, E., 2008. Regulation of retinal blood flow in health and disease. Prog. Retin. Eye Res. 27, 284–330.
Ragaller, M., Richter, T., 2010. Acute lung injury and acute respiratory distress syndrome. J. Emergencies, Trauma, Shock 3, 43–51.
Reimann, M., Prieur, S., Lippold, B., Bornstein, S.R., Reichmann, H., Julius, U., Ziemssen, T., 2009. Retinal vessel analysis in hypercholesterolemic patients before and after LDL apheresis. Atherosclerosis Suppl. 10, 39–43.
Rezoagli, E., Fumagalli, R., Bellani, G., 2017. Definition and epidemiology of acute respiratory distress syndrome. Ann. Transl. Med. 5, 282.
Rittirsch, D., Flierl, M.A., Day, D.E., Nadeau, B.A., McGuire, S.R., Hoesel, L.M., Ipaktchi, K., Zetoune, F.S., Sarma, J.V., Leng, L., Huber-Lang, M.S., Neff, T.A., Bucala, R., Ward, P.A., 2008. Acute lung injury induced by lipopolysaccharide is independent of complement activation. J. Immunol. 180, 7664–7672.
Rubenfeld, G.D., Caldwell, E., Peabody, E., Weaver, J., Martin, D.P., Neff, M., Stern, E.J., Hudson, L.D., 2005. Incidence and outcomes of acute lung injury. N. Engl. J. Med. 353, 1685–1693.
Senn, B., Orgul, S., Keller, U., Dickermann, D., Dubler, B., Vavrecka, J., Gasser, P., Kaiser, H.J., Flammer, J., 1999. Retrobulbar and peripheral capillary blood flow in hypercholesterolemic subjects. Am. J. Ophthalmol. 128, 310–316.
Wang, H.M., Bodenstein, M., Duenges, B., Ganatti, S., Boehme, S., Ning, Y., Roehrig, B., Markstaller, K., 2010. Ventilator-associated lung injury superposed to oleic acid infusion or surfactant depletion: histopathological characteristics of two porcine models of acute lung injury. European surgical research. Europaische chirurgische Forschung. Recherches chirurgicales europeennes 45, 121–133.
Wei, Y., Gong, J., Xu, Z., Duh, E.J., 2016. Nrf2 promotes reparative angiogenesis through regulation of NADPH oxidase-2 in oxygen-induced retinopathy. Free Radical Biol. Med. 99, 234–243.
Wong, T.Y., Klein, R., Sharrett, A.R., Nieto, F.J., Boland, L.L., Couper, D.J., Mosley, T.H., Klein, B.E., Hubbard, L.D., Szklo, M., 2002. Retinal microvascular abnormalities and cognitive impairment in middle-aged persons: the Atherosclerosis Risk in Communities Study. Stroke 33, 1487–1492.
Yamakawa, M., Liu, L.X., Date, T., Belanger, A.J., Vincent, K.A., Akita, G.Y., Kuriyama, T., Cheng, S.H., Gregory, R.J., Jiang, C., 2003. Hypoxia-inducible factor-1 mediates activation of cultured vascular endothelial cells by inducing multiple angiogenic factors. Circ. Res. 93, 664–673.
Yoneda, S., Tanihara, H., Kido, N., Honda, Y., Goto, W., Hara, H., Miyawaki, N., 2001. Interleukin-1 beta mediates ischemic injury in the rat retina. Exp. Eye Res. 73, 661–667.
Yuan, G., Khan, S.A., Luo, W., Nanduri, J., Semenza, G.L., Prabhakar, N.R., 2011. Hypoxia-inducible factor 1 mediates increased expression of NADPH oxidase-2 in response to intermittent hypoxia. J. Cell. Physiol. 226, 2925–2933.
Zhu, P., Beny, J.L., Flammer, J., Luscher, T.F., Haefliger, I.O., 1997. Relaxation by bradykinin in porcine ciliary artery. Role of nitric oxide and K(+)-channels. Investig. Ophthalmol. Vis. Sci. 38, 1761–1767.
Ziebart, A., Hartmann, E.K., Thomas, R., Liu, T., Duenges, B., Schad, A., Bodenstein, M., Thal, S.C., David, M., 2014. Low tidal volume pressure support versus controlled ventilation in early experimental sepsis in pigs. Respir. Res. 15, 101.

International Journal of
Molecular Sciences

MDPI

Article

Short-Time Ocular Ischemia Induces Vascular Endothelial Dysfunction and Ganglion Cell Loss in the Pig Retina

Jenia Kouchek Zadeh [1,*], Andreas Garcia-Bardon [2], Erik Kristoffer Hartmann [2], Norbert Pfeiffer [1], Wael Omran [1], Marion Ludwig [3], Andreas Patzak [3], Ning Xia [4], Huige Li [4] and Adrian Gericke [1]

1 Department of Ophthalmology, University Medical Center, Johannes Gutenberg University Mainz, 55131 Mainz, Germany; norbert.pfeiffer@unimedizin-mainz.de (N.P.); w.omran90@gmail.com (W.O.); adrian.gericke@unimedizin-mainz.de (A.G.)
2 Department of Anesthesiology, University Medical Center, Johannes Gutenberg University Mainz, 55131 Mainz, Germany; a.garciabardon@uni-mainz.de (A.G.-B.); hartmane@uni-mainz.de (E.K.H.)
3 Institute of Vegetative Physiology, Charité-Universitätsmedizin Berlin, Charitéplatz 1, 10117 Berlin, Germany; marion.ludwig@charite.de (M.L.); andreas.patzak@charite.de (A.P.)
4 Department of Pharmacology, University Medical Center, Johanens Gutenberg University Mainz, 55131 Mainz, Germany; xianing@uni-mainz.de (N.X.); huigeli@uni-mainz.de (H.L.)
* Correspondence: je.kouchek@hotmail.de

Received: 20 August 2019; Accepted: 18 September 2019; Published: 21 September 2019

Abstract: Visual impairment and blindness are often caused by retinal ischemia-reperfusion (I/R) injury. We aimed to characterize a new model of I/R in pigs, in which the intraocular pathways were not manipulated by invasive methods on the ocular system. After 12 min of ischemia followed by 20 h of reperfusion, reactivity of retinal arterioles was measured in vitro by video microscopy. Dihydroethidium (DHE) staining, qPCR, immunohistochemistry, quantification of neurons in the retinal ganglion cell layer, and histological examination was performed. Retinal arterioles of I/R-treated pigs displayed marked attenuation in response to the endothelium-dependent vasodilator, bradykinin, compared to sham-treated pigs. DHE staining intensity and messenger RNA levels for *HIF-1α*, *VEGF-A*, *NOX2*, and *iNOS* were elevated in retinal arterioles following I/R. Immunoreactivity to HIF-1α, VEGF-A, NOX2, and iNOS was enhanced in retinal arteriole endothelium after I/R. Moreover, I/R evoked a substantial decrease in Brn3a-positive retinal ganglion cells and noticeable retinal thickening. In conclusion, the results of the present study demonstrate that short-time ocular ischemia impairs endothelial function and integrity of retinal blood vessels and induces structural changes in the retina. HIF-1α, VEGF-A, iNOS, and NOX2-derived reactive oxygen species appear to be involved in the pathophysiology.

Keywords: I/R injury; retinal arterioles; endothelial dysfunction; ganglion cell loss

1. Introduction

Ischemia-reperfusion (I/R) events represent a major reason for various retinal disorders [1,2]. For example, breakdown of retinal blood flow, as observed in central retinal artery occlusion (CRAO), is known to have a deleterious impact on visual acuity after already a short time period and represents an ophthalmic emergency with an incidence of approximately 1 per 100,000 people [3]. The lack of oxygen supply to the retina results in massive visual impairment and often in additional sequelae, such as retinal and vitreous hemorrhage, retinal neovascularization, or neovascular glaucoma [4]. Arterial fibrinolysis has failed to improve the clinical outcome of CRAO compared to conservative

treatment (e.g., aspirin, ocular massage) or was even shown to be harmful [5,6]. These studies suggest that deleterious, yet poorly understood, molecular processes are activated already in the early phase of retinal ischemia. Although duration of ischemia is a major factor determining tissue damage [7–9], the experimental methods to induce retinal or ocular ischemia differ substantially and may also have an impact on the experimental outcome. For example, raising intraocular pressure by cannulation of the anterior chamber and administering saline solution leads to complete occlusion of retinal and ciliary vessels and represents a favorable method to investigate overall alterations within the ocular system due to complete ischemia. An advantage of this method is that it does not require much equipment or technical expertise. However, this technique may also induce tissue damage by mechanical disruption of cellular structures and direct triggering of reactive oxygen species (ROS) production, which may hamper the interpretation of results [10–12]. Other models are based on the administration of endothelin-1 or photosensitive rose bengal to induce a partial, dose-dependent vasoconstriction of blood vessels [8,13,14]. The minimally invasive method of applying rose bengal allows for the investigation of ischemia-related molecular pathways [15,16]. However, since a wide range of ocular diseases is associated with reperfusion injury due to restoration of blood flow [1,17], rose bengal may not be suitable to investigate I/R injury because vascular occlusion is induced permanently with this method. Although application of endothelin-1 represents a non-invasive method to induce endogenous vasoconstriction of vessels, it affects physiological pathways by binding to ET_A and ET_B receptors, which may induce direct release of cytokines and ROS [18].

The goal of this study was to test a new method to induce transient ocular ischemia by complete blockade of arterial blood flow to the eye and brain in pigs, which represent a large animal model with similar ocular characteristics as humans [19–22]. We tested the hypothesis that 12 min of complete ischemia are enough to induce vascular dysfunction and retinal tissue damage. Another objective of this study was to determine potential molecular mechanisms that are activated after 12 min of ischemia and 20 h of reperfusion.

2. Results

2.1. Effects of I/R on Monitoring Parameters

At baseline, cerebral oxygen saturation was similar in I/R- and sham-treated pigs (44.9 ± 3.10% and 45.7 ± 2.08%, respectively). During occlusion of vessels supplying the eyes and brain, cerebral oxygen saturation dropped to 24.5 ± 2.33% in the I/R group, while it remained stable at the same time point in the sham group (48.3 ± 5.41%), indicative of ischemia due to reduced blood flow, as shown in Figure 1A. Furthermore, occlusion caused severe tachycardia in the I/R-treated group (125 ± 11.3 bpm versus 81.5 ± 5.52 bpm in I/R versus sham, respectively), as shown in Figure 1B. Mean arterial pressure (MAP) was similar in both groups at baseline but increased in the I/R group when cerebral blood flow was interrupted (125 ± 14.0 mm Hg versus 73.3 ± 4.08 mm Hg in I/R versus sham, respectively), as shown in Figure 1C.

2.2. Effects of I/R on Vascular Responses in Retinal Arterioles

Baseline diameters measured 5 min after cannulation were similar in retinal arterioles from sham- and I/R-treated pigs, as shown in Table 1. Vascular responses in retinal arterioles were measured after development of myogenic tone, which did also not differ between both groups, as shown in Table 1. Vasoconstriction responses to the thromboxane mimetic, U46619, were similar in retinal arterioles from I/R- and sham-treated pigs, as shown in Table 1 and Figure 2A. Likewise, endothelium-independent vasodilatory responses to sodium nitroprusside (SNP) were similar in I/R- and sham-treated pigs, as shown in Table 1 and Figure 2B. In contrast, responses to the endothelium-dependent vasodilator, bradykinin, were impaired in arterioles of the I/R group. Table 1 and Figure 2 show baseline diameters and maximum diameter changes of both groups in response to pharmacological substances used.

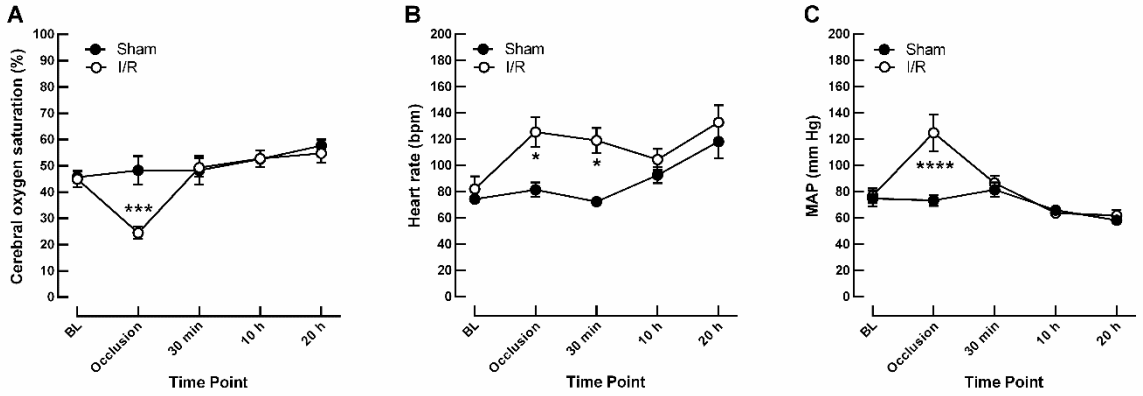

Figure 1. Time courses of cerebral oxygen saturation measured by INVOS™ 5100C (**A**), of heart rate (**B**) and of mean arterial blood pressure (MAP) (**C**) at baseline (BL), during the occlusion time of 12 min (occlusion), 30 min after releasing the occlusion, and after a reperfusion time of 10 and 20 h. Data are expressed as mean ± SE (n = 6 per timepoint and group, * $p < 0.05$, *** $p < 0.001$, **** $p < 0.0001$). I/R = ischemia-reperfusion.

Table 1. Initial diameter (baseline) 5 min after cannulation; basal arteriolar tone after 45 min of equilibration (myogenic tone) in % from baseline. Maximum vascular diameter changes of retinal arterioles to the thromboxane mimetic, U46619, to sodium nitroprusside (SNP) and to bradykinin in % from baseline (myogenic tone). Data are presented as means ± SE.

		Diameter Changes [%]			
	Baseline [µm]	**Myogenic Tone [%]**	**U46619 at 10^{-6} M[%]**	**SNP at 10^{-4} M [%]**	**Bradykinin at 10^{-7} M [%]**
Sham	85.5 ± 20.6	−46.1 ± 5.79	−41.6 ± 9.89	42.3 ± 5.62	82.0 ± 8.85
I/R	91.8 ± 24.7	−42.7 ± 4.18	−35.2 ± 5.11	35.6 ± 8.06	34.5 ± 8.02

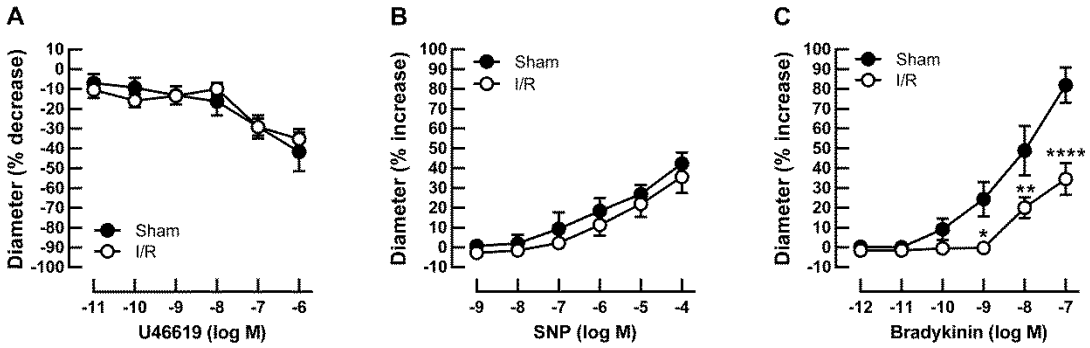

Figure 2. Concentration-dependent responses in retinal arterioles from I/R- and sham-treated pigs to U46619 (**A**), the endothelium-independent vasodilator, SNP (**B**), and to the endothelium-dependent vasodilator, bradykinin (**C**). Data are expressed as mean ± SE (n = 6 per concentration and group; * $p < 0.05$, ** $p < 0.01$, **** $p < 0.0001$).

2.3. Messenger RNA Expression Levels in Isolated Retinal Arterioles

The primer sequences used for PCR analysis are listed in Table 2. In isolated retinal arterioles from I/R-treated pigs, mRNA expression levels were increased for the hypoxic markers, *HIF-1α* and *VEGF-A*, compared to sham-treated pigs (*HIF-1α* ≈ 1.7-fold; * $p < 0.05$ and *VEGF-A* ≈ 2.2-fold, * $p < 0.05$, n = 6 per group), as shown in Figure 3A. In contrast, there were no differences in mRNA expression levels for the inflammatory cytokines, *TNF-α* and *IL-1β*, among both groups, as shown in Figure 3B. Furthermore, I/R elicited markedly increased mRNA expression levels for the prooxidant redox enzyme, *NOX2* (≈ 28-fold, ** $p < 0.01$), as shown in Figure 3C. By analyzing mRNA expression levels of all three nitric oxide synthase isoforms (*NOS*), we found that I/R raised expression for inducible NOS (*iNOS*) by

≈ 2.2-fold (* $p < 0.05$), whereas the expression for endothelial and neuronal NOS (*eNOS* and *nNOS*, respectively) did not differ between the two groups, as shown in Figure 3D.

Table 2. Primer sequences for mRNA expression studies.

Gene Name	Primer Sequence
NOX1	F: TCAGTTTTATTTCTGGCTGCTTGG R: CTTTCTCAGGGTGCGCCTAC
NOX2	F: CACTTCACGCCACGATTCAC R: TTGACTCGGGCGTTCACAC
NOX4	F: GTCCCAGTGTGTCTGCGTTAG R: TCTCGAAATCGTTCTGTCCAGTC
eNOS	F: CTACAGGACCCAAGATGGGC R: TGAAGCAGGGTACAGGGTCT
nNOS	F: ATTTTCGGAGTCACCCTGCG R: AGCTGAAAACCTCATCTGTGTCT
iNOS	F: ACTATTTCTTCCAGCTTAAGAGCC R: CTCGTAGGGAAATACAGCACCA
TNF-α	F: TTCTGCCTACTGCACTTCGAG R: TGAGACGATGATCTGAGTCCTT
IL-1β	F: ATAGTACCTGAACCCGCCAAG R: GTGCAGCACTTCATCTCTTTGG
HIF-1α	F: CGTGCGACCATGAGGAAATG R: GTGAAGTACTTTCCATGTTGCAG
VEGF-A	F: ATAGAGCGAGGCAAGAAAATCCC R: ACACGTCTGCGGATCTTGTA
β-actin	F: TGGACTACCTCCTGTCTGCT R:CCTAGGGGTGGGTTTCTGTG

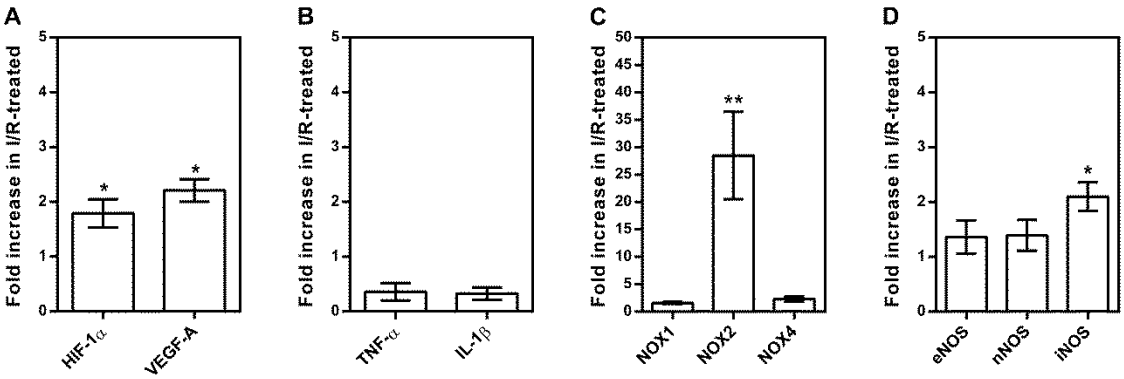

Figure 3. Messenger RNA expression for hypoxic markers (*HIF-1α, VEGF-A*) (**A**), inflammatory cytokines (*TNFα, IL-1ß*) (**B**), prooxidant redox enzymes (*NOX1, NOX2, NOX4*) (**C**), and individual nitric oxide synthase (*NOS*) isoforms (*eNOS, nNOS, iNOS*) (**D**). Data are presented as fold-change in mRNA expression levels in I/R-treated relative to sham-treated pigs. Data are presented as mean ± SE ($n = 6$ per group; * $p < 0.05$, ** $p < 0.01$).

2.4. Immunofluorescence

Immunoreactivity to the hypoxic markers, HIF-1α and VEGF-A, to the prooxidant redox enzyme, NOX2, as well as to iNOS was increased in the endothelium of retinal arterioles from I/R-treated pigs, which is in line with the elevated mRNA expression levels found in the arterioles, as shown in Figure 4.

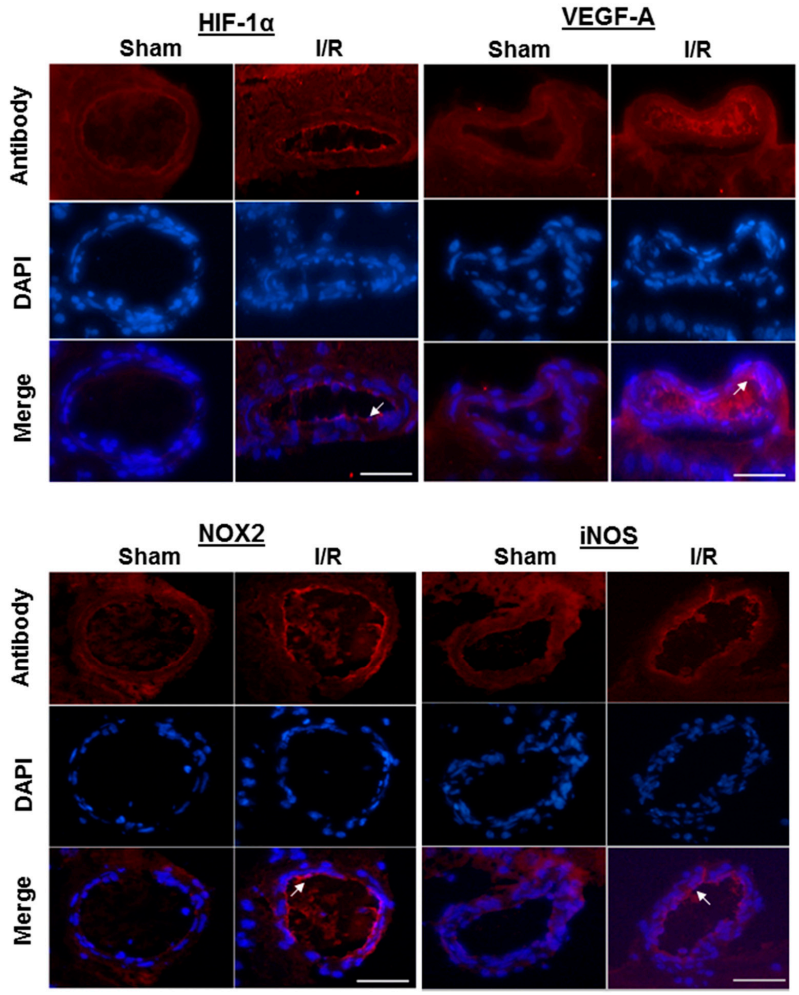

Figure 4. Immunofluorescence micrographs of retinal arteriole cross-sections from sham-treated and I/R-treated pigs stained for HIF-1α, VEGF-A, NOX2, and iNOS. The white arrows point to the endothelial cell layer. Scale bar = 50 μm.

2.5. Levels of Reactive Oxygen Species

Dihydroethidium (DHE) staining of retinal arteriole cross-sections revealed enhanced fluorescence intensity in the vascular wall of arterioles from I/R-treated pigs, indicative of elevated ROS concentrations compared to sham-treated pigs, as shown in Figure 5.

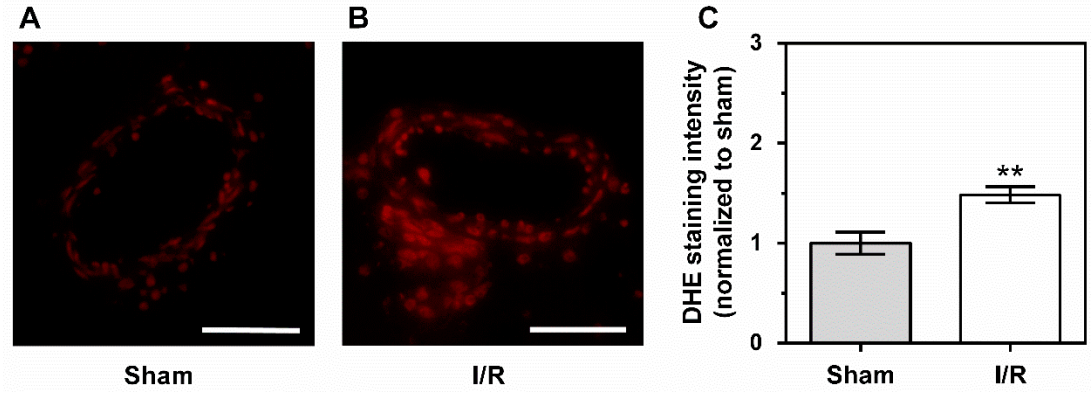

Figure 5. Photomicrographs of dihydroethidium (DHE)-stained retinal arteriole cross-sections from sham- (**A**) and I/R-treated pigs (**B**). DHE staining intensity was markedly increased in I/R-treated pigs (**C**). Data are represented as mean ± SE (n = 6 per group; ** $p < 0.01$). Scale bar = 50 μm.

2.6. Cells in the Retinal Ganglion Cell Layer

To examine whether cell viability was affected in the retinal ganglion cell (RGC) layer of this I/R model, the density of DAPI-positive cells, which represents the overall cell density in the RGC layer, and the density of Brn3a-positive cells, representing the RGC population, was determined. Figure 6 shows the area selected for cell counting from the midperiphery of the porcine retina.

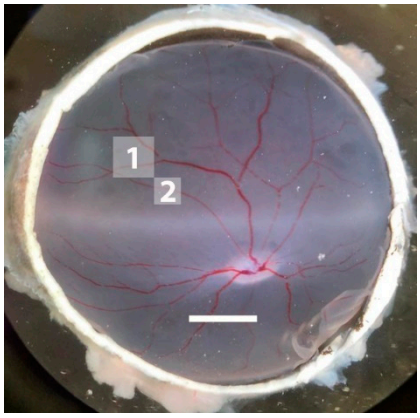

Figure 6. Representative photograph of a pig retina. The marked area labeled with "1" has been used for staining of cells using DAPI and an antibody directed against Brn3a. Just from the area below marked with "2" tissue for histological analysis was taken. Scale bar = 5 mm.

The density of DAPI-stained cell nuclei in the RGC layer did not differ between I/R- and sham-treated pigs (2254 ± 130 cells/mm^2 versus 2009 ± 178 cells/mm^2), as shown in Figure 7. In contrast, a reduction in density of Brn3a-positive cells by 34.3% was observed in I/R-treated pigs compared to sham-treated pigs (424 ± 45.2 cells/mm^2 versus 645 ± 64.4 cells/mm^2), as shown in Figure 7.

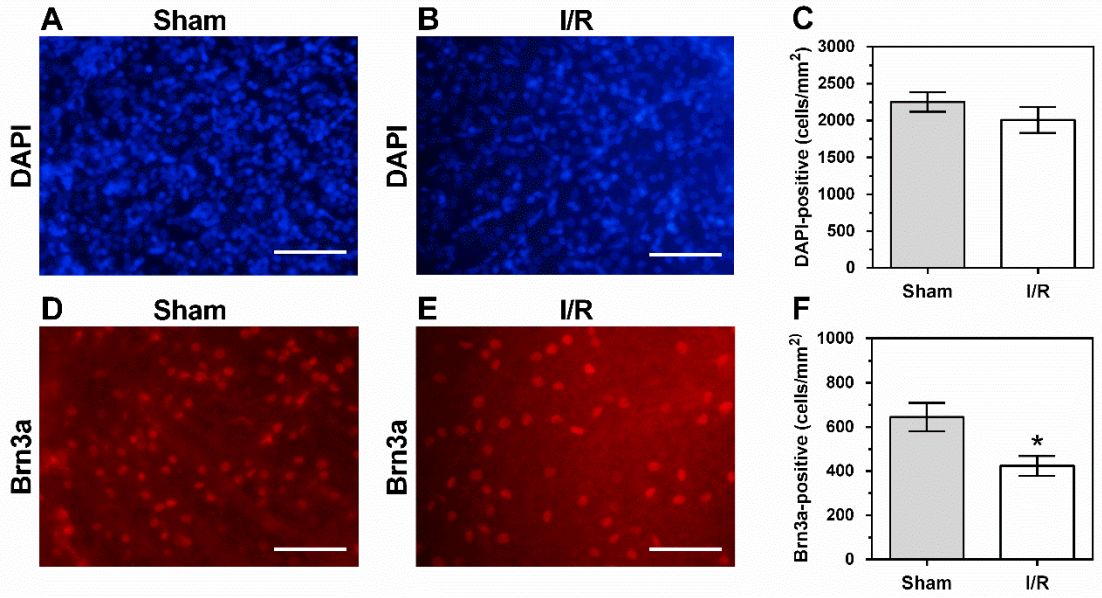

Figure 7. Representative pictures of DAPI-positive cells in sham-treated (**A**) and in I/R-treated pig retinas (**B**). No differences in density of DAPI-positive cells were detected between both groups (**C**). Pictures of Brn3a-stained cells in sham-treated (**D**) and in I/R-treated pigs (**E**). Of note, density of Brn3a-stained cells was markedly reduced in the I/R group (**F**). Data are presented as mean ± SE (n = 6 per group; * $p < 0.05$). Scale bar = 100 µm.

2.7. Retinal Histology

Compared to retinal tissue from sham-treated pigs, as shown in Figure 8A, retinas of I/R- treated pigs displayed fluid accumulation in the nerve fiber layer, especially localized around the arterioles, as shown in Figure 8B. In addition, derangement of the arterial wall architecture was visible in retinal arterioles from the I/R group, suggesting a disturbed vascular integrity. In addition, the RGC layer appeared disorganized in the I/R-treated group. Retinal thickness was markedly increased following I/R-treatment compared to sham-treatment (318 ± 41 µm versus 216 ± 12 µm, respectively), as shown in Figure 8C.

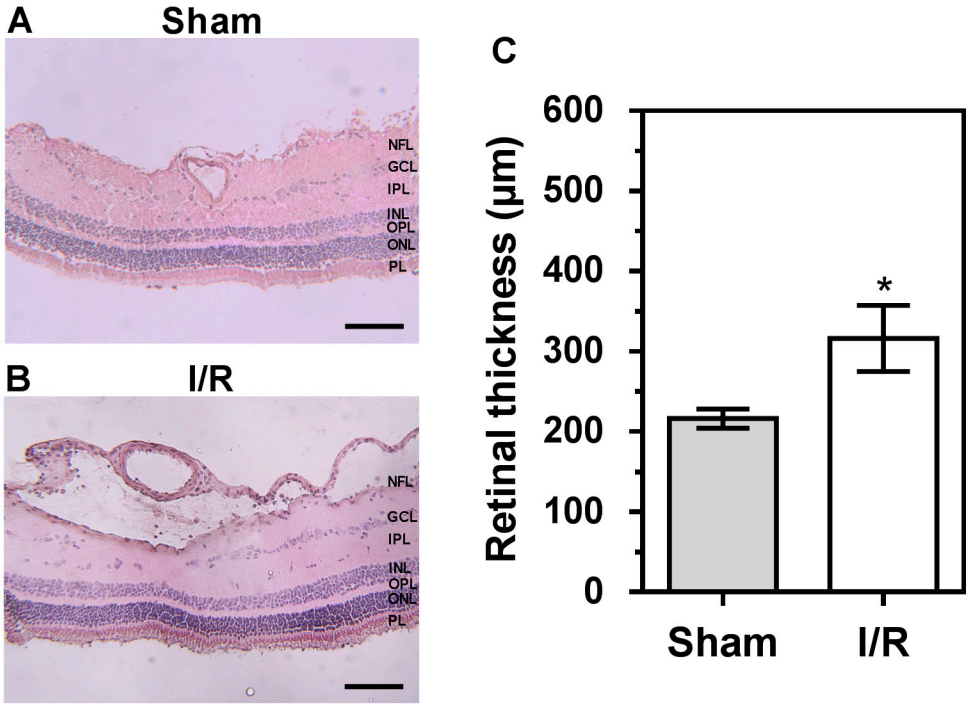

Figure 8. Photomicrographs of retinal cross-sections (H&E staining) from sham-treated (**A**) and I/R-treated pigs (**B**). Quantification of retinal thickness in cryosections revealed increased thickness in I/R-treated pigs (**C**). Data are presented as mean ± SE (n = 6 per group; * $p < 0.05$). NFL = nerve fiber layer; GCL = ganglion cell layer; IPL = inner plexiform layer; INL = inner nuclear layer; OPL = outer plexiform layer; ONL = outer nuclear layer; PL = photoreceptor layer. Scale bar = 100 µm.

3. Discussion

There are several new findings in this study. First, we present a new porcine model of ocular ischemia by inducing global cerebral ischemia. Remarkably, 12 min of ischemia and 20 h of reperfusion resulted in marked endothelial dysfunction of retinal arterioles. Second, ROS levels and mRNA expression levels for *HIF-1α*, *VEGF-A*, *NOX2*, and *iNOS* were elevated in retinal arterioles and immunoreactivity to HIF-1α, VEGF-A, NOX2, and iNOS was increased in retinal arteriole endothelium. Third, a significant loss of RGCs and morphological changes of the retina were observed following I/R. To the best of our knowledge, this is the first model on pigs investigating the effects of short-time ischemia on retinal vascular function and retinal morphology. The findings suggest that retinal tissue is very susceptible to already short periods of ocular ischemia.

A variety of ischemic models in brain research has already been established, starting from cerebral occlusion time periods of 10 min [23] over 30 min to up to 2 h [24], all of them resulting in neuronal ischemic damage of brain structures. In contrast, the time period resulting in irreversible retinal damage remains controversial due to a variety of experimental designs and methods across different species. Of note, retinal ischemia can be triggered by two vessel occlusion (2VO), also termed bilateral

common carotid arteries occlusion (BCCAO), leading to a 50% retinal ischemia, as well as by combined occlusion of vertebral arteries and common carotid arteries, also called four vessel occlusion (4VO), resulting in complete retinal ischemia of 95–100% [25], which is the case in the present study.

In the current study, we observed endothelial dysfunction of retinal arterioles and structural changes in retinal tissue of I/R-treated pigs. Recent studies have been more and more focused on the association between endothelial dysfunction and the severity of vision-threatening diseases like primary open angle glaucoma and diabetic retinopathy due to the important role of an intact endothelium for proper regulation of retinal perfusion [26–28]. In the present study, retinal arteriole dilation after I/R was blunted in response to the endothelium-dependent vasodilator, bradykinin, but not to the endothelium-independent vasodilator, SNP, indicative of endothelial dysfunction. Since NOX2 expression and ROS production were increased in retinal arterioles of I/R-treated pigs, oxidative stress appears to be a trigger factor for endothelial dysfunction. As a consequence of ischemic injury and retinal artery occlusion, retinal damage was previously shown to come along with an increased expression of the hypoxic marker, HIF-1α, and its target genes VEGF, NOX2, and iNOS [14,29], which is supported by the present study. Moreover, several studies suggested iNOS to contribute to the pathophysiology of diabetic retinopathy [30,31]. Furthermore, upregulation of iNOS in endothelial cells induced by I/R was associated with apoptosis, cell migration, and endothelial cell dysfunction [32]. To further search for potential sources of ROS in this model, we investigated expression levels of prooxidant NOX enzymes, which were shown to be involved in various retinal diseases [15,33]. Remarkably, mRNA expression for *NOX2* was elevated in retinal arterioles and immunoreactivity to NOX2 was enhanced in the retinal arteriole endothelium of I/R-treated pigs, suggesting this enzyme to be a potential source of ROS and involved in the onset of endothelial dysfunction in our model. Various laboratories, including our own, have shown a link between hypoxia-induced HIF-1α upregulation and enhanced NOX2 expression in other disease models [34–36]. Moreover, the retinal edema, which we observed in the vicinity of arterioles from I/R-treated pigs suggests that already 12 min of ocular ischemia are sufficient to induce a noticeable disruption of the inner blood–retinal barrier, which is in line with the upregulated VEGF-A expression. We have previously observed similar changes in a porcine model of acute respiratory distress syndrome [34]. VEGF increases vascular permeability and promotes pathological neovascularization in various ocular diseases, such as age-related macular degeneration and diabetic retinopathy, and its expression is also regulated by HIF-1α during hypoxic conditions [37]. A loss of vascular integrity was also shown by increased leakage of sodium fluorescein tracers and infiltration of monocytes into the ischemic eye at 72 h after ischemic stroke using a 90 min transient middle cerebral artery occlusion (MCAO) model in mice [38]. The authors also observed a delayed inflammatory response by increased mRNA levels for proinflammatory cytokines, such as *TNF-α*, after 90 min of ocular ischemia and 8 h of reperfusion, which is in disagreement with our model, but may be explained by differences in species characteristics and the duration of ischemia.

To assess whether retinal neuron viability was affected after 12 min of ischemia and 20 h of reperfusion, we determined overall cell density in the RGC layer by counting DAPI-positive cells and RGC density by counting Brna3a-positive cells. In the retina, Brn3 transcription factors, including Brn3a, are exclusively expressed in RGCs [39]. Although we did not find marked changes in overall cell density, we observed a decrease in RGC density by ≈34% in I/R-treated pigs. These findings suggest that the subgroup of RGCs may be especially vulnerable to I/R. Since the density of Brna3a-positive cells was only 28.6% and 21.1% of the overall cell density in the RGC layer of sham- and I/R-treated pigs, respectively, selective loss of RGCs in the I/R group may have remained undetected when looking only at the overall cell density. The density of Brn3a-positive cells in the sham group was close to previously reported porcine RGC density data of the same retinal region obtained by retrograde labeling of RGCs with Fluoro-Gold [40], suggesting that the Brn3a antibody bound specifically to RGCs. Moreover, the overall cell density was in line with previously reported cell density data obtained by the Nissl staining method [41].

Bardy et al. demonstrated hemodynamic changes and impairment of cell function in miniature pigs by experimental microembolization for 10 min only, which is supported by the present study [42]. A study by Osborne et al. has shown in a rat model of BCCAO that 24 min of blood flow cessation followed by 6 days of reperfusion enhanced glial fibrillary acidic protein expression in the retina, suggesting that this relatively short period of ischemia already affected retinal tissue homeostasis [43].

In contrast to these findings, a series of studies by Hayreh et al. on primates revealed that CRAO elicited retinal damage not before a duration of 105 min, indicative of a high retinal tolerance to ischemic injury [44,45]. One explanation for the discrepancies between the studies may be the extent and type of occlusion of vessels supplying the retina. In those animal models, where the retinal circulation was selectively blocked, residual oxygen and glucose supply to the retina may be maintained by the choroidal network. Conversely, in the models with complete ocular ischemia, including the present one, the choroidal supply is also blocked, which may be a reason for the shorter ischemic tolerance of retinal tissue. Another explanation may be species differences with regard to retinal vascular supply and ischemic tolerance [46]. Although porcine eyes constitute an established and validated model in vision research due to high morphological resemblance to human eyes, e.g., with respect to the mean area of retina and vascularization, ischemia-induced retinal damage is still poorly understood in pigs [20,21].

In conclusion, complete cerebral ischemia presents a feasible method to induce ocular ischemia without direct manipulation of the eye. A disadvantage of this method is that it requires a high level of technical effort and expertise. A major new finding of this study is that only 12 min of ocular ischemia followed by a reperfusion period of 20 h induced endothelial dysfunction in retinal arterioles, retinal thickening, indicative of edema due to vascular leakage, and RGC loss. Hypoxia-induced changes, such as upregulation of HIF-1α, VEGF-A, NOX2, and iNOS, as well as oxidative stress, appear to be involved in the pathophysiology.

4. Materials and Methods

4.1. Animals

All experimental protocols were approved by the Animal Care Committee of Rhineland-Palatinate, Germany (date of approval: 11 June 2013), and adhere to the EU Directive 2010/63/EU for animal experiments. Male German Landrace pigs (*Sus scrofa domesticus*, 12–16 weeks, 33–36 kg) were obtained from a local farm and sedated for transport by an intramuscular injection of azaperone and ketamine (4 mg/kg). After arrival at the research facility, anesthesia was induced by intravenous injection of fentanyl (4 µg/kg), propofol (3 mg/kg), and atracurium (1.5 mg/kg) via an ear vein cannula and maintained by continuous infusion of fentanyl (10 µg/kg/h) and propofol (6 mg/kg/h). After endotracheal intubation, volume-controlled ventilation was maintained with the following settings: tidal volume 8 mL/kg; positive end-expiratory pressure 5 cm H_2O, FiO_2 = 0.3; inspiration to expiration ratio 1:2; and variable respiration rate to achieve an end-tidal pCO_2 < 6 kPa. Rectal temperature was continuously monitored, and body temperature was maintained using a heating blanket throughout the experiment. Arterial and venous catheters were placed via ultrasound guidance into the femoral vessels for central venous vascular access and invasive blood pressure monitoring. Hemodynamic parameters, such as arterial pressure and heart rate, were continuously measured. Cerebral oxygen saturation (rSO_2) was quantified with a self-adherent near infrared spectroscopy probe placed bilaterally on the forehead. The rSO_2 values were updated and displayed in five-second intervals with the INVOS™ 5100C Cerebral/Somatic Oximeter (Somanetics Corporation, Troy, MI, USA), providing a highly sensitive real-time parameter for changes in cerebral blood flow.

4.2. Materials

Components for the Krebs–Henseleit buffer were obtained from Carl Roth GmbH, Karlsuhe, Germany. The vasodilator, bradykinin (Sigma-Aldrich Chemie GmbH, Steinheim, Germany; purity

≥98%), induces endothelium-dependent vasodilation in various blood vessels, including porcine retinal arterioles [47,48]. The endothelium-independent vasodilator, sodium nitroprusside (SNP; Sigma-Aldrich; purity ≥99%) is a donor of nitric oxide (NO) [49]. The vasoconstrictor, U46619 (Cayman Chemical, Ann Arbor, MI, U.S.; purity ≥98%), is a thromboxane A2 (TP) receptor agonist [50]. The stock solution of U46619 was dissolved in dimethyl sulfoxide (DMSO), whereas bradykinin and sodium nitroprusside were dissolved in phosphate buffered saline (PBS).

Antibodies against NOX2 (ab129068, 1:100), VEGF-A (ab9570, 1:100), and iNOS (ab15323, 1:100) were purchased from Abcam, Berlin, Germany. The antibody directed against HIF-1α (NB100-654, 1:100) was obtained from Bio-Techne GmbH, Wiesbaden, Germany. For the NOX2, HIF-1α, and VEGF-A antibodies used in this study, we have previously shown an increased immunoreactivity in retinal arteriole endothelium of hypoxic pigs with acute respiratory distress syndrome [34]. The secondary antibody was coupled with Rhodamine Red-X (111-035-045, 1:200) and was purchased from Dianova GmbH, Hamburg, Germany. For immunostaining of RGCs, a goat polyclonal brain-specific homebox/POU domain protein 3A (Brn3a) antibody purchased from Santa Cruz Biotechnology (sc-31984, Santa Cruz, CA, USA, 1:750) was used. The antibody was directed against an epitope close to the N-terminus of the human Brn3a protein and was shown to be suitable for RGC detection in rats and mice [51,52]. The amino acid sequence of this region is identical in humans, pigs, mice, and rats. In pilot experiments performed in porcine retinal-cross sections, we found positive immunoreactivity only in a portion of cells localized in the RGC layer, suggesting specific binding to RGCs. Donkey anti-goat IgG Alexa Fluor 568 (A11057, Life Technologies, Carlsbad, CA, USA 1:400) was used as secondary antibody.

4.3. Surgical Procedure

Cerebral ischemia was induced in six pigs (I/R group). After sternotomy, carotid and right vertebral inflow were occluded by clamping the innominate artery, containing right and left carotid and right subclavian artery, just distal of the aortic arch. The left subclavian artery was clamped equally proximal to occlude inflow via the left vertebral artery. Effective clamping and consecutive cerebral ischemia were confirmed by an INVOS™ 5100C Cerebral/Somatic Oximeter (Medtronic GmbH, Meerbuch, Germany) and by an increase of blood pressure and heart rate, as well as by dilated non-reactive pupils. After 12 min, clamping was released, and blood flow restored. After initial stabilization, pigs were monitored, and normal hemodynamic parameters were maintained for the next 20 h. Sham surgery was also conducted in six pigs. In this group, apart from the occlusion of arteries, the same surgical preparation was conducted as in the I/R group.

4.4. Measurement of Vascular Reactivity in Retinal Arterioles

After pigs had been monitored for 20 h following I/R, they were sacrificed by inducing cardiac arrest via application of high doses of propofol (200 mg) and potassium chloride (40 mmol) intravenously. Next, the eyes were enucleated and transferred into ice-cold Krebs–Henseleit buffer of the following ionic composition (in mM): 118.3 NaCl, 4.7 KCl, 2.5 CaCl2, 1.2 MgSO4, 1.2 KH2PO4, 25 NaHCO3, 11 glucose. After opening the eye globe, the retina was carefully isolated as described previously [34]. Retinal arterioles of the first order were then isolated and cleaned from surrounding retinal tissue by Vannas scissors and fine-point tweezers. Vascular measurements were conducted after cannulation of blood vessels onto two micropipettes as described previously [53,54]. Only when the luminal arteriole diameter decreased by at least 30% in response to 100 mM KCl, the vessel was used for experiments. Concentration–response curves were started after development of basal tone, which was achieved after an equilibration time of 45 min. A myogenic tone of 30%–50% of the initial diameter was defined as preconstricted for the following concentration–response curves to vasodilators. If not achieved, the thromboxane mimetic, U46619 (Cayman Chemical, Ann Arbor, MI, U.S.), was titrated into the circulating Krebs–Henseleit buffer to achieve proper preconstriction.

4.5. Measurement of Reactive Oxygen Species

Retinal arterioles together with surrounding retinal tissue were isolated immediately after enucleation, embedded in Tissue Tek OCT compound (Sakura Finetek Europe, Alphen aan den Rijn, Netherlands), frozen in liquid nitrogen, and stored at −80 °C until use. For staining, cryosections of 10 µM thickness were placed on Superfrost Plus slides (Thermo Fisher Scientific, Menzel-Gläser, Braunschweig, Germany) and 1 mL of 5 µM dihydroethidium (DHE, Thermo Fisher Scientific, Waltham, MA, U.S.) solution was dropped onto each slide. Then, all slides were placed in a light-protected and humidified chamber and incubated at 37 °C for 30 min. Oxidized DHE sections were analyzed as described previously [34,55].

4.6. Quantitative PCR

Directly after enucleation, vessels were isolated in cold Krebs–Henseleit buffer using fine-point tweezers and microscissors, washed in cold phosphate buffered solution (PBS, Thermo Fisher Scientific, Braunschweig, Germany), transferred into a 1.5 mL tube, and snap-frozen. Homogenization of tissue was performed in lysis buffer (1.0% NP40, 0.5% sodium deoxycholate, 0.1% SDS, 10 mmol/l NaF, 80 mmol/l TRIS, pH 7.5). Quantitative PCR was performed according to the manufacturer's protocol by using a light cycler (LC480, Roche Diagnostics, Mannheim, Germany) and a StepOnePlus device (Applied Biosystems, Foster City, CA, USA). SYBR Green (Thermo Fisher Scientific) was utilized for fluorescent detection of DNA generated during PCR. Relative mRNA levels were quantified using comparative threshold (CT) normalized to the β-actin gene. Primer sequences are presented in Table 2.

4.7. Immunohistochemistry

Retinal tissue containing first-order retinal arterioles was excised for immunohistochemical evaluation and embedded in Tissue Tek OCT compound (Sakura Finetek Europe). After freezing in liquid nitrogen, the tissue was stored at −80 °C until use. Frozen sections of 10 µm thickness were cut and fixed in 4% paraformaldehyde (pH 7.4) solution for 20 min. Next, slides were rinsed with PBS and incubated at room temperature with blocking solution containing 0.1% Triton-X-100 and 0.1% bovine serum albumin for 30 min. Next, primary antibodies directed against HIF-1α, VEGF-A, NOX2, and iNOS were diluted in blocking solution and incubated for 2 h at room temperature. Thereafter, each slide was washed in PBS three times for 5 min and incubated for 1 h at room temperature with a secondary Rhodamine Red-X-coupled antibody (Dianova GmbH). For negative controls, the primary antibody was omitted.

For immunohistochemical visualization of RGCs, retinas were carefully separated from the pigment epithelium by injection of Krebs buffer. In each retina, the optic disc was used as a reference point. To minimize localization-dependent variations in RGC density, we have chosen a retinal piece of 3 × 3 mm localized in the nasal superior midperiphery of the retina. The lower temporal corner of this area was localized 7 mm nasally and 7 mm superior to the optic disc center, as shown in Figure 6. We have chosen this area because the retinal midperiphery represents the major part of the porcine retina containing ≈70% of the RGCs and has a relatively homogeneous RGC density [40]. A pair of compasses was used to localize and measure the area, which was harvested for cell staining. After careful excision of the retinal piece and fixation with 4% paraformaldehyde for 30 min, the tissue was washed in PBS + 0.5% Triton-X-100 twice for 10 min and then frozen for 15 min at −80 ° C. Following this procedure, the tissue was thawed at room temperature and then washed twice with PBS and 0.5% Triton-X-100. A primary antibody for Brn3a, an established tool for RGC staining [51,52], was diluted in blocking buffer containing PBS + 2% Triton-X-100 + 2% fetal calf serum (FCS). After incubation overnight at 4 °C, residual antibody was removed by washing the tissue three times for 10 min with PBS + 0. 5% Triton-X-100. Then, retinal tissue was incubated with the secondary antibody for 2 h at room temperature. Subsequently, the tissue was washed three times for 10 min with PBS and mounted with 4',6-diamidino-2-phenylindole (DAPI)-containing medium (VECTASHIELD®

Mounting Medium with DAPI, H-1200, BIOZOL Diagnostica Vertrieb GmbH, Eching, Germany) and cover-slipped. Next, in each stained piece of retina, 10 areas, each representing 0.138 mm^2, were photographed by fluorescence microscopy. Brn3a- and DAPI-positive cells were counted in all 10 areas manually and semi-automatically using a macro [56] installed in ImageJ cell counting software (version 1.52a) [57]. The counting procedure included the following steps: convert to 8-bit, subtract background, auto threshold, run nucleus counter (smallest 800, largest 7000) as described elsewhere [58]. The mean cell number was then determined for the 10 counted areas per piece of tissue, and the cell density per mm^2 calculated.

4.8. Retinal Histology

Retinal cryosections of 10 µM thickness, each containing a cross-section of a first-order retinal arteriole taken from an area 2 mm superior to the visual streak, as shown in Figure 6, were fixed with 4% paraformaldehyde (Histofix, Roth, Karlsruhe, Germany) for 20 min at room temperature. Next, tissue sections were washed with purified water twice for 5 min, immersed in hematoxylin for 3 min, and washed another time with purified water for 5 min. Sections were placed into 95% ethanol for 1 min, followed by 1 min of staining in eosin solution. Subsequently, tissue dehydration was done by ascending ethanol series (70%, 96%, and 100%) and washing in xylene (3 × 5 min). Subsequently, the glass slides were mounted with Eukitt quick-hardening mounting medium (Sigma-Aldrich, Steinheim, Germany) and visualized by transmitted light microscopy (Nikon, Yurakucho, Tokyo, Japan). Retinal thickness was measured at five standardized positions, and the average was calculated for each retinal cross section.

4.9. Statistical Methods

Time courses of tissue oxygenation, heart rate, and mean arterial pressure, as well as concentration–response curves, were compared by two-way analysis of variance (ANOVA) for repeated measurements and the Sidak's multiple comparisons test. A two-sided unpaired t-test was used to compare ROS levels, mRNA expression levels (ΔCT values), cell density, and retinal thickness. Data are presented as mean ± SE, and n represents the number of pigs per group. The significance level was set at 0.05.

5. Conclusions

In conclusion, we developed a new porcine model, which induces endothelial dysfunction of retinal arterioles by ocular and global brain ischemia and leads to retinal pathological changes, such as edema and loss of RGCs after only 12 min of ischemia and 20 h of reperfusion. Moreover, our data suggest that the HIF-1α-VEGF-A-NOX2 pathway plays a crucial role in inducing retinal vascular endothelial dysfunction in the early phase of ocular ischemia.

Author Contributions: Conceptualization, J.K.Z., A.G.-B., E.K.H., and A.G.; Data curation, J.K.Z., A.G.-B., W.O., M.L., and N.X.; Formal analysis, A.G.-B., M.L., A.P., and A.G.; Funding acquisition, N.P. and A.G.; Methodology, J.K.Z., A.G.-B., E.K.H., M.L., N.X., and A.G.; Project administration, E.K.H., N.X., and A.G.; Resources, A.G.-B., E.K.H., N.P., A.P., H.L., and A.G.; Software, M.L., A.P., and N.X.; Supervision, N.P. and A.P.; Validation, H.L.; Visualization, J.K.Z., W.O., and A.G.; Writing—original draft, J.K.Z. and A.G.; Writing—review & editing, A.P. and H.L.

Funding: This research received no external funding.

Conflicts of Interest: The authors declare no conflict of interest.

Abbreviations

BL	Baseline
Brn3a	Brain specific homebox/POU domain protein 3A
CRAO	Central retinal artery occlusion
DAPI	4′,6-diamidino-2-phenylindole
DHE	Dihydroethidium
DMSO	Dimethyl sulfoxide
eNOS	Endothelial nitric oxide synthase
FCS	Fetal calf serum
GCL	Ganglion cell layer
HIF-1α	Hypoxia-inducible factor-1α
HR	Heartrate
iNOS	Inducible nitric oxide synthase
INL	Inner nuclear layer
IL	Interleukin
IPL	Inner plexiform layer
I/R	Ischemia-reperfusion
MAP	Mean arterial blood pressure
NFL	Nerve fiber layer
nNOS	Neuronal nitric oxide synthase
NOX	Nicotinamide adenine dinucleotide phosphate oxidase
ONL	Outer nuclear la
OPL	Outer plexiform layer
PBS	Phosphate-buffered saline
RGC	Retinal ganglion cell
ROS	Reactive oxygen species
SNP	Sodium nitroprusside
TNF- α	Tumor necrosis factor alpha
U46619	9,11-dideoxy-9α,11α-methanoepoxy prostaglandin F2α
VEGF-A	Vascular endothelial growth factor

References

1. Gao, S.; Andreeva, K.; Cooper, N.G. Ischemia-reperfusion injury of the retina is linked to necroptosis via the ERK1/2-RIP3 pathway. *Mol. Vis.* **2014**, *20*, 1374–1387. [PubMed]
2. Renner, M.; Stute, G.; Alzureiqi, M.; Reinhard, J.; Wiemann, S.; Schmid, H.; Faissner, A.; Dick, H.B.; Joachim, S.C. Optic Nerve Degeneration after Retinal Ischemia/Reperfusion in a Rodent Model. *Front Cell Neurosci.* **2017**, *11*, 254. [CrossRef] [PubMed]
3. Rumelt, S.; Dorenboim, Y.; Rehany, U. Aggressive systematic treatment for central retinal artery occlusion. *Am. J. Ophthalmol.* **1999**, *128*, 733–738. [CrossRef]
4. Terelak-Borys, B.; Skonieczna, K.; Grabska-Liberek, I. Ocular ischemic syndrome—A systematic review. *Med. Sci. Monit.* **2012**, *18*, 138–144. [CrossRef] [PubMed]
5. Feltgen, N.; Neubauer, A.; Jurklies, B.; Schmoor, C.; Schmidt, D.; Wanke, J.; Maier-Lenz, H.; Schumacher, M.; Group, E.A.-S. Multicenter study of the European assessment group for lysis in the eye (EAGLE) for the treatment of central retinal artery occlusion: Design issues and implications. EAGLE Study report no. 1: EAGLE Study report no. 1. *Graefes. Arch. Clin. Exp. Ophthalmol.* **2006**, *244*, 950–956. [CrossRef] [PubMed]
6. Schumacher, M.; Schmidt, D.; Jurklies, B.; Gall, C.; Wanke, I.; Schmoor, C.; Maier-Lenz, H.; Solymosi, L.; Brueckmann, H.; Neubauer, A.S.; et al. Central retinal artery occlusion: Local intra-arterial fibrinolysis versus conservative treatment, a multicenter randomized trial. *Ophthalmology* **2010**, *117*, 1367–1375. [CrossRef] [PubMed]
7. Xu, Z.; Alloush, J.; Beck, E.; Weisleder, N. A murine model of myocardial ischemia-reperfusion injury through ligation of the left anterior descending artery. *J. Vis. Exp.* **2014**. [CrossRef] [PubMed]

8. Masuzawa, K.; Jesmin, S.; Maeda, S.; Kaji, Y.; Oshika, T.; Zaedi, S.; Shimojo, N.; Yaji, N.; Miyauchi, T.; Goto, K. A model of retinal ischemia-reperfusion injury in rats by subconjunctival injection of endothelin-1. *Exp. Biol. Med. (Maywood)* **2006**, *231*, 1085–1089. [PubMed]
9. Larpthaveesarp, A.; Gonzalez, F.F. Transient middle cerebral artery occlusion model of neonatal stroke in P10 Rats. *J. Vis. Exp.* **2017**. [CrossRef]
10. Hartsock, M.J.; Cho, H.; Wu, L.; Chen, W.J.; Gong, J.; Duh, E.J. A mouse model of retinal ischemia-reperfusion injury through elevation of intraocular pressure. *J. Vis. Exp.* **2016**. [CrossRef]
11. Hein, T.W.; Ren, Y.; Potts, L.B.; Yuan, Z.; Kuo, E.; Rosa, R.H., Jr.; Kuo, L. Acute retinal ischemia inhibits endothelium-dependent nitric oxide-mediated dilation of retinal arterioles via enhanced superoxide production. *Invest Ophthalmol. Vis. Sci.* **2012**, *53*, 30–36. [CrossRef] [PubMed]
12. Zheng, G.Y.; Zhang, C.; Li, Z.G. Early activation of caspase-1 after retinal ischemia and reperfusion injury in mice. *Chin. Med. J.* **2004**, *117*, 717–721.
13. Aktas, Z.; Gurelik, G.; Akyurek, N.; Onol, M.; Hasanreisoglu, B. Neuroprotective effect of topically applied brimonidine tartrate 0.2% in endothelin-1-induced optic nerve ischaemia model. *Clin. Exp. Ophthalmol.* **2007**, *35*, 527–534. [CrossRef] [PubMed]
14. Goldenberg-Cohen, N.; Dadon, S.; Avraham, B.C.; Kramer, M.; Hasanreisoglu, M.; Eldar, I.; Weinberger, D.; Bahar, I. Molecular and histological changes following central retinal artery occlusion in a mouse model. *Exp. Eye Res.* **2008**, *87*, 327–333. [CrossRef]
15. Masuda, T.; Shimazawa, M.; Hara, H. Retinal Diseases Associated with Oxidative Stress and the Effects of a Free Radical Scavenger (Edaravone). *Oxid. Med. Cell. Longev.* **2017**, *2017*, 9208489. [CrossRef]
16. Kruk, J.; Kubasik-Kladna, K.; Aboul-Enein, H.Y. The role oxidative stress in the pathogenesis of eye diseases: Current status and a dual role of physical activity. *Mini. Rev. Med. Chem.* **2015**, *16*, 241–257. [CrossRef] [PubMed]
17. Carden, D.L.; Granger, D.N. Pathophysiology of ischaemia-reperfusion injury. *J. Pathol.* **2000**, *190*, 255–266. [CrossRef]
18. Kowalczyk, A.; Kleniewska, P.; Kolodziejczyk, M.; Skibska, B.; Goraca, A. The role of endothelin-1 and endothelin receptor antagonists in inflammatory response and sepsis. *Arch. Immunol. Ther. Exp. (Warsz)* **2015**, *63*, 41–52. [CrossRef] [PubMed]
19. Sanchez, I.; Martin, R.; Ussa, F.; Fernandez-Bueno, I. The parameters of the porcine eyeball. *Graefes Arch. Clin. Exp. Ophthalmol.* **2011**, *249*, 475–482. [CrossRef] [PubMed]
20. Ruiz-Ederra, J.; Garcia, M.; Hernandez, M.; Urcola, H.; Hernandez-Barbachano, E.; Araiz, J.; Vecino, E. The pig eye as a novel model of glaucoma. *Exp. Eye Res.* **2005**, *81*, 561–569. [CrossRef]
21. Galdos, M.; Bayon, A.; Rodriguez, F.D.; Mico, C.; Sharma, S.C.; Vecino, E. Morphology of retinal vessels in the optic disk in a Gottingen minipig experimental glaucoma model. *Vet. Ophthalmol.* **2012**, *15*, 36–46. [CrossRef] [PubMed]
22. Stone, J.; Johnston, E. The topography of primate retina: A study of the human, bushbaby, and new- and old-world monkeys. *J. Comp. Neurol.* **1981**, *196*, 205–223. [CrossRef] [PubMed]
23. Onken, M.; Berger, S.; Kristian, T. Simple model of forebrain ischemia in mouse. *J. Neurosci. Methods* **2012**, *204*, 254–261. [CrossRef] [PubMed]
24. Chiang, T.; Messing, R.O.; Chou, W.H. Mouse model of middle cerebral artery occlusion. *J. Vis. Exp.* **2011**. [CrossRef] [PubMed]
25. Block, F.; Schwarz, M.; Sontag, K.H. Retinal ischemia induced by occlusion of both common carotid arteries in rats as demonstrated by electroretinography. *Neurosci. Lett.* **1992**, *144*, 124–126. [CrossRef]
26. Bukhari, S.M.; Kiu, K.Y.; Thambiraja, R.; Sulong, S.; Rasool, A.H.; Liza-Sharmini, A.T. Microvascular endothelial function and severity of primary open angle glaucoma. *Eye* **2016**, *30*, 1579–1587. [CrossRef]
27. Resch, H.; Garhofer, G.; Fuchsjager-Mayrl, G.; Hommer, A.; Schmetterer, L. Endothelial dysfunction in glaucoma. *Acta Ophthalmol.* **2009**, *87*, 4–12. [CrossRef]
28. Lim, L.S.; Ling, L.H.; Ong, P.G.; Foulds, W.; Tai, E.S.; Wong, E.; Lee, S.Y.; Wong, D.; Cheung, C.M.; Wong, T.Y. Dynamic responses in retinal vessel caliber with flicker light stimulation in eyes with diabetic retinopathy. *Invest. Ophthalmol. Vis. Sci.* **2014**, *55*, 5207–5213. [CrossRef]
29. Cheng, L.; Yu, H.; Yan, N.; Lai, K.; Xiang, M. Hypoxia-inducible factor-1alpha target genes contribute to retinal neuroprotection. *Front. Cell. Neurosci.* **2017**, *11*. [CrossRef]

30. Mishra, A.; Newman, E.A. Inhibition of inducible nitric oxide synthase reverses the loss of functional hyperemia in diabetic retinopathy. *Glia* **2010**, *58*, 1996–2004. [CrossRef]
31. Carr, B.C.; Emigh, C.E.; Bennett, L.D.; Pansick, A.D.; Birch, D.G.; Nguyen, C. Towards a treatment for diabetic retinopathy: Intravitreal toxicity and preclinical safety evaluation of inducible nitric oxide synthase inhibitors. *Retina* **2017**, *37*, 22–31. [CrossRef] [PubMed]
32. Zhu, T.; Yao, Q.; Wang, W.; Yao, H.; Chao, J. iNOS Induces vascular endothelial cell migration and apoptosis via autophagy in ischemia/reperfusion injury. *Cell. Physiol. Biochem.* **2016**, *38*, 1575–1588. [CrossRef] [PubMed]
33. Chan, E.C.; van Wijngaarden, P.; Liu, G.S.; Jiang, F.; Peshavariya, H.; Dusting, G.J. Involvement of Nox2 NADPH oxidase in retinal neovascularization. *Invest. Ophthalmol. Vis. Sci.* **2013**, *54*, 7061–7067. [CrossRef] [PubMed]
34. Zadeh, J.K.; Ruemmler, R.; Hartmann, E.K.; Ziebart, A.; Ludwig, M.; Patzak, A.; Xia, N.; Li, H.; Pfeiffer, N.; Gericke, A. Responses of retinal arterioles and ciliary arteries in pigs with acute respiratory distress syndrome (ARDS). *Exp. Eye Res.* **2019**, *184*, 152–162. [CrossRef]
35. Yuan, G.; Khan, S.A.; Luo, W.; Nanduri, J.; Semenza, G.L.; Prabhakar, N.R. Hypoxia-inducible factor 1 mediates increased expression of NADPH oxidase-2 in response to intermittent hypoxia. *J. Cell. Physiol.* **2011**, *226*, 2925–2933. [CrossRef] [PubMed]
36. Nanduri, J.; Vaddi, D.R.; Khan, S.A.; Wang, N.; Makarenko, V.; Semenza, G.L.; Prabhakar, N.R. HIF-1alpha activation by intermittent hypoxia requires NADPH oxidase stimulation by xanthine oxidase. *PLoS ONE* **2015**, *10*, e0119762. [CrossRef]
37. Kurihara, T.; Westenskow, P.D.; Friedlander, M. Hypoxia-inducible factor (HIF)/vascular endothelial growth factor (VEGF) signaling in the retina. *Adv. Exp. Med. Biol.* **2014**, *801*, 275–281. [PubMed]
38. Ritzel, R.M.; Pan, S.J.; Verma, R.; Wizeman, J.; Crapser, J.; Patel, A.R.; Lieberman, R.; Mohan, R.; McCullough, L.D. Early retinal inflammatory biomarkers in the middle cerebral artery occlusion model of ischemic stroke. *Mol. Vis.* **2016**, *22*, 575–588. [PubMed]
39. Pan, L.; Yang, Z.; Feng, L.; Gan, L. Functional equivalence of Brn3 POU-domain transcription factors in mouse retinal neurogenesis. *Development* **2005**, *132*, 703–712. [CrossRef]
40. Garca, M.; Ruiz-Ederra, J.; Hernandez-Barbachano, H.; Vecino, E. Topography of pig retinal ganglion cells. *J. Comp. Neurol.* **2005**, *486*, 361–372. [CrossRef]
41. Hebel, R. Distribution of retinal ganglion cells in five mammalian species (pig, sheep, ox, horse, dog). *Anat. Embryol. (Berl)* **1976**, *150*, 45–51. [PubMed]
42. Bardy, M.; Tsacopoulos, M. Metabolic changes in the retina after experimental microembolism in the miniature pig (author's transl). *Klin. Monbl. Augenheilkd.* **1978**, *172*, 451–460. [PubMed]
43. Osborne, N.N.; Block, F.; Sontag, K.H. Reduction of ocular blood flow results in glial fibrillary acidic protein (GFAP) expression in rat retinal Muller cells. *Vis. Neurosci.* **1991**, *7*, 637–639. [CrossRef] [PubMed]
44. Hayreh, S.S.; Kolder, H.E.; Weingeist, T.A. Central retinal artery occlusion and retinal tolerance time. *Ophthalmology* **1980**, *87*, 75–78. [CrossRef]
45. Hayreh, S.S.; Zimmerman, M.B.; Kimura, A.; Sanon, A. Central retinal artery occlusion. retinal survival time. *Exp. Eye Res.* **2004**, *78*, 723–736. [CrossRef]
46. Hayreh, S.S.; Weingeist, T.A. Experimental occlusion of the central artery of the retina. IV: Retinal tolerance time to acute ischaemia. *Br. J. Ophthalmol.* **1980**, *64*, 818–825. [CrossRef]
47. Leeb-Lundberg, L.M.; Marceau, F.; Muller-Esterl, W.; Pettibone, D.J.; Zuraw, B.L. International union of pharmacology. XLV. Classification of the kinin receptor family: From molecular mechanisms to pathophysiological consequences. *Pharmacol. Rev.* **2005**, *57*, 27–77. [CrossRef] [PubMed]
48. Dalsgaard, T.; Kroigaard, C.; Bek, T.; Simonsen, U. Role of calcium-activated potassium channels with small conductance in bradykinin-induced vasodilation of porcine retinal arterioles. *Invest. Ophthalmol. Vis. Sci.* **2009**, *50*, 3819–3825. [CrossRef]
49. Friederich, J.A.; Butterworth, J.F. t. Sodium nitroprusside: Twenty years and counting. *Anesth. Analg.* **1995**, *81*, 152–162.
50. Coleman, R.A.; Humphrey, P.P.; Kennedy, I.; Levy, G.P.; Lumley, P. Comparison of the actions of U-46619, a prostaglandin H2-analogue, with those of prostaglandin H2 and thromboxane A2 on some isolated smooth muscle preparations. *Br. J. Pharmacol.* **1981**, *73*, 773–778. [CrossRef]

51. Nadal-Nicolas, F.M.; Jimenez-Lopez, M.; Sobrado-Calvo, P.; Nieto-Lopez, L.; Canovas-Martinez, I.; Salinas-Navarro, M.; Vidal-Sanz, M.; Agudo, M. Brn3a as a marker of retinal ganglion cells: Qualitative and quantitative time course studies in naive and optic nerve-injured retinas. *Invest. Ophthalmol. Vis. Sci.* **2009**, *50*, 3860–3868. [CrossRef] [PubMed]
52. Galindo-Romero, C.; Aviles-Trigueros, M.; Jimenez-Lopez, M.; Valiente-Soriano, F.J.; Salinas-Navarro, M.; Nadal-Nicolas, F.; Villegas-Perez, M.P.; Vidal-Sanz, M.; Agudo-Barriuso, M. Axotomy-induced retinal ganglion cell death in adult mice: Quantitative and topographic time course analyses. *Exp. Eye Res.* **2011**, *92*, 377–387. [CrossRef] [PubMed]
53. Gericke, A.; Mayer, V.G.; Steege, A.; Patzak, A.; Neumann, U.; Grus, F.H.; Joachim, S.C.; Choritz, L.; Wess, J.; Pfeiffer, N. Cholinergic responses of ophthalmic arteries in M3 and M5 muscarinic acetylcholine receptor knockout mice. *Invest. Ophthalmol. Vis. Sci.* **2009**, *50*, 4822–4827. [CrossRef] [PubMed]
54. Manicam, C.; Staubitz, J.; Brochhausen, C.; Grus, F.H.; Pfeiffer, N.; Gericke, A. The gatekeepers in the mouse ophthalmic artery: Endothelium-dependent mechanisms of cholinergic vasodilation. *Sci. Rep.* **2016**, *6*, 20322. [CrossRef]
55. Laspas, P.; Zhutdieva, M.B.; Brochhausen, C.; Musayeva, A.; Zadeh, J.K.; Pfeiffer, N.; Xia, N.; Li, H.; Wess, J.; Gericke, A. The M1 muscarinic acetylcholine receptor subtype is important for retinal neuron survival in aging mice. *Sci. Rep.* **2019**, *9*, 5222. [CrossRef] [PubMed]
56. Schindelin, J.; Arganda-Carreras, I.; Frise, E.; Kaynig, V.; Longair, M.; Pietzsch, T.; Preibisch, S.; Rueden, C.; Saalfeld, S.; Schmid, B.; et al. Fiji: An open-source platform for biological-image analysis. *Nat Methods* **2012**, *9*, 676–682. [CrossRef] [PubMed]
57. Schneider, C.A.; Rasband, W.S.; Eliceiri, K.W. NIH Image to ImageJ: 25 years of image analysis. *Nat Methods* **2012**, *9*, 671–675. [CrossRef]
58. Teister, J.; Anders, F.; Beck, S.; Funke, S.; von Pein, H.; Prokosch, V.; Pfeiffer, N.; Grus, F. Decelerated neurodegeneration after intravitreal injection of alpha-synuclein antibodies in a glaucoma animal model. *Sci. Rep.* **2017**, *7*, 6260. [CrossRef] [PubMed]

Hindawi
Oxidative Medicine and Cellular Longevity
Volume 2019, Article ID 5181429, 17 pages
https://doi.org/10.1155/2019/5181429

Research Article

Apolipoprotein E Deficiency Causes Endothelial Dysfunction in the Mouse Retina

Jenia Kouchek Zadeh,[1] **Mayagozel B. Zhutdieva**,[1] **Panagiotis Laspas**,[1] **Can Yuksel**,[1] **Aytan Musayeva**,[1] **Norbert Pfeiffer**,[1] **Christoph Brochhausen**,[2,3] **Matthias Oelze**,[4] **Andreas Daiber**,[4] **Ning Xia**,[5] **Huige Li**,[5] **and Adrian Gericke**[1]

[1]*Department of Ophthalmology, University Medical Center, Johannes Gutenberg University Mainz, Langenbeckstr. 1, 55131 Mainz, Germany*
[2]*Institute of Pathology, University Medical Center, Johannes Gutenberg University Mainz, Langenbeckstr. 1, 55131 Mainz, Germany*
[3]*Institute of Pathology, University of Regensburg, Franz-Josef-Strauss-Allee 11, 93053 Regensburg, Germany*
[4]*Center of Cardiology 1, Molecular Cardiology, University Medical Center, Johannes Gutenberg University Mainz, Langenbeckstr. 1, 55131 Mainz, Germany*
[5]*Department of Pharmacology, University Medical Center, Johannes Gutenberg University Mainz, Obere Zahlbacher Str. 67, 55131 Mainz, Germany*

Correspondence should be addressed to Jenia Kouchek Zadeh; je.kouchek@hotmail.de

Academic Editor: Sonia de Pascual-Teresa

Objective. Atherogenic lipoproteins may impair vascular reactivity consecutively causing tissue damage in multiple organs via abnormal perfusion and excessive reactive oxygen species generation. We tested the hypothesis that chronic hypercholesterolemia causes endothelial dysfunction and cell loss in the retina. *Methods*. Twelve-month-old apolipoprotein E-deficient (ApoE-/-) mice and age-matched wild-type controls were used in this study ($n = 8$ per genotype for each experiment). Intraocular pressure, blood pressure, and ocular perfusion pressure were determined. Retinal arteriole responses were studied *in vitro*, and reactive oxygen and nitrogen species were quantified in the retinal and optic nerve cryosections. The expression of the lectin-like oxidized low-density lipoprotein receptor-1 (LOX-1) and the NADPH oxidase isoforms, NOX1, NOX2, and NOX4, were determined in retinal cryosections by immunofluorescence microscopy. Pro- and antioxidant redox genes were quantified in retinal explants by PCR. Moreover, cell number in the retinal ganglion cell layer and axon number in the optic nerve was calculated. *Results*. Responses to the endothelium-dependent vasodilator, acetylcholine, were markedly impaired in retinal arterioles of ApoE-/- mice ($P < 0.01$). LOX-1 ($P = 0.0007$) and NOX2 ($P = 0.0027$) expressions as well as levels of reactive oxygen species ($P = 0.0022$) were increased in blood vessels but not in other retinal structures. In contrast, reactive nitrogen species were barely detectable in both mouse genotypes. Messenger RNA for HIF-1α, VEGF-A, NOX1, and NOX2, but also for various antioxidant redox genes was elevated in the retina of ApoE-/- mice. Total cell number in the retinal ganglion cell layer did not differ between ApoE-/- and wild-type mice ($P = 0.2171$). Also, axon number in the optic nerve did not differ between ApoE-/- and wild-type mice ($P = 0.6435$). *Conclusion.* Apolipoprotein E deficiency induces oxidative stress and endothelial dysfunction in retinal arterioles, which may trigger hypoxia in the retinal tissue. Oxidative stress in nonvascular retinal tissue appears to be prevented by the upregulation of antioxidant redox enzymes, resulting in neuron preservation.

1. Introduction

Hypercholesterolemia is a main risk factor for atherosclerosis and thus a primary cause of cardiovascular organ dysfunction [1–3]. Critical molecular events in atherogenesis are oxidative alterations of lipoproteins and phospholipids, activation of endothelial cells, and infiltration of the vascular wall by macrophages, which is facilitated by reactive oxygen species (ROS) [4, 5]. In the human retina, elevated serum cholesterol levels have been associated with reduced

retinal vascular hyperemic responses to flicker light stimulation [6, 7]. Also, familial risk for cardiovascular disease was reported to be associated with alterations in the retinal vascular function [8]. In addition, hypercholesterolemia has been linked to the pathogenesis of retinal artery and vein occlusion, which constitute major reasons for severe visual impairment and blindness [9–11]. Moreover, a recent meta-analysis reported on an association between hyperlipidemia and an increased risk of glaucoma [12], which is one of the leading causes of vision impairment worldwide characterized by progressive loss of retinal ganglion cells (RGCs), visual field defects, and specific morphological changes of the optic nerve [13–15]. One of the heavily discussed risk factors for glaucoma is impaired ocular perfusion, and vascular endothelial dysfunction is suggested to contribute to abnormalities in ocular perfusion observed in glaucoma patients [16, 17]. Hence, hypercholesterolemia might be linked to glaucoma via inducing vascular endothelial dysfunction in the eye. Despite these findings, the specific effects of hypercholesterolemia on retinal vascular function are unknown at the molecular level. Moreover, it remains to be established whether chronic hypercholesterolemia has an influence on RGC viability. Hence, the aim of the present study was to test the hypothesis that chronic hypercholesterolemia affects retinal arteriole reactivity and RGC survival. We used apolipoprotein E-deficient mice (ApoE-/-) for our studies, because they develop spontaneous severe hypercholesterolemia and atherosclerotic lesions in various blood vessels similar to those found in humans [18–20].

2. Materials and Methods

2.1. Animals. All animals were treated in accordance with the guidelines of EU Directive 2010/63/EU for animal experiments and were approved by the Animal Care Committee of Rhineland-Palatinate, Germany. Mice deficient in the gene coding for apolipoprotein E (ApoE-/-) and age-matched wild-type controls (C57BL/6J) were obtained from The Jackson Laboratory, Bar Harbour, ME, USA. Male mice were fed with a standard rodent chow (Altromin, Lage, Germany) and used for experiments at the age of 12 months. In a previous study using mice from our mouse stock and the same chow, plasma low-density lipoprotein (LDL) and total cholesterol levels were increased by more than 5-fold in 6-month-old ApoE-/- mice compared to wild-type controls [21]. Mice were housed under standardized conditions (12 hours light/dark cycle, temperature of $22 \pm 2^{\circ}C$, humidity of $55 \pm 10\%$, and free access to food and tap water).

2.2. Measurement of Intraocular Pressure, Blood Pressure, and Cholesterol. Intraocular pressure (IOP) was measured noninvasively in conscious mice ($n = 8$ per genotype) using the Icare® TONOLAB rebound tonometer (Bon Optic, Lübeck, Germany) designed for mice and rats. Before each examination, topical anaesthesia (proparacaine 0.5% eye drops, URSAPHARM Arzneimittel GmbH, Saarbrücken, Germany) was applied onto the ocular surface. Per eye, 12 IOP values were taken and the overall mean of all 24 measurements was calculated for each mouse. Blood pressure measurements with a computerized tail-cuff system (CODA® Monitor, Kent Scientific, Torrington, CT, USA) were conducted in conscious restrained mice ($n = 8$ per genotype). Before measurement, mice were trained for two consecutive days to become acclimatized to the procedure. Mice were placed in restraint tubes to prevent excessive movement during measurement and placed on a warming platform (32-35°C). After tails were cuffed, an acclimatization time of 5 minutes allowed mice to warm up before the start of the experiment. Each session consisted of 20 measuring cycles, of which the first 5 cycles were used for acclimatization and were excluded from the analysis. The average of the following 15 cycles was taken as the reading for each mouse. Ocular perfusion pressure was expressed as the difference between arterial blood pressure and intraocular pressure (IOP). We calculated systolic, diastolic, and mean ocular perfusion pressure, respectively. After mice ($n = 8$ per genotype) had been killed by CO_2 exposure, blood was collected from the heart, and serum total cholesterol was determined using the scil Reflovet® Plus (scil animal care company GmbH, Viernheim, Germany).

2.3. Measurements of Retinal Arteriole Reactivity. Retinal arteriole reactivity was measured in isolated retinas using videomicroscopy as previously described [22, 23]. First, mice ($n = 8$ per genotype) were sacrificed by CO_2 exposure, and per mouse one eye was isolated and put into cold Krebs–Henseleit buffer. After preparation of the ophthalmic artery, isolation of the retina, cannulation of the ophthalmic artery, and placing the retina onto a transparent plastic platform, retinal arterioles were pressurized to 50 mm Hg. First-order retinal arterioles were then imaged under bright-field conditions and their responses measured after 30 minutes of equilibration. Concentration-response curves for the thromboxane mimetic, U46619 (10^{-11} to 10^{-6} M; Cayman Chemical, Ann Arbor, MI, USA), were conducted. Vessels were then preconstricted to 50–70% of the initial luminal diameter by titration of U46619 and responses to the endothelium-dependent vasodilator, acetylcholine (10^{-9} to 10^{-4} M; Sigma-Aldrich, Taufkirchen, Germany), and to the endothelium-independent nitric oxide (NO) donor, sodium nitroprusside (SNP, 10^{-9} to 10^{-4} M, Sigma-Aldrich), were measured.

2.4. Quantification of Reactive Oxygen Species. ROS formation was determined in 10 μm cryosections of the retina and optic nerve by dihydroethidium- (DHE-, 1 μm) derived fluorescence according to a modified protocol for vascular cryosections ($n = 8$ per genotype) [24]. In retinal sections, the fluorescence (518 nm/605 nm excitation/emission) was measured in blood vessels and in individual layers of the inner retina as previously described [25–27].

2.5. Immunfluorescence Analysis. Immunostainings were used to quantify reactive nitrogen species (RNS) in cryopreserved retinal and optic nerve cross-sections ($n = 8$ per genotype) stained with an antibody directed against nitrotyrosine (for details see Table 1). Moreover, antibodies directed

Table 1: Specifications of antibodies used for immunofluorescence analysis.

Antibody	Article number, company	Species, clonality	Dilution
Nitrotyrosine	06-284, Merck Millipore, Darmstadt, Germany	Rabbit, polyclonal	1 : 100
NOX1	ab131088, Abcam, Waltham, MA, USA	Rabbit, polyclonal	1 : 200
NOX2	ab129068, Abcam, Waltham, MA, USA	Rabbit, monoclonal	1 : 200
NOX4	ab109225, Abcam, Waltham, MA, USA	Rabbit, monoclonal,	1 : 200
LOX-1	bs-2044R, Biozol Diagnostica Vertrieb GmbH, Eching, Germany	Rabbit, polyclonal	1 : 100
FITC-coupled secondary antibody (for nitrotyrosine staining)	111-095-003, dianova GmbH, Hamburg, Germany	Goat anti-rabbit, polyclonal	1 : 200
Rhodamine red-X-coupled secondary antibody (for NOX1, NOX, NOX4 and LOX-1 staining)	111-295-003, dianova GmbH, Hamburg, Germany	Goat anti-rabbit, polyclonal	1 : 200

against the isoforms of nicotinamide adenine dinucleotide phosphate oxidase (NOX), NOX1, NOX2, and NOX4, respectively, and against the lectin-like oxidized low-density lipoprotein receptor-1 (LOX-1) were used to quantify the respective proteins in retinal cross-sections of 7 μm thickness (for antibody details see Table 1). Fixation of tissue sections for 20 minutes in paraformaldehyde (4%) was followed by preincubation with bovine serum albumin (1%) for 30 minutes and then by the respective primary antibody for 2 hours at room temperature. All primary antibodies displayed pronounced immunoreactivity in the thoracic aorta from ApoE-/- mice (positive control), but not from wild-type mice, at the concentrations used for retinal immunostainings, suggesting that they were suitable to detect the respective gene products. After washing the slides in PBS (3×5 min), the secondary antibody was applied for 1 hour at room temperature (for details see Table 1). Negative control sections were incubated with a blocking medium and the secondary antibody. Finally, slides were washed in PBS (3×5 min) and were mounted using VECTASHIELD® Mounting Medium with DAPI (BIOZOL Diagnostica Vertrieb GmbH, Eching, Germany) and cover-slipped. Subsequently, the fluorescence was measured in blood vessels and in individual layers of the inner retina.

2.6. Real-Time PCR. Messenger RNA for the hypoxic markers, *HIF-1α* and *VEGF-A*; the prooxidant redox enzymes, *NOX1*, *NOX2*, and *NOX*; the antioxidant redox enzymes, *catalase*, *GPx1*, *HO-1*, *SOD1*, *SOD2* and *SOD3*; and for the nitric oxide synthase (*NOS*) isoforms, *eNOS*, *iNOS*, and *nNOS*, was quantified in the retina of ApoE-/- and wild-type mice ($n = 8$ per genotype) by real-time PCR. After mice had died by CO_2 exposure, the one eye per mouse was immediately excised and transferred into cooled phosphate-buffered solution (PBS, Invitrogen, Karlsruhe, Germany) to isolate the retina under a dissecting microscope. Next, the isolated retina was transferred into 1.5 ml plastic tube, rapidly frozen in liquid nitrogen, and stored at -80°C. Later, tissue samples were homogenized (FastPrep; MP Biomedicals, Illkirch, France), and the expression of genes was measured by SYBR Green-based quantitative real-time PCR, as previously described [28]. RNA was isolated using peqGOLD TriFast™ (PEQLAB) and cDNA was generated with the High-Capacity cDNA Reverse Transcription Kit (Applied Biosystems, Darmstadt, Germany). Real-time PCR reactions were performed on a StepOnePlus™ Real-Time PCR System (Applied Biosystems) using SYBR® Green JumpStart™ Taq ReadyMix™ (Sigma-Aldrich) and 20 ng cDNA. Relative mRNA levels of target genes were quantified using comparative threshold (CT) normalized to housekeeping gene TATA-binding protein (TBP). Messenger RNA expression is presented as the fold-change in ApoE-/- mice versus wild-type mice. The PCR primer sequences are listed in Table 2.

2.7. Cell Counting in Retinal Wholemounts. Post mortem, one eye per mouse ($n = 8$ per genotype) was excised and fixed in 4% paraformaldehyde (Sigma-Aldrich) for 30 minutes. Next, a retinal wholemount was prepared in cold PBS, transferred onto a glass slide, and stained with cresyl blue as previously described [29]. After the staining procedure, sixteen predefined areas per wholemount, eight central and eight peripheral, of 150 μm × 200 μm were photographed by a blinded investigator as reported in detail previously [25, 30, 31]. Per photograph, all cresyl blue-positive cells were counted manually by a blinded investigator using the cell counter plugin for ImageJ software (NIH, http://rsb.info.nih.gov/ij/) as previously described [25, 31]. The mean cell density (cells/mm^2) was calculated and multiplied with the wholemounts' surface area to obtain the total number of cells per retina.

2.8. Axon Counting in Optic Nerve Cross-Sections. Per mouse, one optic nerve was isolated ($n = 8$ per genotype), placed in fixative solution, and embedded in agar 100 resin. Afterwards, semithin cross-sections were cut with an ultramicrotome (Ultracut E, Leica, Bensheim, Germany), placed on glass slides, and stained with 1% toluidine blue in 1% sodium borate according to standard protocols. Each cross-section

Table 2: Sequences of the primers used for real-time PCR analysis.

Gene	Forward	Reverse
HIF-1α	TCATCAGTTGCCACTTCCCCAC	CCGTCATCTGTTAGCACCATCAC
VEGF-A	ACTTGTGTTGGGAGGAGGATGTC	AATGGGTTTGTCGTGTTTCTGG
NOX1	GGAGGAATTAGGCAAAATGGATT	GCTGCATGACCAGCAATGTT
NOX2	CCAACTGGGATAACGAGTTCA	GAGAGTTTCAGCCAAGGCTTC
NOX4	TGTAACAGAGGGAAAACAGTTGGA	GTTCCGGTTACTCAAACTATGAAGAGT
eNOS	CCTTCCGCTACCAGCCAGA	CAGAGATCTTCACTGCATTGGCTA
iNOS	CAGCTGGGCTGTACAAACCTT	CATTGGAAGTGAAGCGTTTCG
nNOS	TCCACCTGCCTCGAAACC	TTGTCGCTGTTGCCAAAAAC
Catalase	CAAGTACAACGCTGAGAAGCCTAAG	CCCTTCGCAGCCATGTG
GPx1	CCCGTGCGCAGGTACAG	GGGACAGCAGGGTTTCTATGTC
HO-1	GGTGATGCTGACAGAGGAACAC	TAGCAGGCCTCTGACGAAGTG
SOD1	CCAGTGCAGGACCTCATTTTAAT	TCTCCAACATGCCTCTCTTCATC
SOD2	CCTGCTCTAATCAGGACCCATT	CGTGCTCCCACACGTCAAT
SOD3	TTCTTGTTCTACGGCTTGCTACTG	AGCTGGACTCCCCTGGATTT
TBP	CTT CGT GCA AGA AAT GCT GAA T	CAG TTG TCC GTG GCT CTC TTA TT

Table 3: Intraocular pressure, blood pressure, ocular perfusion pressure, and total serum cholesterol in wild-type and ApoE-/- mice ($n = 8$ per genotype).

Systemic parameters	Wild type	ApoE-/-	P value
Intraocular pressure (mm hg)	11.95 ± 0.5491	11.56 ± 0.6165	0.6428
Blood pressure (mm hg)			
Systolic	98.68 ± 4.341	105.7 ± 4.263	0.2701
Diastolic	67.74 ± 3.959	63.23 ± 4.606	0.4702
Mean	77.73 ± 3.907	77.06 ± 3.941	0.9051
Ocular perfusion pressure (mm hg)			
Systolic	86.73 ± 4.024	94.12 ± 3.925	0.2098
Diastolic	55.79 ± 3.631	51.68 ± 4.390	0.4817
Mean	65.79 ± 3.568	65.50 ± 3.647	0.9566
Total cholesterol (mg/dL)	145.1 ± 5.642	511.0 ± 12.21	**<0.0001**

was examined using bright-field microscopy by a blinded investigator. Five nonoverlapping fields of 60 μm × 80 μm (one central and four peripheral) were photographed per cross-section. Axons were counted manually by a blinded investigator using ImageJ software. The mean axon density (axons/mm^2) was calculated and multiplied by the cross-sectional area to obtain the total number of axons per optic nerve as described recently in detail [25, 31].

2.9. Statistical Analysis. Data are presented as mean ± SE, and n represents the number of mice per group. Constriction responses to U46619 are presented as percent change in luminal diameter from resting diameter, while responses to SNP and acetylcholine are presented as percent change in luminal diameter from the preconstricted diameter. Comparison between concentration-responses was made using two-way ANOVA for repeated measurements. For comparisons of IOP, blood pressure, ocular perfusion pressure, total serum cholesterol, fluorescent intensity, mRNA expression levels, and cell and axon numbers, an unpaired t-test was used. The level of significance was set at 0.05.

3. Results

3.1. Intraocular Pressure, Blood Pressure, Ocular Perfusion Pressure, and Total Serum Cholesterol. No differences in intraocular pressure, blood pressure, and ocular perfusion pressure were detected between ApoE-/- and wild-type mice. Total serum cholesterol was markedly elevated in ApoE-/- mice compared to wild-type mice ($P < 0.0001$, $n = 8$ per genotype). The data are presented in Table 3.

3.2. Responses of Retinal Arterioles. The initial luminal diameter of retinal arterioles was similar in both mouse genotypes (20.52 ± 0.9656 μm and 21.58 ± 0.9808 μm in ApoE-/- and wild-type mice, respectively, $P = 0.4550$, $n = 8$ per genotype).

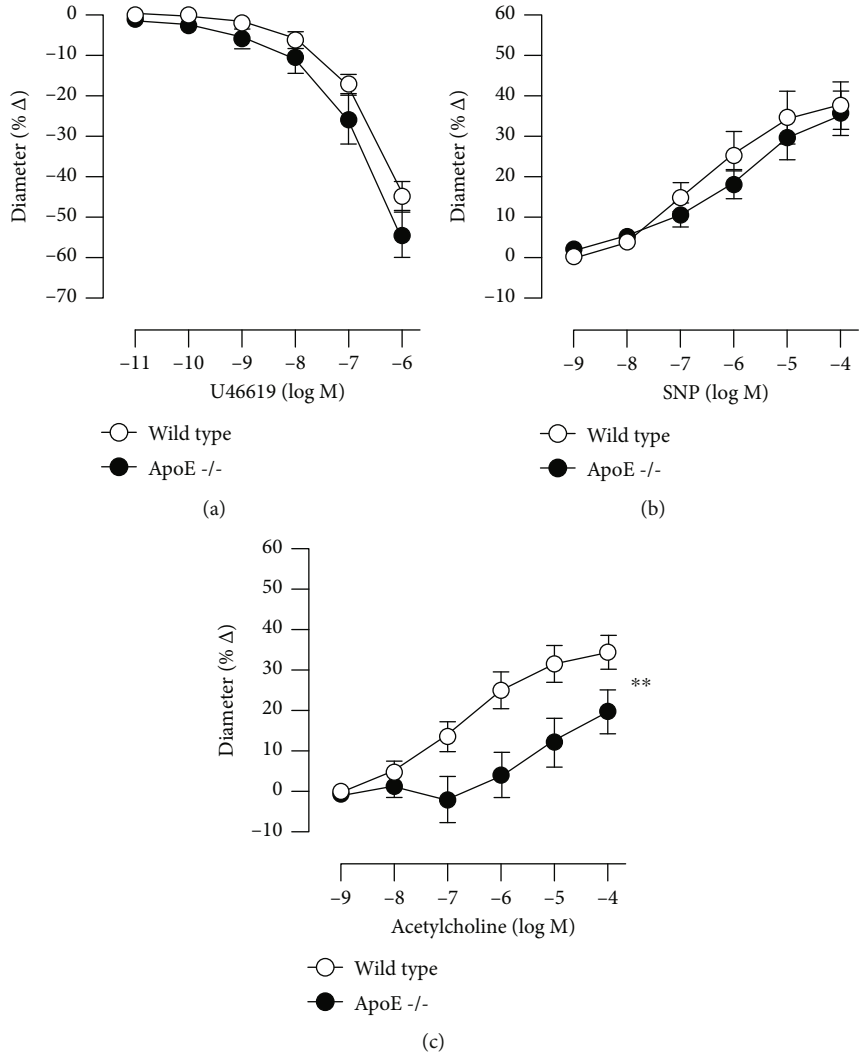

Figure 1: Responses of retinal arterioles from ApoE−/− and wild-type mice to the thromboxane mimetic, U46619 (a), the endothelium-independent vasodilator, SNP (b), and to the endothelium-dependent vasodilator, acetylcholine (c). Values are presented as mean ± SE ($n = 8$ per concentration and genotype; $^{**}P < 0.01$).

U46619 elicited concentration-dependent vasoconstriction of retinal arterioles that was similar in ApoE-/- and wild-type mice (54.50 ± 5.441% versus 44.86 ± 3.495%, ApoE-/- versus wild-type mice at 10^{-6} M; $P > 0.05$; Figure 1(a)). The endothelium-independent vasodilator, SNP, elicited concentration-dependent vasodilation that did also not differ between both mouse genotypes (35.77 ± 5.531% versus 37.70 ± 5.837%, ApoE-/- versus wild-type mice at 10^{-4} M; $P > 0.05$; Figure 1(b)). In contrast, the endothelium-dependent vasodilator, acetylcholine, produced concentration-dependent vasodilation, which was impaired in arterioles from ApoE-/- mice (19.79 ± 5.576% versus 34.41 ± 4.175%, ApoE-/- versus wild-type mice at 10^{-4} M; $P < 0.01$; Figure 1(c)).

3.3. ROS and RNS Formation in the Retina and Optic Nerve. Staining of retinal sections with DHE revealed increased fluorescence intensity specifically in retinal blood vessels from ApoE−/− mice, indicative of elevated ROS levels ($P = 0.0022$, ApoE-/- versus wild-type mice, $n = 8$ per genotype; Figures 2(a), 2(b), and 2(e)). No differences in fluorescence intensity where found between both genotypes in the individual layers of the inner retina ($n = 8$ per genotype; Figures 2(a), 2(b), and 2(e)). Similarly, in cross-sections of the optic nerve, no differences in DHE fluorescence intensity were found between wild-type and ApoE−/− mice ($n = 8$ per genotype; Figures 2(c)–2(e)). Immunoreactivity to nitrotyrosine was negligible in blood vessels and in all inner retinal layers of both mouse genotypes ($n = 8$ per genotype; Figures 3(a), 3(b), 3(d) and 3(e)), suggesting that RNS levels were very low and not increased in ApoE-/- mice (Figure 3(g)). In optic nerve cross-sections of both genotypes, some green hyperfluorescent spots were visible (Figures 3(c) and 3(f)), but no differences in immunoreactivity to nitrotyrosine were detectable between wild-type and ApoE−/− mice ($n = 8$ per genotype; Figure 3(g)).

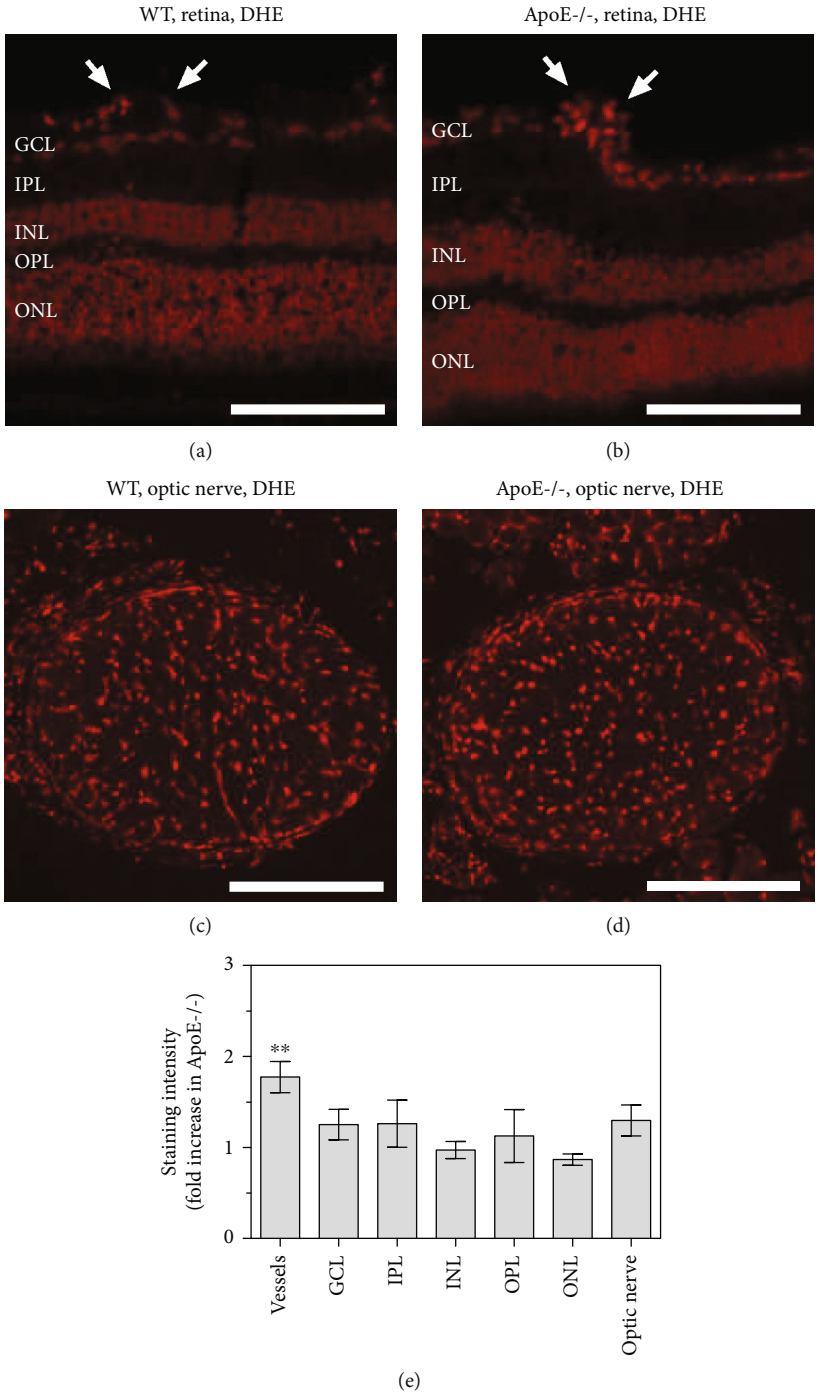

Figure 2: DHE stainings of retinal cross-sections (a, b) and of optic nerve cross-sections (c, d) from wild-type and ApoE-/- mice, respectively. Staining intensity was increased in retinal blood vessels from ApoE-/- mice but did neither differ in any of the retinal layers nor in the optic nerve between both genotypes (e). The white arrows point to retinal blood vessel cross-sections. GCL: ganglion cell layer; IPL: inner plexiform layer; INL: inner nuclear layer; OPL: outer plexiform layer; ONL: outer nuclear layer. Values are presented as mean ± SE ($n = 8$ per genotype; $^{**}P < 0.01$). Scale bar = 100 μm.

3.4. NOX1, NOX2, and NOX4 Expressions in the Retina. Immunoreactivity to NOX1 did not differ between blood vessels and any of the inner retinal layers of ApoE−/− and wild-type mice ($n = 8$ per genotype; Figures 4(a)–4(g)). In contrast, immunoreactivity to NOX2 was markedly increased in retinal blood vessels from ApoE-/- mice ($P = 0.0027$, ApoE-/- versus wild-type mice, $n = 8$ per genotype), but did not differ in individual retinal layers of both mouse genotypes (Figures 4(h)–4(n)). NOX4 immunoreactivity was similar in blood vessels and all retinal layers of both mouse genotypes ($n = 8$ per genotype; Figures 4(o)–4(u)).

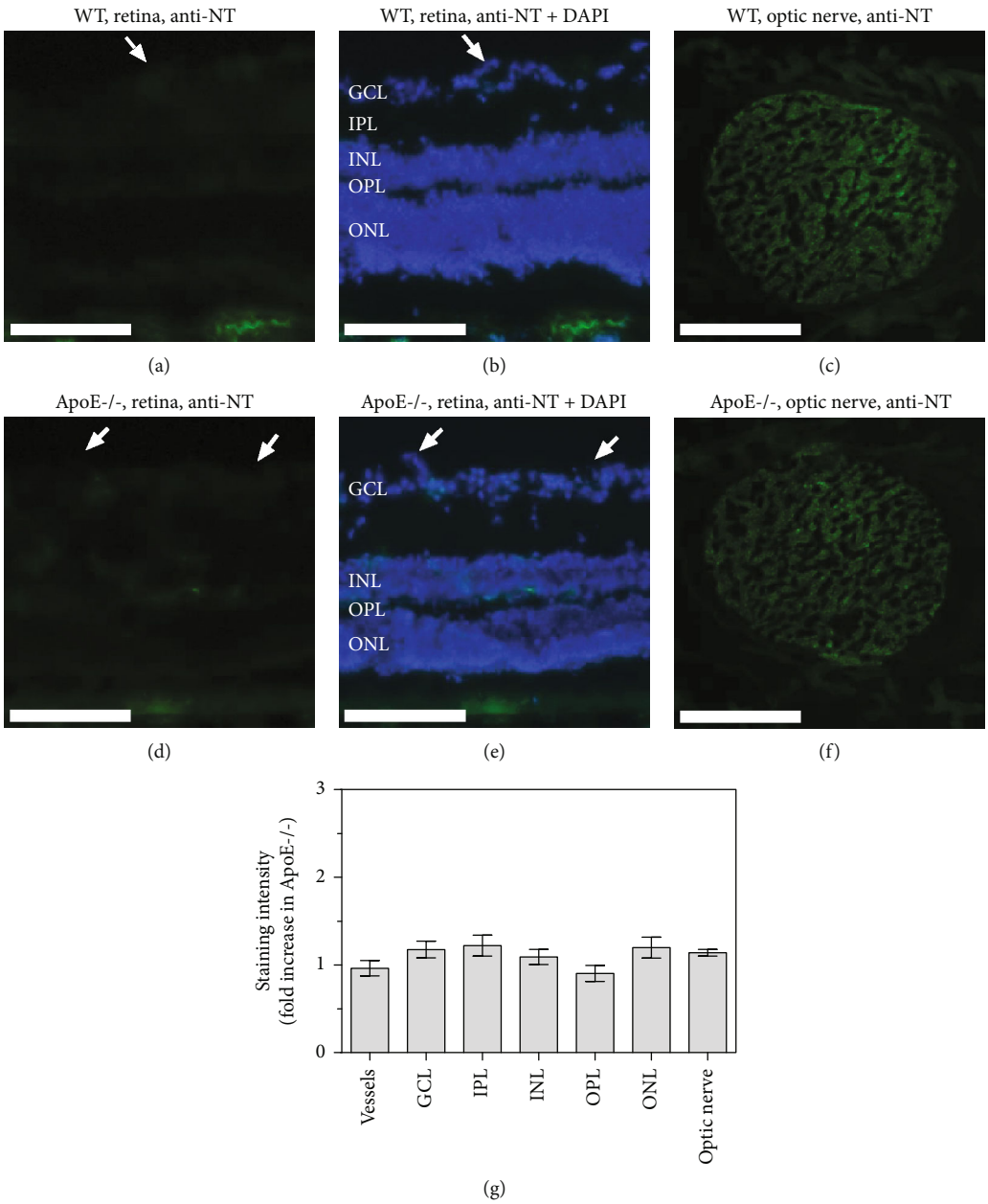

Figure 3: Nitrotyrosine immunostainings (anti-NT) in retinal cross-sections and optic nerve cross-sections from wild-type (a–c) and ApoE-/- mice (d–f). Immunoreactivity to nitrotyrosine was negligible in the inner retina of both genotypes (a, d). In optic nerve cross-sections, some green hyperfluorescent spots were visible, but no differences in fluorescent intensity were observed between both genotypes (g). The white arrows point to retinal blood vessels cross-sections. GCL: ganglion cell layer; IPL: inner plexiform layer; INL: inner nuclear layer; OPL: outer plexiform layer; ONL: outer nuclear layer. Values are presented as mean ± SE ($n = 8$ per genotype). Scale bar = 100 μm.

3.5. Expression of LOX-1 in the Retina. Immunoreactivity to LOX-1, which serves as a receptor for ox-LDL, was faint in the inner retina of wild-type mice. Also, immunoreactivity in blood vessels was not pronounced in retinas of wild-type mice ($n = 8$ per genotype; Figures 5(a)–5(c)). The immunoreactivity pattern in individual retinal layers from ApoE-/- mice resembled the one from wild-type mice. However, strong immunoreactivity was seen in retinal blood vessels from ApoE-/- mice ($n = 8$ per genotype; Figures 5(c)–5(e)). The staining intensity was markedly stronger in retinal blood vessels from ApoE-/- mice compared to wild-type mice ($P = 0.0007$, $n = 8$ per genotype; Figure 5(f)).

3.6. Expression of Hypoxic and Redox Genes in the Retina. In the retina of ApoE-/- mice, mRNA for both hypoxic markers, *HIF-1α* and *VEGF-A*, was slightly but significantly elevated compared to wild-type mice (1.7-fold for *HIF-1α*, $P = 0.0013$ and 1.4-fold for *VEGF-A*, $P = 0.0095$, $n = 8$ per genotype), indicative of a hypoxic condition (Figure 6(a)). Also, mRNA for the prooxidant redox genes, *NOX1* and *NOX2*,

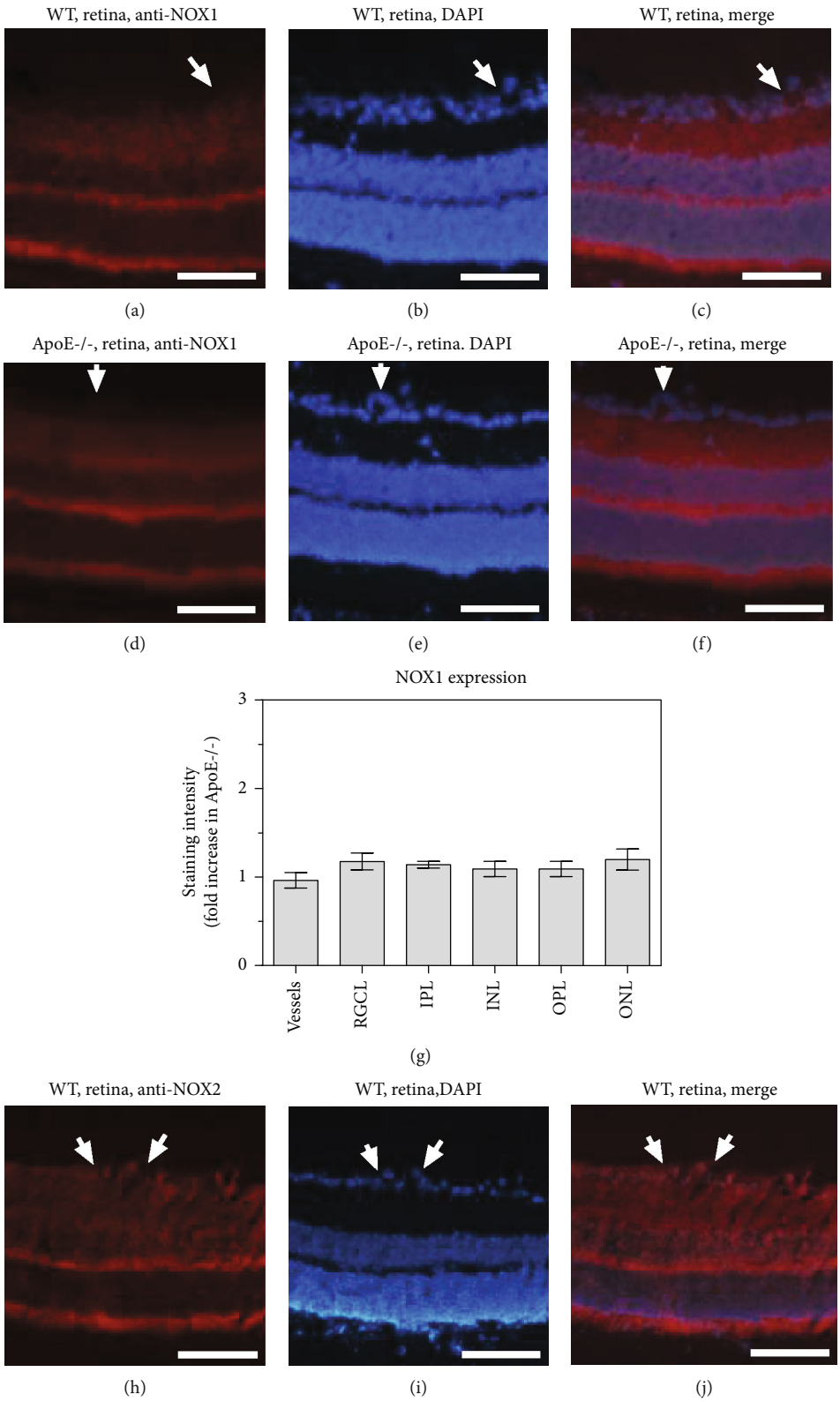

Figure 4: Continued.

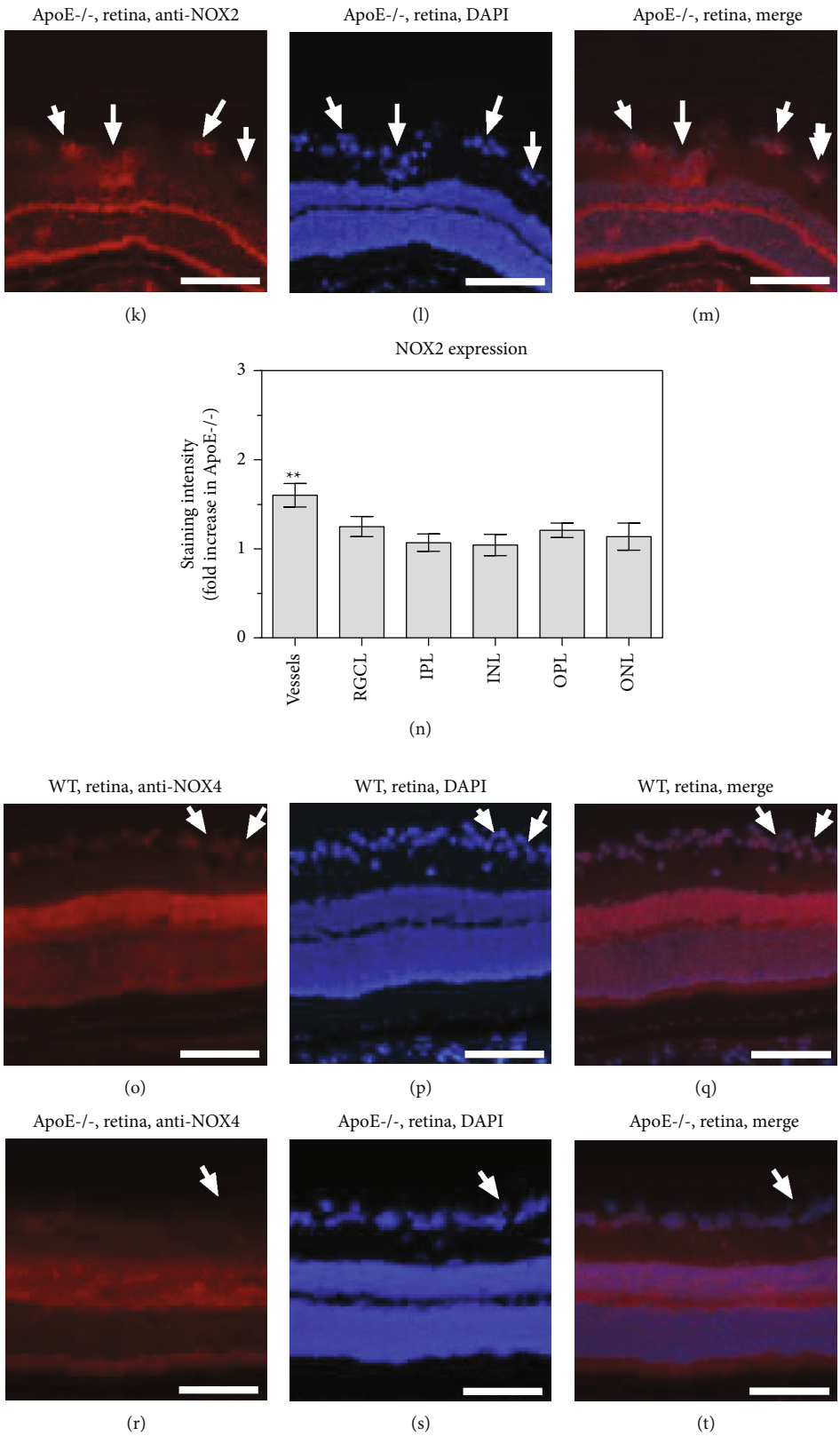

Figure 4: Continued.

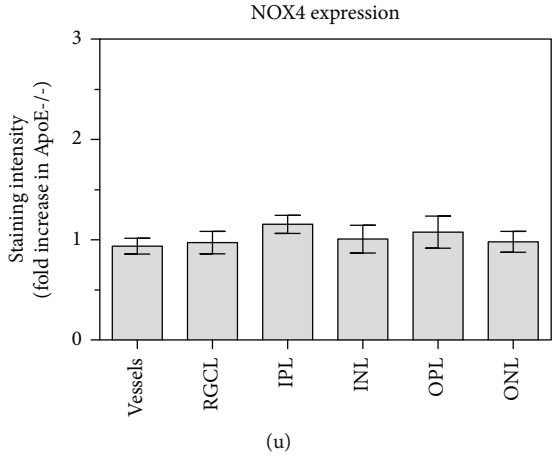

Figure 4: Immunostainings for NOX1 (a–g), NOX2 (h–n), and NOX4 (o–u) in retinal cross-sections from wild-type and ApoE-/- mice. Immunoreactivity to NOX1 was similar in blood vessels and all retinal layers in both mouse genotypes (g). In contrast, immunoreactivity to NOX2 was increased in retinal blood vessels from ApoE-/- mice but did not differ in individual retinal layers of both mouse groups (n). Immunoreactivity to NOX4 was also similar throughout the retina in both genotypes (u). The white arrows point to retinal blood vessel cross-sections. GCL: ganglion cell layer; IPL: inner plexiform layer; INL: inner nuclear layer; OPL: outer plexiform layer; ONL: outer nuclear layer. Values are presented as mean ± SE ($n = 8$ per genotype; $^{**}P < 0.01$). Scale bar = 100 μm.

was increased in the retina from ApoE-/- mice compared to wild-type mice (2.0-fold for *NOX1*, $P = 0.0053$ and 2.1-fold for *NOX2*, $P = 0.0312$, $n = 8$ per genotype; Figure 6(b)). Among the three nitric oxide synthase (NOS) isoforms, mRNA expression for inducible (*iNOS*) and neuronal NOS (*nNOS*) was found to be increased (1.3-fold for *iNOS*, $P = 0.0009$ and 2.6-fold for *nNOS*, $P = <0.0001$, $n = 8$ per genotype; Figure 6(c)). Interestingly, also mRNA expression for all antioxidant redox genes tested was elevated (5.2-fold for *catalase*, $P < 0.0001$; 1.4-fold for *GPx-1*, $P = 0.0063$; 2.0-fold for *HO-1*, $P = 0.0005$; 1.3-fold for *SOD1*, $P = 0.0180$; 1.4-fold for *SOD2*, $P = 0.0383$; 3.1-fold for *SOD3*, $P = 0.0006$, $n = 8$ per genotype; Figure 6(d)).

3.7. Retinal Ganglion Cell Layer Cells and Optic Nerve Axons. Total cell number in the RGC layer was 108 063 ± 2 745 and 102 255 ± 3 558 in ApoE-/- and wild-type mice and did not differ between both genotypes ($P = 0.2171$, $n = 8$ per genotype; Figure 7). The number of axons in the optic nerve, representing the axons of RGCs, did also not differ between both genotypes. The axon number was 46 790 ± 1 493 and 45 554 ± 2 145 in ApoE-/- and wild-type mice, respectively, and was not different between both mouse genotypes ($P = 0.6435$, $n = 8$ per genotype; Figure 7).

4. Discussion

There are several major new findings emerging from this experimental study. First, the lack of apolipoprotein E had no effect on intraocular pressure, blood pressure, and ocular perfusion pressure but affected reactivity of retinal arterioles to the endothelium-dependent vasodilator, acetylcholine, indicative of endothelial dysfunction. Second, ROS levels, but not RNS levels, were found to be elevated in retinal arterioles of ApoE-/- mice. In contrast, neither ROS nor RNS were increased in individual retinal layers and the optic nerve of ApoE-/- mice suggesting that oxidative stress is limited to the vasculature and nitrosative stress is negligible. Also, immunoreactivity to LOX-1 and NOX2, but not to NOX1 or NOX4 was elevated in retinal vessels of ApoE-/- mice, suggesting that a mechanism involving LOX-1, NOX2, and ROS may be involved in mediating endothelial dysfunction. The lack of apolipoprotein E was associated with increased retinal mRNA expression for the hypoxia markers, *HIF-1α* and *VEGF-A*, as well as of redox genes coding for the prooxidant enzymes *NOX1* and *NOX2*. However, mRNA expression for the antioxidant redox genes *SOD1*, *SOD3*, *SOD3*, *GPx1*, *HO-1*, and *catalase* were also increased, suggesting that enhanced ROS production is associated with a compensation by antioxidant enzymes. Third, total cell number in the RGC layer and axon number in the optic nerve was not affected by the lack of apolipoprotein E. These findings illustrate that apolipoprotein E deficiency causes oxidative stress and endothelial dysfunction in retinal arterioles, but no oxidative damage in nonvascular retinal tissue probably by effective buffering of excessive ROS and RNS generation by antioxidant redox enzymes.

During hypercholesterolemia, oxidized low-density lipoproteins (ox-LDLs) have been shown to trigger the expression of prooxidant enzymes and thus, ROS generation, in the vascular wall via involvement of LOX-1 [32]. Of note, the expression LOX-1, which serves as a receptor for ox-LDL, was reported to be upregulated in hypercholesterolemia via positive feedback mechanisms involving the transcription factor NF-κB [33, 34]. In agreement with these studies, we found increased LOX-1 expression and increased ROS levels in the vascular wall of retinal blood vessels from ApoE-/- mice. In many vascular beds, high ROS concentrations elicit endothelial dysfunction, reflected by a reduced endothelium-dependent vasodilation, in part by affecting eNOS bioactivity and by inactivation of nitric oxide [32, 35, 36]. These mechanisms have also been described in cerebral blood vessels of

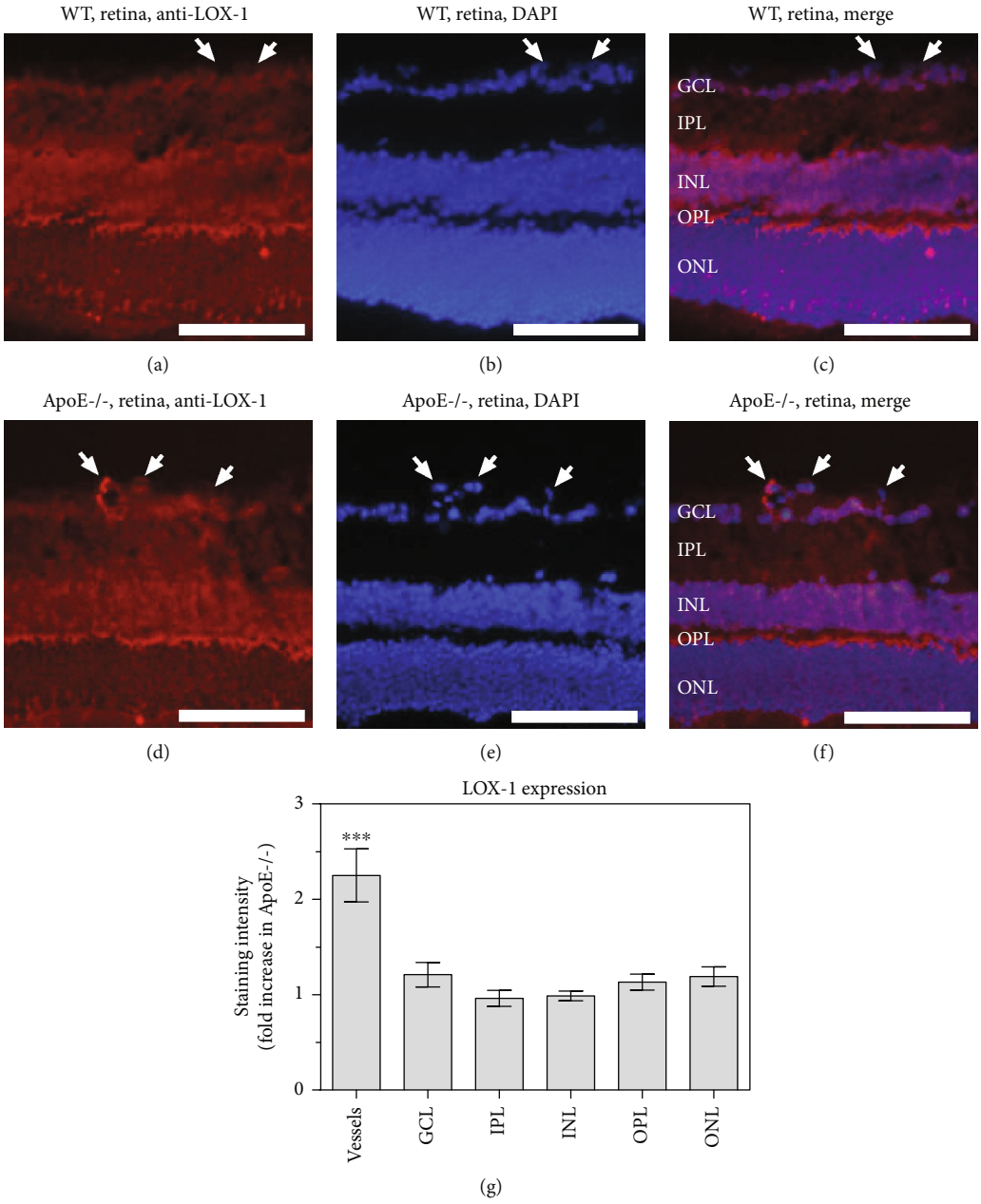

Figure 5: Immunostainings for the ox-LDL receptor, LOX-1, in retinal cross-sections from wild-type (a–c) and ApoE-/- mice (d–f), respectively. Staining intensity was increased in blood vessels from ApoE-/- mice (g) but did not differ in any of the retinal layers between both genotypes. GCL: ganglion cell layer; IPL: inner plexiform layer; INL: inner nuclear layer; OPL: outer plexiform layer; ONL: outer nuclear layer. Values are presented as mean ± SE ($n = 8$ per genotype; $^{***}P < 0.001$). Scale bar = 100 μm.

various hypercholesterolemic animal models, including ApoE-/- mice [37–40]. Likewise, in the human retina, elevated serum cholesterol levels have been associated with reduced retinal vascular hyperemic responses to flicker light stimulation, which are in part nitric oxide synthase-dependent [6, 7]. However, the molecular effects of hypercholesterolemia on retinal endothelial function have not been elucidated so far. The findings of the present study suggest that LOX-1, NOX2, and ROS are involved in mediating hypercholesterolemia-induced endothelial dysfunction in the retina, which is in concert with a study in cerebral blood vessels reporting that NOX2-derived ROS abrogated nitric oxide function in ApoE-/- mice [40].

We excluded the possibility that endothelial dysfunction was triggered by differences in IOP, blood pressure, or ocular perfusion pressure between ApoE-/- and wild-type mice. Arterial hypertension is a trigger factor of endothelial dysfunction in various blood vessels, including ocular and cerebral vessels [41, 42]. Conversely, low ocular perfusion pressure was associated with glaucoma prevalence, incidence, and progression [43]. Similar to the present findings, most of the previous studies reported that blood pressure does not

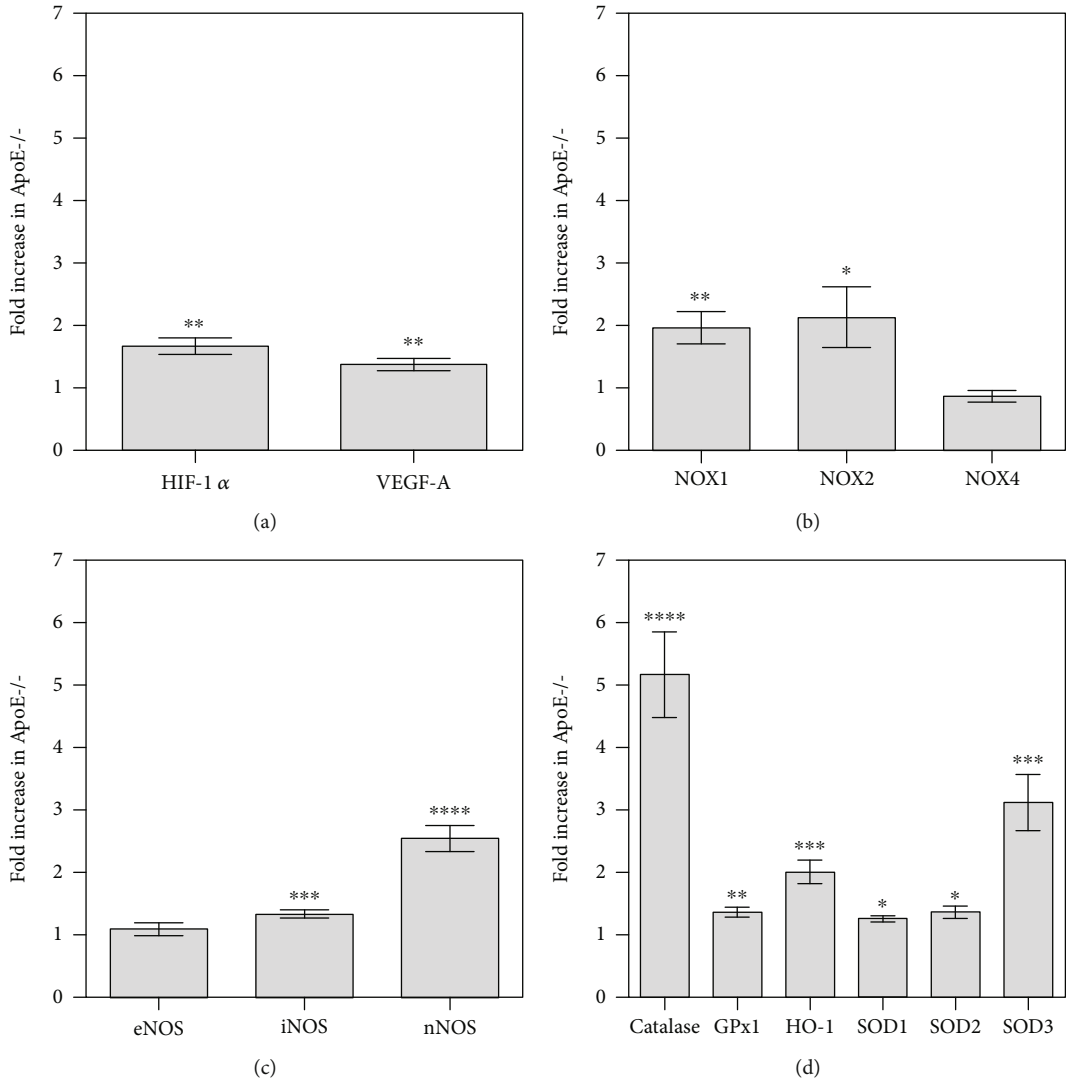

Figure 6: Messenger RNA expression of hypoxic markers ((a) HIF-1α, VEGF-A), prooxidant ((b) NOX1, NOX2, and NOX4), the three nitric oxide synthase isoforms ((c) eNOS, iNOS, and nNOS), and of the antioxidant redox enzymes ((d) catalase, GPx1, HO-1, SOD1, SOD2, and SOD3) in retinal samples from wild-type and ApoE-/- mice. Data are presented as the fold-change (mean ± SE) in ApoE-/- versus wild-type mice ($n = 8$ per genotype, $^{*}P < 0.05$, $^{**}P < 0.01$, $^{***}P < 0.001$, $^{****}P < 0.0001$).

differ in ApoE-/- and wild-type mice and is stable with age [20, 44–46]. Interestingly, other previous studies in ApoE-/- mice revealed that some small blood vessels do not develop endothelial dysfunction [47, 48]. One possible explanation for these findings is that endothelium-derived hyperpolarizing factor- (EDHF-) dependent vasodilation mechanisms are less affected by hypercholesterolemia [47]. In mouse retinal arterioles, however, endothelium-dependent vasodilation is mainly mediated by eNOS and, during eNOS deficiency, by nNOS and COX-2 metabolites, suggesting that EDHF pathways play only a negligible role [49, 50].

An intriguing question concerning many retinal diseases is how endothelial dysfunction affects neuron survival. So far only indirect links between impaired vascular responses and the onset and progression retinal pathologies exist. For example, reduced responses of retinal arterioles to various stimuli have been reported in patients with diabetic retinopathy and glaucoma [51, 52]. Other studies in humans suggest that certain polymorphisms of the gene coding for eNOS, which plays a major role in endothelial function of retinal arterioles, have a risk association for onset or progression of diabetic retinopathy and of some forms of glaucoma [53–57]. However, in animal models characterized by reduced responsiveness to the endothelium-dependent vasodilator, acetylcholine, such as eNOS-deficient and M_3 receptor-deficient mice, no loss of RGCs has been detected [22, 25, 30, 50]. On the other hand, in diabetic mice, eNOS deficiency was reported to promote the progression of diabetic retinopathy, suggesting that endothelial dysfunction might accelerate pathophysiological processes in the retina [58].

The retinal vasculature supplies the inner retinal layers, while the outer layers are supplied by choroidal blood vessels [59]. Hence, impaired blood supply due to abnormal

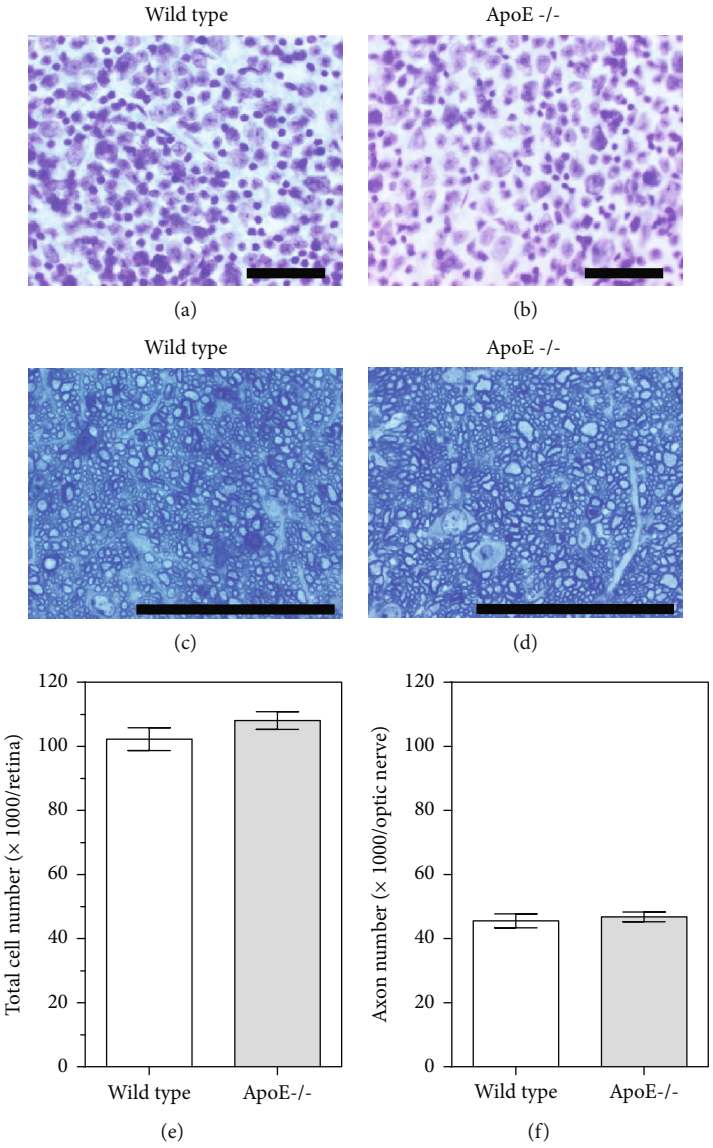

Figure 7: Example photographs taken from retinal wholemounts stained with cresyl blue and optic nerve cross-sections stained with toluidine blue of wild-type (a, c) and ApoE-/- mice (b, d). Total cell number in the RGC layer (e) and axon number (f) in the optic nerve was similar in wild-type and ApoE-/- mice. Values are presented as mean ± SE ($n = 8$ per genotype). Scale bar = 50 μm.

reactivity of retinal vessels is supposed to affect primarily the inner retinal cell layers, such as the RGC layer. Intriguingly, previous studies in genetically modified animal models of atherosclerosis, including ApoE-/- mice, reported on pathological changes in outer retinal layers, such as lipoidal degenerations and basal deposits in the Bruch's membrane that resemble alterations observed in ageing human eyes, with some functional and morphologic alterations similar to those found in age-related macular degeneration [60–63]. In support of this concept, some studies in humans found a positive association of serum cholesterol levels with age-related macular degeneration [64, 65].

In contrast, the effects of apolipoprotein E deficiency on RGC survival have not been studied in detail so far. A recent meta-analysis reported that hyperlipidemia was associated with an increased risk of glaucoma, a disease characterized by progressive RGC and visual field loss [12]. However, the original studies included in the meta-analysis displayed highly heterogenic results [12]. Also, studies on the association of apolipoprotein E gene polymorphisms with glaucoma reported heterogenic results [66–69]. Interestingly, a study in mice found that apolipoprotein E deficiency was even protective against RGC death induced by elevated intraocular pressure or optic nerve crush [70]. In the present study, 12-month-old ApoE-/- mice and age-matched wild-type controls had a similar total cell number in the RGC layer, which comprises RGCs, displaced amacrine cells, vascular cells, and glial cells. Moreover, no differences in optic nerve axon number, which reflects the number of RGCs, have been detected, suggesting that apolipoprotein E deficiency has no effect of RGC viability. The mRNA expression data of the present study, however, revealed increased expression levels for *HIF-1α* and

VEGF-A together with increased levels for *NOX1* and *NOX2* indicating that abnormal vascular function in the retina may have triggered hypoxia and ROS generation. However, also a variety of antioxidant redox genes was shown to be upregulated in the retina of ApoE-/- mice, suggesting that compensatory antioxidant pathways have been activated, which may have buffered excessive ROS and RNS generation and, thus, their potential deleterious effects on cell viability.

Apart from its role in the regulation of cholesterol homeostasis in the peripheral circulation, apolipoprotein E is expressed in the central nervous system including the retina and optic nerve, where it takes part in cholesterol transport and intracellular exchange of metabolites between neurons and glial cells [71–73]. One study reported that activated retinal glial cells promote neurite outgrowth in RGCs via involvement of apolipoprotein E [73]. However, studies of retinal histology and function have shown only minor changes in ApoE-/- mice [74, 75]. In support of this concept, detailed neurocognitive and retinal studies in a 40-year-old patient with severe dysbetalipoproteinemia due to total absence of apolipoprotein E failed to demonstrate any functional and morphological defects [76]. These findings suggest that redundant mechanisms exist in the retina to compensate for the lack of apolipoprotein E.

5. Conclusions

Our study demonstrates that chronic apolipoprotein E deficiency promotes endothelial dysfunction in retinal arterioles. The presented data also suggest that LOX-1, NOX2, and ROS, but not RNS, are involved in this process. Although the mRNA expression for prooxidant enzymes was increased in the retina of ApoE-/- mice, mRNA for antioxidant enzymes was also upregulated, indicating that oxidative stress in retinal tissue appears to be quenched by antioxidant mechanisms, which results in preservation of RGC viability. Hence, our data also suggest that apolipoprotein E deficiency and endothelial dysfunction of the retinal vasculature are not deleterious to RGCs, at least in the absence of additional pathophysiological stimuli.

Abbreviations

ApoE-/-: Apolipoprotein E-deficient mouse
DAPI: 4′,6-Diamidino-2-phenylindole
DHE: Dihydroethidium
EDHF: Endothelium-derived hyperpolarizing factor
eNOS: Endothelial nitric oxide synthase
GPx1: Glutathinone peroxidase 1
HIF-1α: Hypoxia-inducible factior-1α
HO-1: Heme oxygenase-1
iNOS: Inducible nitric oxide synthase
IOP: Intraocular pressure
nNOS: Neuronal nitric oxide synthase
NOX: Nicotinamide adenine dinucleotide phosphate oxidase
LDL: Low-density lipoprotein
LOX-1: Lectin-like oxidized low-density lipoprotein receptor-1
PBS: Phosphate-buffered saline
RGC: Retinal ganglion cell
RNS: Reactive nitrogen species
ROS: Reactive oxygen species
SNP: Sodium nitroprusside
SOD: Superoxide dismutase
TNF-α: Tumor necrosis factor alpha
U46619: 9,11-Dideoxy-9α,11α-methanoepoxy prostaglandin F2α
VEGF-A: Vascular endothelial growth factor a.

Data Availability

The data used to support the findings of this study are available from the corresponding author upon request.

Disclosure

Part of this study will be presented in the PhD thesis of Jenia Kouchek Zadeh. Part of the data in the manuscript were presented as a poster at the congress of the Annual Meeting of the Association for Research in Vision and Ophthalmology (ARVO) 2014 in Orlando, FL, USA. The conference abstract was published in IOVS 2014, Vol.55, 4352.

Conflicts of Interest

The authors state that there is no conflict of interests.

Authors' Contributions

A.G. and H.L. designed the study. A.G., A.M., C.Y., J.K.Z., M.B.Z., P.L., C.B., and N.X. conducted the experiments. A.G., J.K.Z., M.B.Z., and N.X. analyzed data. A.D., C.B., M.O., and N.P. contributed essential materials and reagents. A.G. and J.K.Z. wrote the manuscript. All authors read and approved the final manuscript.

Acknowledgments

We are grateful to Ms. Gisela Reifenberg, Department of Pharmacology, University Medical Center, Johannes Gutenberg University Mainz, for her technical assistance with PCR; to Ms. Karin Molter, Institute of Pathology, University Medical Center, Johannes Gutenberg University Mainz, for her expert assistance with optic nerve embedding procedures; and to Ms. Jessica Rudolph for her technical assistance with blood pressure measurements. A.G. and H.L. received financial support for the work by the intramural Science Transfer Program of the University Medical Center Mainz.

References

[1] L. J. Mundal, J. Igland, M. B. Veierød et al., "Impact of age on excess risk of coronary heart disease in patients with familial hypercholesterolaemia," *Heart*, vol. 104, no. 19, pp. 1600–1607, 2018.

[2] J. P. Appleton, P. Scutt, N. Sprigg, and P. M. Bath, "Hypercholesterolaemia and vascular dementia," *Clinical Science*, vol. 131, no. 14, pp. 1561–1578, 2017.

[3] M. G. Wong, C. Wanner, J. Knight, and V. Perkovic, "Lowering cholesterol in chronic kidney disease: is it safe and effective?," *European Heart Journal*, vol. 36, no. 43, pp. 2988–2995, 2015.

[4] H. Mollazadeh, F. Carbone, F. Montecucco, M. Pirro, and A. Sahebkar, "Oxidative burden in familial hypercholesterolemia," *Journal of Cellular Physiology*, vol. 233, no. 8, pp. 5716–5725, 2018.

[5] U. Forstermann, N. Xia, and H. Li, "Roles of vascular oxidative stress and nitric oxide in the pathogenesis of atherosclerosis," *Circulation Research*, vol. 120, no. 4, pp. 713–735, 2017.

[6] M. Reimann, S. Prieur, B. Lippold et al., "Retinal vessel analysis in hypercholesterolemic patients before and after LDL apheresis," *Atherosclerosis Supplements*, vol. 10, no. 5, pp. 39–43, 2009.

[7] M. Sharifizad, K. J. Witkowska, G. C. Aschinger et al., "Factors determining flicker-induced retinal vasodilation in healthy subjects," *Investigative Ophthalmology & Visual Science*, vol. 57, no. 7, pp. 3306–3312, 2016.

[8] S. Seshadri, S. E. Karimzad, H. Shokr, and D. Gherghel, "Retinal vascular function in asymptomatic individuals with a positive family history of cardiovascular disease," *Acta Ophthalmologica*, vol. 96, no. 8, pp. e956–e962, 2018.

[9] N. Cheung, L. Lim, J. J. Wang et al., "Prevalence and risk factors of retinal arteriolar emboli: the Singapore Malay Eye Study," *American Journal of Ophthalmology*, vol. 146, no. 4, pp. 620–624, 2008.

[10] T. Stojakovic, H. Scharnagl, W. März, B. R. Winkelmann, B. O. Boehm, and O. Schmut, "Low density lipoprotein triglycerides and lipoprotein(a) are risk factors for retinal vascular occlusion," *Clinica Chimica Acta*, vol. 382, no. 1-2, pp. 77–81, 2007.

[11] R. Marcucci, A. Sodi, B. Giambene et al., "Cardiovascular and thrombophilic risk factors in patients with retinal artery occlusion," *Blood Coagulation & Fibrinolysis*, vol. 18, no. 4, pp. 321–326, 2007.

[12] S. Wang and X. Bao, "Hyperlipidemia, blood lipid level, and the risk of glaucoma: a meta-analysis," *Investigative Ophthalmology & Visual Science*, vol. 60, no. 4, pp. 1028–1043, 2019.

[13] H. A. Quigley and A. T. Broman, "The number of people with glaucoma worldwide in 2010 and 2020," *The British Journal of Ophthalmology*, vol. 90, no. 3, pp. 262–267, 2006.

[14] Y. C. Tham, X. Li, T. Y. Wong, H. A. Quigley, T. Aung, and C. Y. Cheng, "Global prevalence of glaucoma and projections of glaucoma burden through 2040: a systematic review and meta-analysis," *Ophthalmology*, vol. 121, no. 11, pp. 2081–2090, 2014.

[15] M. Yoshida, S. Kunimatsu-Sanuki, K. Omodaka, and T. Nakazawa, "Structure/function relationship between wide-scan binocular OCT images and the integrated visual field in glaucoma patients," *Clinical & Experimental Ophthalmology*, vol. 44, no. 6, pp. 526–528, 2016.

[16] H. Resch, G. Garhofer, G. Fuchsjäger-Mayrl, A. Hommer, and L. Schmetterer, "Endothelial dysfunction in glaucoma," *Acta Ophthalmologica*, vol. 87, no. 1, pp. 4–12, 2009.

[17] J. Barthelmes, M. P. Nägele, V. Ludovici, F. Ruschitzka, I. Sudano, and A. J. Flammer, "Endothelial dysfunction in cardiovascular disease and Flammer syndrome-similarities and differences," *The EPMA Journal*, vol. 8, no. 2, pp. 99–109, 2017.

[18] Y. Nakashima, A. S. Plump, E. W. Raines, J. L. Breslow, and R. Ross, "ApoE-deficient mice develop lesions of all phases of atherosclerosis throughout the arterial tree," *Arteriosclerosis and Thrombosis*, vol. 14, no. 1, pp. 133–140, 1994.

[19] R. Sun, J. Tian, J. Zhang, L. Wang, J. Guo, and Y. Liu, "Monitoring inflammation injuries in the progression of atherosclerosis with contrast enhanced ultrasound molecular imaging," *PLoS One*, vol. 12, no. 10, article e0186155, 2017.

[20] Q. N. Dinh, S. Chrissobolis, H. Diep et al., "Advanced atherosclerosis is associated with inflammation, vascular dysfunction and oxidative stress, but not hypertension," *Pharmacological Research*, vol. 116, pp. 70–76, 2017.

[21] P. Wohlfart, H. Xu, A. Endlich et al., "Antiatherosclerotic effects of small-molecular-weight compounds enhancing endothelial nitric-oxide synthase (eNOS) expression and preventing eNOS uncoupling," *The Journal of Pharmacology and Experimental Therapeutics*, vol. 325, no. 2, pp. 370–379, 2008.

[22] A. Gericke, J. J. Sniatecki, E. Goloborodko et al., "Identification of the muscarinic acetylcholine receptor subtype mediating cholinergic vasodilation in murine retinal arterioles," *Investigative Ophthalmology & Visual Science*, vol. 52, no. 10, pp. 7479–7484, 2011.

[23] A. Gericke, E. Goloborodko, N. Pfeiffer, and C. Manicam, "Preparation steps for measurement of reactivity in mouse retinal arterioles *Ex Vivo*," *Journal of Visualized Experiments*, vol. 135, no. 135, 2018.

[24] M. Oelze, A. Warnholtz, J.. Faulhaber et al., "NADPH oxidase accounts for enhanced superoxide production and impaired endothelium-dependent smooth muscle relaxation in BK$\beta 1^{-/-}$ Mice," *Arteriosclerosis, Thrombosis, and Vascular Biology*, vol. 26, no. 8, pp. 1753–1759, 2006.

[25] P. Laspas, M. B. Zhutdieva, C. Brochhausen et al., "The M_1 muscarinic acetylcholine receptor subtype is important for retinal neuron survival in aging mice," *Scientific Reports*, vol. 9, no. 1, article 5222, 2019.

[26] J. K. Zadeh, R. Ruemmler, E. K. Hartmann et al., "Responses of retinal arterioles and ciliary arteries in pigs with acute respiratory distress syndrome (ARDS)," *Experimental Eye Research*, vol. 184, pp. 152–161, 2019.

[27] J. K. Zadeh, A. Garcia-Bardon, E. K. Hartmann et al., "Short-time ocular ischemia induces vascular endothelial dysfunction and ganglion cell loss in the pig retina," *International Journal of Molecular Sciences*, vol. 20, no. 19, article 4685, 2019.

[28] N. Xia, S. Horke, A. Habermeier et al., "Uncoupling of endothelial nitric oxide synthase in perivascular adipose tissue of diet-induced obese mice," *Arteriosclerosis, Thrombosis, and Vascular Biology*, vol. 36, no. 1, pp. 78–85, 2016.

[29] P. Laspas, O. W. Gramlich, H. D. Müller et al., "Autoreactive antibodies and loss of retinal ganglion cells in rats induced by immunization with ocular antigens," *Investigative Ophthalmology & Visual Science*, vol. 52, no. 12, pp. 8835–8848, 2011.

[30] P. Laspas, E. Goloborodko, J. J. Sniatecki et al., "Role of nitric oxide synthase isoforms for ophthalmic artery reactivity in mice," *Experimental Eye Research*, vol. 127, pp. 1–8, 2014.

[31] P. Laspas, J. J. Sniatecki, C. Brochhausen et al., "Effect of the M_1 muscarinic acetylcholine receptor on retinal neuron number studied with gene-targeted mice," *Journal of Molecular Neuroscience*, vol. 56, no. 2, pp. 472–479, 2015.

[32] A. J. Kattoor, S. H. Kanuri, and J. L. Mehta, "Role of ox-LDL and LOX-1 in atherogenesis," *Current Medicinal Chemistry*, vol. 26, no. 9, pp. 1693–1700, 2019.

[33] T. Aoyama, T. Sawamura, Y. Furutani et al., "Structure and chromosomal assignment of the human lectin-like oxidized low-density-lipoprotein receptor-1 (LOX-1) gene," *The Biochemical Journal*, vol. 339, no. 1, Part 1, pp. 177–184, 1999.

[34] L. Pérez, A. Vallejos, C. Echeverria, D. Varela, C. Cabello-Verrugio, and F. Simon, "OxHDL controls LOX-1 expression and plasma membrane localization through a mechanism dependent on NOX/ROS/NF-κB pathway on endothelial cells," *Laboratory Investigation*, vol. 99, no. 3, pp. 421–437, 2019.

[35] N. J. Alp, M. A. McAteer, J. Khoo, R. P. Choudhury, and K. M. Channon, "Increased endothelial tetrahydrobiopterin synthesis by targeted transgenic GTP-cyclohydrolase I overexpression reduces endothelial dysfunction and atherosclerosis in ApoE-knockout mice," *Arteriosclerosis, Thrombosis, and Vascular Biology*, vol. 24, no. 3, pp. 445–450, 2004.

[36] M. Simionescu, "Implications of early structural-functional changes in the endothelium for vascular disease," *Arteriosclerosis, Thrombosis, and Vascular Biology*, vol. 27, no. 2, pp. 266–274, 2007.

[37] E. Rossitch Jr., E. Alexander 3rd, P. M. Black, and J. P. Cooke, "L-arginine normalizes endothelial function in cerebral vessels from hypercholesterolemic rabbits," *The Journal of Clinical Investigation*, vol. 87, no. 4, pp. 1295–1299, 1991.

[38] J. Kitayama, F. M. Faraci, S. R. Lentz, and D. D. Heistad, "Cerebral vascular dysfunction during hypercholesterolemia," *Stroke*, vol. 38, no. 7, pp. 2136–2141, 2007.

[39] K. Yamashiro, A. B. Milsom, J. Duchene et al., "Alterations in nitric oxide and endothelin-1 bioactivity underlie cerebrovascular dysfunction in ApoE-deficient mice," *Journal of Cerebral Blood Flow and Metabolism*, vol. 30, no. 8, pp. 1494–1503, 2010.

[40] A. A. Miller, T. M. de Silva, C. P. Judkins, H. Diep, G. R. Drummond, and C. G. Sobey, "Augmented superoxide production by Nox2-containing NADPH oxidase causes cerebral artery dysfunction during hypercholesterolemia," *Stroke*, vol. 41, no. 4, pp. 784–789, 2010.

[41] O. de Montgolfier, A. Pinçon, P. Pouliot et al., "High systolic blood pressure induces cerebral microvascular endothelial dysfunction, neurovascular unit damage, and cognitive decline in mice," *Hypertension*, vol. 73, no. 1, pp. 217–228, 2019.

[42] S. H. Tsai, W. Xie, M. Zhao, Rosa RH Jr, T. W. Hein, and L. Kuo, "Alterations of ocular hemodynamics impair ophthalmic vascular and neuroretinal function," *The American Journal of Pathology*, vol. 188, no. 3, pp. 818–827, 2018.

[43] V. P. Costa, A. Harris, D. Anderson et al., "Ocular perfusion pressure in glaucoma," *Acta Ophthalmologica*, vol. 92, no. 4, pp. e252–e266, 2014.

[44] L. V. d'Uscio, M. Barton, S. Shaw, and T. F. Lüscher, "Chronic ET_A receptor blockade prevents endothelial dysfunction of small arteries in apolipoprotein E-deficient mice," *Cardiovascular Research*, vol. 53, no. 2, pp. 487–495, 2002.

[45] J. Ketonen, S. Merasto, I. Paakkari, and E. M. Mervaala, "High sodium intake increases vascular superoxide formation and promotes atherosclerosis in apolipoprotein E-deficient mice," *Blood Pressure*, vol. 14, no. 6, pp. 373–382, 2005.

[46] C. J. Hartley, A. K. Reddy, S. Madala et al., "Hemodynamic changes in apolipoprotein E-knockout mice," *American Journal of Physiology-Heart and Circulatory Physiology*, vol. 279, no. 5, pp. H2326–H2334, 2000.

[47] T. Beleznai, H. Takano, C. Hamill et al., "Enhanced K^+-channel-mediated endothelium-dependent local and conducted dilation of small mesenteric arteries from $ApoE^{-/-}$ mice," *Cardiovascular Research*, vol. 92, no. 2, pp. 199–208, 2011.

[48] S. E. Wolfle and C. de Wit, "Intact endothelium-dependent dilation and conducted responses in resistance vessels of hypercholesterolemic mice in vivo," *Journal of Vascular Research*, vol. 42, no. 6, pp. 475–482, 2005.

[49] A. Gericke, E. Goloborodko, J. J. Sniatecki, A. Steege, L. Wojnowski, and N. Pfeiffer, "Contribution of nitric oxide synthase isoforms to cholinergic vasodilation in murine retinal arterioles," *Experimental Eye Research*, vol. 109, pp. 60–66, 2013.

[50] A. Gericke, I. Wolff, A. Musayeva et al., "Retinal arteriole reactivity in mice lacking the endothelial nitric oxide synthase (eNOS) gene," *Experimental Eye Research*, vol. 181, pp. 150–156, 2019.

[51] G. Garhöfer, C. Zawinka, H. Resch, P. Kothy, L. Schmetterer, and G. T. Dorner, "Reduced response of retinal vessel diameters to flicker stimulation in patients with diabetes," *The British Journal of Ophthalmology*, vol. 88, no. 7, pp. 887–891, 2004.

[52] S. T. Venkataraman, C. Hudson, R. Rachmiel et al., "Retinal arteriolar vascular reactivity in untreated and progressive primary open-angle glaucoma," *Investigative Ophthalmology & Visual Science*, vol. 51, no. 4, pp. 2043–2050, 2010.

[53] B. S. Cheema, H. S. kohli, R. Sharma, A. Bhansali, and M. Khullar, "Endothelial nitric oxide synthase gene polymorphism and type 2 diabetic retinopathy among Asian Indians," *Acta Diabetologica*, vol. 49, no. 6, pp. 481–488, 2012.

[54] I. Cilenšek, S. Mankoč, M. G. Petrovič, and D. Petrovič, "The 4a/4a genotype of the VNTR polymorphism for endothelial nitric oxide synthase (eNOS) gene predicts risk for proliferative diabetic retinopathy in Slovenian patients (Caucasians) with type 2 diabetes mellitus," *Molecular Biology Reports*, vol. 39, no. 6, pp. 7061–7067, 2012.

[55] S. Zhao, T. Li, B. Zheng, and Z. Zheng, "Nitric oxide synthase 3 (NOS3) 4b/a, T-786C and G894T polymorphisms in association with diabetic retinopathy susceptibility: a meta-analysis," *Ophthalmic Genetics*, vol. 33, no. 4, pp. 200–207, 2012.

[56] J. W. Jeoung, D. M. Kim, S. Oh, J. S. Lee, S. S. Park, and J. Y. Kim, "The relation between endothelial nitric oxide synthase polymorphisms and normal tension glaucoma," *Journal of Glaucoma*, vol. 26, no. 11, pp. 1030–1035, 2017.

[57] Y. Xiang, Y. Dong, X. Li, and X. Tang, "Association of common variants in eNOS gene with primary open angle glaucoma: a meta-analysis," *Journal of Ophthalmology*, vol. 2016, Article ID 1348347, 11 pages, 2016.

[58] Q. Li, A. Verma, P. Y. Han et al., "Diabetic eNOS-knockout mice develop accelerated retinopathy," *Investigative Ophthalmology & Visual Science*, vol. 51, no. 10, pp. 5240–5246, 2010.

[59] D.-Y. Yu, S. J. Cringle, P. K. Yu et al., "Retinal capillary perfusion: spatial and temporal heterogeneity," *Progress in Retinal and Eye Research*, vol. 70, pp. 23–54, 2019.

[60] A. C. Provost, L. Vede, K. Bigot et al., "Morphologic and electroretinographic phenotype of SR-BI knockout mice after a long-term atherogenic diet," *Investigative Ophthalmology & Visual Science*, vol. 50, no. 8, pp. 3931–3942, 2009.

[61] S. Dithmar, C. A. Curcio, N. A. le, S. Brown, and H. E. Grossniklaus, "Ultrastructural changes in Bruch's membrane of apolipoprotein E-deficient mice," *Investigative Ophthalmology & Visual Science*, vol. 41, no. 8, pp. 2035–2042, 2000.

[62] G. Malek, L. V. Johnson, B. E. Mace et al., "Apolipoprotein E allele-dependent pathogenesis: a model for age-related retinal degeneration," *Proceedings of the National Academy of Sciences of the United States of America*, vol. 102, no. 33, pp. 11900–11905, 2005.

[63] M. Rudolf, B. Winkler, Z. Aherrahou, L. C. Doehring, P. Kaczmarek, and U. Schmidt-Erfurth, "Increased expression of vascular endothelial growth factor associated with accumulation of lipids in Bruch's membrane of LDL receptor knockout mice," *The British Journal of Ophthalmology*, vol. 89, no. 12, pp. 1627–1630, 2005.

[64] J. A. Mares-Perlman, W. E. Brady, R. Klein, G. VandenLangenberg, B. E. Klein, and M. Palta, "Dietary fat and age-related maculopathy," *Archives of Ophthalmology*, vol. 113, no. 6, pp. 743–748, 1995.

[65] L. Hyman, A. P. Schachat, Q. He, M. C. Leske, and for the Age-Related Macular Degeneration Risk Factors Study Group, "Hypertension, cardiovascular disease, and age-related macular Degeneration," *Archives of Ophthalmology*, vol. 118, no. 3, pp. 351–358, 2000.

[66] T. Ressiniotis, P. G. Griffiths, M. Birch, S. Keers, and P. F. Chinnery, "The role of apolipoprotein E gene polymorphisms in primary open-angle glaucoma," *Archives of Ophthalmology*, vol. 122, no. 2, pp. 258–261, 2004.

[67] M. Zetterberg, G. Tasa, M. S. Palmér et al., "Apolipoprotein E polymorphisms in patients with primary open-angle glaucoma," *American Journal of Ophthalmology*, vol. 143, no. 6, pp. 1059-1060, 2007.

[68] F. Mabuchi, S. Tang, D. Ando et al., "The apolipoprotein E gene polymorphism is associated with open angle glaucoma in the Japanese population," *Molecular Vision*, vol. 11, pp. 609–612, 2005.

[69] C. Y. Lam, B. J. Fan, D. Y. Wang et al., "Association of apolipoprotein E polymorphisms with normal tension glaucoma in a Chinese population," *Journal of Glaucoma*, vol. 15, no. 3, pp. 218–222, 2006.

[70] K. Omodaka, K. M. Nishiguchi, M. Yasuda et al., "Neuroprotective effect against axonal damage-induced retinal ganglion cell death in apolipoprotein E-deficient mice through the suppression of kainate receptor signaling," *Brain Research*, vol. 1586, pp. 203–212, 2014.

[71] P. S. Hauser, V. Narayanaswami, and R. O. Ryan, "Apolipoprotein E: from lipid transport to neurobiology," *Progress in Lipid Research*, vol. 50, no. 1, pp. 62–74, 2011.

[72] A. Amaratunga, C. R. Abraham, R. B. Edwards, J. H. Sandell, B. M. Schreiber, and R. E. Fine, "Apolipoprotein E is synthesized in the retina by Müller glial cells, secreted into the vitreous, and rapidly transported into the optic nerve by retinal ganglion cells," *The Journal of Biological Chemistry*, vol. 271, no. 10, pp. 5628–5632, 1996.

[73] B. Lorber, M. Berry, M. R. Douglas, T. Nakazawa, and A. Logan, "Activated retinal glia promote neurite outgrowth of retinal ganglion cells via apolipoprotein E," *Journal of Neuroscience Research*, vol. 87, no. 12, pp. 2645–2652, 2009.

[74] A. Saadane, A. Petrov, N. Mast et al., "Mechanisms that minimize retinal impact of apolipoprotein E absence," *Journal of Lipid Research*, vol. 59, no. 12, pp. 2368–2382, 2018.

[75] J. M. Ong, N. C. Zorapapel, K. A. Rich et al., "Effects of cholesterol and apolipoprotein E on retinal abnormalities in ApoE-deficient mice," *Investigative Ophthalmology & Visual Science*, vol. 42, no. 8, pp. 1891–1900, 2001.

[76] A. C. Mak, C. R. Pullinger, L. F. Tang et al., "Effects of the absence of apolipoprotein e on lipoproteins, neurocognitive function, and retinal function," *JAMA Neurology*, vol. 71, no. 10, pp. 1228–1236, 2014.

8.4 Weitere Publikationen

Teile dieser Dissertation wurden in internationalen Fachzeitschriften publiziert und auf wissenschaftlichen Kongressen präsentiert.

1. *Elevated Intraocular Pressure Causes Abnormal Reactivity of Mouse Retinal Arterioles.*
   Gericke A, Mann C, **Zadeh JK**, Musayeva A, Wolff I, Wang M, Pfeiffer N, Daiber A, Li H, Xia N, Prokosch V. Oxidative Medicine and Cellular Longevity, Dec 2019, PMID:31976030

2. *Retinal Arteriole Reactivity in Mice Lacking the Endothelial Nitric Oxide Synthase (eNOS) Gene.*
   Gericke A, Wolff I, Musayeva A, **Zadeh JK**, Manicam C, Pfeiffer N, Li H, Xia N. Experimental Eye Research, Apr 2019, PMID: 30716330

3. *The M_1 Muscarinic Acetylcholine Receptor Subtype is Important for Retinal Neuron Survival in Aging Mice.* Laspas P, Zhutdieva MB, Brochhausen C, Musayeva A, **Zadeh JK**, Pfeiffer N, Xia N, Li H, Wess J, Gericke A. Scientific Reports, Mar 2019, PMID: 30914695

4. *Compensatory Vasodilator Mechanisms in the Ophthalmic Artery of Endothelial Nitric Oxide Synthase Gene Knockout Mice.* Manicam C, Ginter N, Li H, Xia N, Goloborodko E, **Zadeh JK**, Musayeva A, Pfeiffer N, Gericke A
   Scientific Reports, Aug 2017, PMID: 28769073

<u>Posterbeiträge auf wissenschaftlichen Konferenzen:</u>

Responses of Retinal Arterioles and Ciliary Arteries in Pigs with Acute Respiratory Distress Syndrome (ARDS).
Zadeh JK, Ruemmler R, Hartmann EK, Ziebart A, Ludwig M, Patzak A, Xia N, Li H, Pfeiffer N, Gericke A
Deutsche Ophthalmologische Gesellschaft, DOG Kongress, Bonn, Deutschland, 2018

8.5 Eidesstaatliche Erklärung

Hiermit erkläre ich an Eides statt, dass ich diese Dissertation selbstständig und nur unter Verwendung der angegebenen Hilfsmittel angefertigt habe. Ich habe keinen vorherigen Promotionsversuch unternommen.

Mainz, 2020

Jenia Kouchek Zadeh

8.6 Lebenslauf

Jenia Kouchek Zadeh

PERSONAL DATA

Date of Birth	January 24, 1991
Place of Birth	Kirn, Germany
Citizenship	German

PROFESSIONAL EXPERIENCE

Since Jul 2019	**Medical Affairs Manager at Allergan Gmbh** ▪ Medical Science Liaison Management ▪ Medical Management Inhouse
Dec 2016 – Jun 2019	**Ph.D. position at Universitätsmedizin Mainz** ▪ Ophthalmo- Pharmacology and Physiology, PD. Dr. Adrian Gericke ▪ Investigation of oxidative stress on endothelial dependent dilatory mechanisms in retinal arterioles induced by three different diseases
Dec 2015 – Nov 2016	**Pharmacist at Jordan Apotheke in Erlangen**
May 2015 – Oct 2015	**Internship at Meilwald-/Kolibri-Apotheke in Erlangen**
Nov 2014 – Apr 2015	**Internship at the University of Florida in Orlando, College of Pharmacy** ▪ Translational Research Institute for Diabetes and Metabolism (TRI) ▪ Florida Hospital
Nov 2014	**Scholarship from Bayerische Apothekerstiftung**

EDUCATION

Nov 2015	**3rd Staatsexamen, Munich** Licensed Pharmacist
Oct 2014	**2nd Staatsexamen** Friedrich-Alexander Universität Erlangen-Nürnberg
OCT 2010 – OCT 2014	**Studies of Pharmacy** Friedrich-Alexander Universität Erlangen-Nürnberg
2001 – 2010	**Abitur** Kurfürstliches Schloss in Mainz

Jun 2008 – Jul 2008 **Education First**

Languages

- German: native
- Farsi: native
- English: fluent
- Spanish: basic

EDV

- Advanced skills in MS Word, MS Power Point, MS Excel
- Advanced skills in Image J, Statistica

Certificates

- Certificate of Modular course 4, Translational Animal Research Center
- Certificate of essential statistics course

Mainz, 02.11.2020